INDIVIDUAL WELFARE MAXIMIZATION IN ELECTRICITY MARKETS INCLUDING CONSUMER AND FULL TRANSMISSION SYSTEM MODELING

BY

JAMES DANIEL WEBER

B.S., University of Wisconsin - Platteville, 1995
M.S., University of Illinois at Urbana-Champaign, 1997

THESIS

Submitted in partial fulfillment of the requirements
for the degree of Doctor of Philosophy in Electrical Engineering
in the Graduate College of the
University of Illinois at Urbana-Champaign, 1999

Urbana, Illinois

RED-BORDERED FORM

ABSTRACT

This dissertation presents a new algorithm that allows a market participant to maximize its individual welfare in the electricity spot market. The use of such an algorithm in determining market equilibrium points, called Nash equilibria, is also demonstrated.

The start of the algorithm is a spot market model that uses the optimal power flow (OPF), with a full representation of the transmission system. The OPF is also extended to model consumer behavior, and a thorough mathematical justification for the inclusion of the consumer model in the OPF is presented. The algorithm utilizes price and dispatch sensitivities, available from the Hessian matrix of the OPF, to help determine an optimal change in an individual's bid. The algorithm is shown to be successful in determining local welfare maxima, and the prospects for scaling the algorithm up to realistically sized systems are very good.

Assuming a market in which all participants maximize their individual welfare, economic equilibrium points, called Nash equilibria, are investigated. This is done by iteratively solving the individual welfare maximization algorithm for each participant until a point is reached where all individuals stop modifying their bids. It is shown that these Nash equilibria can be located in this manner. However, it is also demonstrated that equilibria do not always exist, and are not always unique when they do exist.

It is also shown that individual welfare is a highly nonconcave function resulting in many local maxima. As a result, a more global optimization technique, using a genetic algorithm (GA), is investigated. The genetic algorithm is successfully demonstrated on several systems. It is also shown that a GA can be developed using special niche methods, which allow a GA to converge to several local optima at once.

Finally, the last chapter of this dissertation covers the development of a new computer visualization routine for power system analysis: contouring. The contouring algorithm is demonstrated to be useful in visualizing bus-based and transmission line-based quantities.

ACKNOWLEDGMENTS

I would like to thank Professor Thomas J. Overbye for his knowledge, guidance, and support throughout my doctoral studies. He and his family have been a great help to me. I would also like to thank all the other professors who have helped and continue to help me in my academic career. I also say thanks the University of Illinois Power Affiliates Program and Grainger Foundation for their generous financial support.

PowerWorld Corporation also deserves my thanks. Working there has given me great insight into turning research into a commercial product, and has also inspired much of the direction of my research. Also, thank you for providing me the flexibility to complete my doctoral studies.

Lastly, I would like to thank my family. My brothers Scott and Brian, and sister-in-law Andrea continue to be a source of inspiration, support and friendship. My mother and father, Jan and Gene, deserve great thanks for their unconditional love and support which have allowed me and my brothers continued success in our personal lives and careers. Finally, I say thank you to my fiancé Amelia Fuller who has made the last two years of my doctoral work a joy. I look forward to our future life together.

TABLE OF CONTENTS

Page

LIST OF TABLES

LIST OF FIGURES

NOTATION AND TERMINOLOGY

General conventions on notation

All vector and matrix variables are in bold (e.g., **h** is a vector and h is a scalar).
All vectors are column vectors.
Subscript p and subscript q signify a relation to real and reactive power, respectively.

Variable Definitions

x = state variables and other controls (e.g., tap ratios)

$\mathbf{s} = \begin{bmatrix} \mathbf{s}_p^T & \mathbf{s}_q^T \end{bmatrix}^T$ = the supply vector

$\mathbf{d} = \begin{bmatrix} \mathbf{d}_p^T & \mathbf{d}_q^T \end{bmatrix}^T$ = the demand vector

$\hat{\mathbf{s}} = \begin{bmatrix} \hat{\mathbf{s}}_p^T & \hat{\mathbf{s}}_q^T \end{bmatrix}^T$ = augmented supply vector including zeros where no suppliers exists

$\hat{\mathbf{d}} = \begin{bmatrix} \hat{\mathbf{d}}_p^T & \hat{\mathbf{d}}_q^T \end{bmatrix}^T$ = augmented demand vector including zeros where no loads exist

$C(\mathbf{s}) = C(\mathbf{s}_p, \mathbf{s}_q) = \sum_{\text{all suppliers}} C_k(\mathbf{s}_p, \mathbf{s}_q)$ = suppliers' cost

$B(\mathbf{d}) = B(\mathbf{d}_p, \mathbf{d}_q) = \sum_{\text{all consumers}} B_k(\mathbf{d}_p, \mathbf{d}_q)$ = consumers' benefit

$$\mathbf{h}(\mathbf{x},\mathbf{s},\mathbf{d}) = \begin{bmatrix} \hat{\mathbf{h}}(\mathbf{x}) - \hat{\mathbf{s}} + \hat{\mathbf{d}} \\ \overline{\mathbf{h}}(\mathbf{x}) \end{bmatrix} = \begin{bmatrix} \mathbf{h}_p(\mathbf{x},\mathbf{s}_p,\mathbf{d}_p) \\ \mathbf{h}_q(\mathbf{x},\mathbf{s}_q,\mathbf{d}_q) \\ \overline{\mathbf{h}}(\mathbf{x}) \end{bmatrix} = \text{equality constraints}$$

$\mathbf{h}_p(\mathbf{x},\mathbf{s}_p,\mathbf{d}_p) = \hat{\mathbf{h}}_p(\mathbf{x}) - \hat{\mathbf{s}}_p + \hat{\mathbf{d}}_p$ = real power flow equations

$\mathbf{h}_q(\mathbf{x},\mathbf{s}_q,\mathbf{d}_q) = \hat{\mathbf{h}}_q(\mathbf{x}) - \hat{\mathbf{s}}_q + \hat{\mathbf{d}}_q$ = reactive power flow equations

$$\mathbf{g}(\mathbf{x},\mathbf{s},\mathbf{d}) = \begin{bmatrix} \mathbf{s}_{\min} - \mathbf{s} \\ \mathbf{s} - \mathbf{s}_{\max} \\ \mathbf{d}_{\min} - \mathbf{d} \\ \mathbf{d} - \mathbf{d}_{\max} \\ \overline{\mathbf{g}}(\mathbf{x}) \end{bmatrix} = \text{inequality constraints}$$

L, $\overline{L}$ = Lagrange functions

$\boldsymbol{\lambda} = \begin{bmatrix} \boldsymbol{\lambda}_h^T & \boldsymbol{\lambda}_g^T & \boldsymbol{\lambda}_f^T \end{bmatrix}^T$ = Lagrange multiplier vector

$\boldsymbol{\lambda}_h = \begin{bmatrix} \boldsymbol{\lambda}_{\hat{h}}^T & \boldsymbol{\lambda}_{\overline{h}}^T \end{bmatrix}^T = \begin{bmatrix} \boldsymbol{\lambda}_{\hat{h}p}^T & \boldsymbol{\lambda}_{\hat{h}q}^T & \boldsymbol{\lambda}_{\overline{h}}^T \end{bmatrix}^T$ = Lagrange multiplier vector for power flow equations and other equality constraints

$\boldsymbol{\lambda}_g = \begin{bmatrix} \boldsymbol{\lambda}_{gs\min}^T & \boldsymbol{\lambda}_{gs\max}^T & \boldsymbol{\lambda}_{gd\min}^T & \boldsymbol{\lambda}_{gd\max}^T & \boldsymbol{\lambda}_{\overline{g}}^T \end{bmatrix}^T$ = Lagrange multiplier vector for inequality constraints

$\tilde{\boldsymbol{\lambda}}_{\hat{h}s} = \begin{bmatrix} \tilde{\boldsymbol{\lambda}}_{\hat{h}sp}^T & \tilde{\boldsymbol{\lambda}}_{\hat{h}sq}^T \end{bmatrix}^T$ = reduced Lagrange multiplier vector, including only entries for power flow equations that include a supply of real or reactive power

$\tilde{\boldsymbol{\lambda}}_{\hat{h}d} = \begin{bmatrix} \tilde{\boldsymbol{\lambda}}_{\hat{h}dp}^T & \tilde{\boldsymbol{\lambda}}_{\hat{h}dq}^T \end{bmatrix}^T$ = reduced Lagrange multiplier vector, including only entries for power flow equations that include a demand of real or reactive power

$\tilde{\boldsymbol{\lambda}}_f = \left[\tilde{\boldsymbol{\lambda}}_{fp}^T \quad \tilde{\boldsymbol{\lambda}}_{fq}^T\right]^T$ = Lagrange multiplier vector for additional constraints

$\mathbf{p} = \left[\mathbf{p}_s^T \;\vdots\; \mathbf{p}_d^T\right]^T = \left[\mathbf{p}_{sp}^T \quad \mathbf{p}_{sq}^T \;\vdots\; \mathbf{p}_{dp}^T \quad \mathbf{p}_{dq}^T\right]^T$ = price vector for variable suppliers and variable consumers (includes real and reactive prices)

$\mathbf{D}(\mathbf{p})$ = the functional inverse of $\dfrac{\partial B(\mathbf{d})}{\partial \mathbf{d}}$

$\mathbf{S}(\mathbf{p})$ = the functional inverse of $\dfrac{\partial C(\mathbf{s})}{\partial \mathbf{s}}$

Terminology

- Supplier : Economic entity that offers the sale of products to the market (e.g., a generator).
- Supply : The products the supplier offers to the market (e.g., output of generator in MWh).
- Generation : A particular kind of supply.
- Consumer : Economic entity that requests the purchase of products from the market (e.g., a load).
- Demand : The products the consumer purchases from the market (e.g., input to a load in MWh).
- Load : A particular kind of demand.

1. INTRODUCTION

Electricity markets throughout the world continue to be opened to competitive forces. The underlying objective of introducing competition to these markets is to make them more efficient. It is a general concept of capitalism that if fair and equitable market structures are created, which give all market participants incentives to maximize their own individual welfare, then the market as a whole will behave in a manner which maximizes welfare for everyone. If this objective is to be achieved, the electricity industry needs new algorithms to help market participants behave in an efficient manner, helping them maximize their own welfare. It is imperative that these algorithms model the economics of the electricity market while maintaining the detail necessary to represent the underlying engineering requirements. This dissertation presents a new algorithm which allows a market participant to maximize its individual welfare, while taking into account the full model of the electrical transmission system.

Before continuing further, it is useful to introduce general market structures and to look at the history of the electricity industry to motivate the desire for restructuring. Section 1.1 will introduce electricity market structures, while Sections 1.2 and 1.3 will discuss the history of the electricity industry throughout the world leading up to the creation of these market structures.

1.1 Electricity Market Structures

In most industries, competitive market structures give suppliers of the commodity direct access to the consumer as shown in Figure 1.1.

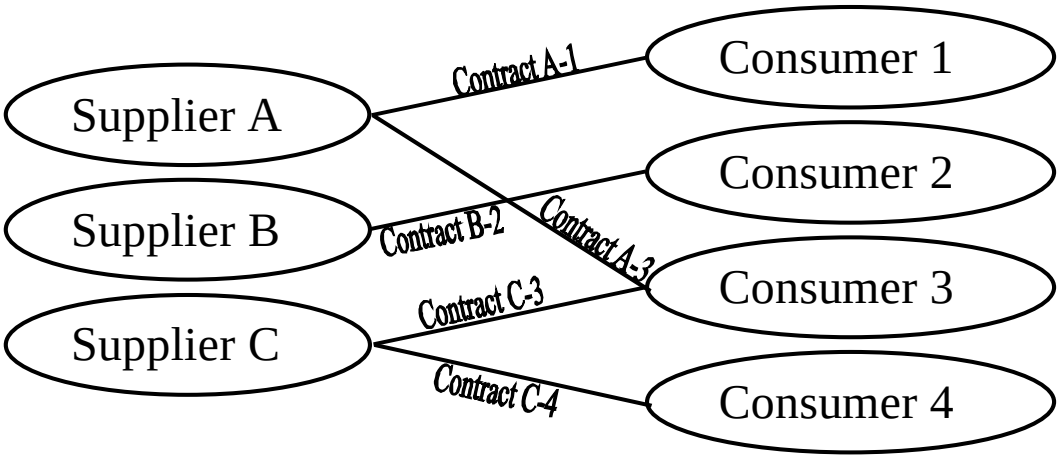

Figure 1.1 Bilateral Market Model

As an example consider the commodity of long distance telephone service. In this industry, suppliers such as MCI, Sprint, and AT&T sell their commodity directly to the retail consumer. The supplier and consumer then enter into a bilateral contract, where the supplier agrees to provide long distance telephone service, while the consumer agrees to a fee schedule for this service. The advantage of this bilateral market model is that no restrictions are placed on the structure of the contract. This gives flexibility, allowing all participants in the market the opportunity to find the exact kind of service they desire at the price they desire.

While this model is appropriate for most markets, the electricity market exhibits two distinguishing characteristics that make the formation of a bilateral market model difficult: (1) the inability to store electrical energy practically, and (2) the sharing of a common, essentially uncontrollable, transmission network. The inability to practically store electrical energy can result in extreme price volatility due to shortages during times of peak demand. This market behavior has already been exhibited in the limited wholesale markets of today, with prices during times of high demand reaching more than 100 times normal market prices [1]. Markets with this kind of price volatility will have difficulty reaching equilibrium.

The sharing of a common transmission network is common to other markets, such as the long distance telephone market. What distinguishes the electricity market network, however, is the uncontrollability of the network flows. In telephone networks, information flow is controlled through computer software which performs call routing. Routers determine the exact physical path of the phone call, giving the system operator precise control of the network flow [2]. There are nearly no network flow controllers available in electricity markets, with a small number of phase-shifting transformers and flexible ac transmission devices (FACTs) as exceptions. Because the network flows are not controllable, the action of one player in the market directly affects the ability of other players to participate in the market. In the long distance telephone market this is not seen. If AT&T sells service to your neighbor, this does not prevent MCI from selling service to you. With electricity, however, there are many ancillary services [3],[4] that must be supplied and limits that must be adhered to along with delivery of the product in order for the electric transmission system to maintain integrity. One example of this is ensuring that the transmission line limits are adhered to at all times. In systems where transmission congestion is encountered, the actions of players directly affect who can get power to the local market. This creates a potential for cooperative behavior among several generators and loads that would limit the competition in a local area of the system. Additionally, electric transmission system losses are affected by an individual player's actions that, as a result, can affect all players in the market. How to account for losses can be very difficult because of their nonlinear nature.

Because of these characteristics, all the work in setting up new market structures in the electric power industry throughout the world has involved the development of power pools. In this market model, a pool operator takes bids from suppliers and consumers and dispatches generation and load in an economic manner based on the bids. This economic manner will be

described shortly. The suppliers and consumers do not directly interact with one another, but only indirectly through the pool operator. The advantage of this arrangement is that the pool operator can internalize the problems of congestion management, loss allocation, and other ancillary services. The pool operator in this model is responsible for the economic infrastructure of accepting and awarding bids, as well as the engineering system infrastructure of maintaining the transmission system. In some markets, such as in California, these two tasks are assigned to separate organizations. The economic organization is called the power pool, or power exchange, while the engineering organization is called the independent system operator (ISO).

The methods which have been used to dispatch generation and load in an economic manner have been based on one of two methods: last accepted bid and spot pricing theory. In the last accepted bid method, market participants submit blocks of generation and sometimes load along with associated prices. All the supply bids are then aggregated and sorted by price in ascending order to create the *aggregate supply curve*. If consumer bidding is included, then all the demand bids are aggregated and sorted by price in descending order to create the *aggregate demand curve*. The curves are then plotted against one another, and the point were they cross defines the *market clearing price (MCP)*. All bids to the left of this point are then accepted and all suppliers are paid the MCP for the blocks of generation which were bid, and all consumers must pay the MCP for the blocks of demand which were bid. This is depicted in Figure 1.2. Examples of markets which used the last accepted bid methods are England and Wales [5], New Zealand [6], and the state of California in the Western United States [7].

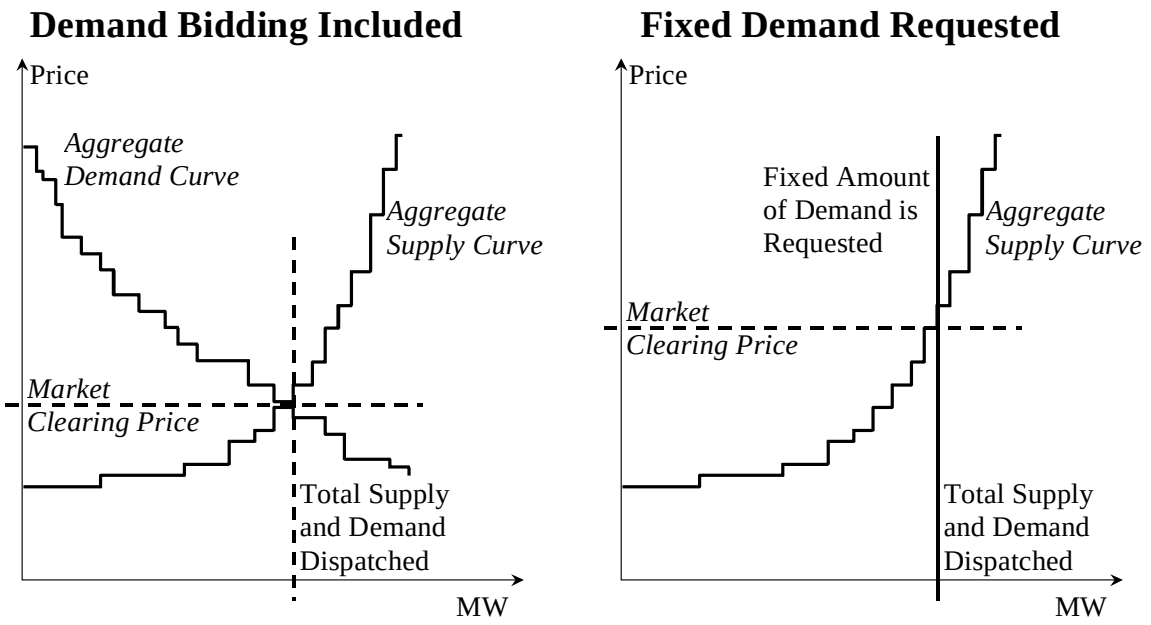

Figure 1.2 Last Accepted Bid Dispatch Model

The other method used to dispatch generation and load in an economic manner is to use spot pricing theory as described in [8]. This is the method which is used throughout this dissertation and will be discussed in great detail throughout. In this method suppliers and sometimes consumers submit bid curves to the pool operator and an optimization routine is used to determine the dispatch results. Suppliers are then paid a price according to their bids and consumers must pay a price according to their bids. Examples of markets which using spot pricing methods are Australia [5], the PJM interconnection in the Eastern United States [9], Argentina [5], and the New England region of the United States [10].

Electricity market structures have been introduced, but the impetus for creating them is still not clear. Sections 1.2 and 1.3 discuss the history of the electricity industry, concentrating on what has lead to the creation of market structures throughout the world.

1.2 History of the Electricity Industry in the United States

After the formation of the electric utility industry in the early 1900s in the United States, utilities went through a period of merging and consolidation up through the 1920s. During this time the U.S. began forming what would ultimately become the interconnected electric system that exists today. From the middle 1930s through the early 1970s the industry went through an incredible expansion, with electricity demand growing at rates of approximately 7% each year. Increasing economies of scale marked this period of time as ever larger plants were built at lower costs per megawatt of capacity. Throughout this time the price of electricity continued to drop even as the demand increased.

During the 1970s this began to change. Oil prices increased dramatically during and after the 1973-1974 oil embargo. This, along with high inflation, resulted in increased energy costs. As a result of these events, the United States began striving for energy self-sufficiency. Energy conservation programs increased in number and the development of renewable resources such as solar, wind, waste, or geothermal was begun in earnest.

These events led to new legislation in the United States to help achieve the United States' energy goals. This new legislation was encapsulated in the Public Utility Regulatory Policy Act (PURPA) of 1978 [11]. The goals of PURPA were

> to encourage (1) conservation of energy supplied by electric utilities; (2) the optimization of the efficiency of use of facilities and resources by electric utilities; and (3) equitable rates to electric consumers. (16 USC Sec. 2611 of [11])

In order to achieve these goals, PURPA created a new class of electricity supply called the qualifying facility (QF). QFs were intended to be small generation plants that used alternative fuel sources such as wind, solar, waste, or geothermal. Under PURPA, the electric utilities were required to purchase electricity from the QFs. PURPA stated that

> the rates for such purchase (1) shall be just and reasonable to the electric consumers of the electric utility and in the public interest, and (2) shall not discriminate against qualifying cogenerators or qualifying small power producers. (16 USC Sec. 824-3 of [11])

QFs were the beginning of competition in the United States. Traditionally, electric utilities had been vertically integrated monopolies. The utility built the generators that supplied the power, built the wires that transported the electricity to each community and to each individual consumer, and directly billed the consumer for this bundled service. QFs became a threat to the generation side of this monopoly. However, the utility still maintained its monopoly as it was in control of the method of distributing the product to the consumer: the transmission and distribution systems.

Throughout the 1970s and 1980s the United States government began to deregulate many industries including telecommunications (1969), trucking (1977), air travel (1978), and natural gas (late 1980s). This push to remove direct government control from markets was undertaken to develop more efficient market-based economies. With this trend in government policy, the move toward a competitive market in the electricity industry was on the horizon.

If the industry were to move towards a truly competitive marketplace, access to the product distribution channel needed to be opened. The first step toward this end was another legislative act, the 1992 Energy Policy Act [12]. This was followed in 1996 by orders from the Federal Energy Regulatory Commission (FERC): FERC Order 888 [13] and FERC Order 889 [14]. The stated goal of FERC Order 888 was to promote "wholesale competition through open access non-discriminatory transmission services by public utilities." How best to set up markets to achieve this goal is being decided in the federal and state governments throughout the United States [15]. Three markets have been created in the United States thus far in California [7], the Pennsylvania-New Jersey-Maryland (PJM) Interconnection [9], and New England [10].

1.3 History of Electricity Industry Reform throughout the World

While energy conservation and energy self-sufficiency were the motivating goals in the United States, electricity industry reform in other parts of the world have been for vastly different reasons. Throughout much of the world, the electricity industry has always been a state-owned monopoly. Problems due to the inefficiency of state-owned industries have been the motivation behind reform in many countries. These problems have resulted in poor electricity service along with financial shortages of capital investment. Several example experiences are discussed below.

1.3.1 United Kingdom

The United Kingdom (UK) electricity industry was formerly a state-owned industry. In 1947, many important industries throughout the UK became government owned and operated, including the electricity industry. In 1957, the government control was extended by the passage of the Central Electricity Generating Board (CEGB) which gave the government control over the generation and transmission systems and all related investment decisions.

While this may have been an important step in rebuilding the post-war UK, several decades later industry inefficiencies became a heavy burden on the government. One major example of inefficiency was the government policy of sustaining the national coal industry through purchases from the national electricity industry from 1957 through the 1980s. Throughout this time, the electricity industry was pressured and eventually required to purchase British coal at prices which were well above world prices. With the electric utilities forced to pay such high prices, "electricity prices became excessively high, and the British coal industry in essence became dependent on the electricity industry for survival"[5]. Eventually due to inefficiencies like these, Britain began to consider the viability of continuing the government-owned industries.

In 1979, under the leadership of Margaret Thatcher, a conservative government was elected to power in Britain initiating the privatization of the government-owned industries. Industries were auctioned off and several present-day companies were formed such as British Aerospace (1981), Cable and Wireless (1981), British Telecommunications (1984), British Airways (1987), and British Steel (1988) [5]. The last major industry to be deregulated was the electric utility industry. The start of this was the Electricity Act of 1983 which encouraged the creation of non-utility power producers, similar to PURPA (1978) and the Energy Policy Act (1992) in the United States. Finally, the restructuring was completely implemented in the Electricity Act of 1989.

A new industry structure was phased in over several years. The transmission system was restructured by requiring all companies with ownership in the electric transmission grid in the UK to divest their shares of the grid and a new publicly-traded company, the National Grid Company (NGC), was created to manage this grid. For generation, The nonnuclear generation was assigned to two companies, National Power and PowerGen, accounting for 46% and 28% of the generation, respectively. For distribution, twelve former regional area boards were privatized to create regional electricity companies (RECs).

The UK power pool was then developed with the National Grid Company acting as the pool operator. The NGC forecasts the demand each day and represents this by 48 half-hour segments. The suppliers then submit block bids for each half-hour, and the NGC determines the dispatch using the last accepted bid method discussed previously.

The new market structure has been generally successful, but some concern has been expressed regarding the price volatility as well as a concern over possible unfair practices of the two dominant generation companies. Some attempts have been made to remedy these concerns.

In 1994, the regulatory authorities in the UK forced the two dominant companies to sell 15% of their capacities (9% of the entire UK market) to try and reduce duopoly behavior. Also in late 1995, each company attempted a takeover of an REC, prompting the regulatory authorities to deny each request on the grounds that the takeovers would "pose significant detriments to competition"[5].

1.3.2 South America

South America is an example of a region that has also restructured its state-owned monopolies. In 1982, Chile officially reorganized its electric power industry. Argentina followed in 1992, Peru in 1993, Bolivia and Colombia in 1994, and then Brazil and Venezuela in 1996 [16]. Examples of inefficiencies included power rationing throughout Colombia in 1992-1993 and an inability to raise capital for investment in the industry in Bolivia and Peru. As a result of the reforms, a dramatic improvement in economic efficiency as well as better service has been seen in many countries. In Argentina for instance, availability of thermal generation went from an all-time low of 47% in 1992 to 75% in 1996, while electricity prices dropped from an average of more than $50 per MWh to $30 per MWh [16].

As in the United States, the countries throughout South America have required "open-access schemes… which permit open and nondiscriminatory use of their transmission systems"[16]. This open-access has enabled the development of market structures that allow competition to flourish. Most of the market structures in South America have determined generation dispatch and prices using spot pricing theory.

1.3.3 Australia

Up until recently, the electricity in Australia has been provided by publicly-owned state utilities which met the needs of each individual state. Transmission ties between the states were either nonexistent or extremely weak. The state governments were responsible for control and operation of the industry as well as for planning. The national government was only peripherally involved in regulation through legal requirements such as foreign ownership limits and taxation [5]. Because Australia's population of 18 million people is spread over an area approximately the size if the 48 contiguous states of the United States, these separate power systems made economic sense.

Because of the inefficiencies of government-owned industries, however, Australia has looked to restructure its electricity industry. The reform effort has been under way since 1991 with discussions between the industry and government resulting in the National Electricity Code, which was completed in September of 1996. The National Electricity Code established the rules and procedures for operating in the national electricity market (NEM).

The electricity grid in Australia will remain under regulation of the states until early 2000. At this time, the Australia Competition and Consumer Commission (ACCC) will take over regulation of the grid. Methods for pricing transmission services have not been completely determined at this stage. Also, because of the geographical limitations, initially the NEM will be limited to the southeastern part of Australia encompassing the states of New South Wales and Victoria, and the Australia Capital Territory. In order to expand the market, new interstate transmission connections have been planned to tie to Queensland to the North, South Australia to the West, and Tasmania via a sub-sea link.

The Australia market will utilize a combination of bilateral contracts in the long-term (more than a month ahead) and short-term (days ahead) markets, and a spot pricing for the half-hour markets to match supply and demand. All suppliers with net exports larger than 30 MW will be required to participate in the market, while smaller suppliers will be given an option. Initially, consumers with demand of greater than 10 MW will be given the option to participate in the market. Eventually, however, all customers will be given this option. Full competition is slated to begin in 2001.

1.4 The Need for Simulation Tools

Regardless of what market structures are implemented, there is a need for many new kinds of economic and engineering analysis tools. In engineering analysis, tools such as available transfer capability (ATC) calculators are needed to determine the distance from which consumers can purchase their electricity products [17],[18]. In economic analysis, tools that help predict future price trends are needed to help create a stable market. Other tools are needed to bridge the gap between engineering and economic analysis in order to analyze the impact of underlying engineering constraints on the market. One such tool that bridges this gap is an individual welfare maximization algorithm which includes a full transmission system model. This tool would allow an individual to determine its optimal bidding behavior in an electric power pool. This tool is developed in this dissertation.

The applications of welfare maximization tool would be varied. For example, transmission system congestion can subdivide a market into several regions with vastly different prices. By including the full transmission system model, market situations like this can be represented. For market participants the presence of transmission congestion could present opportunities to sell

generation into such a subdivided market in which local demand might be high and the number of potential sellers low. Tools are needed to help market participants devise optimal bidding strategies. Engineers at an ISO or other planning agency could also use such a tool to help with long-term system forecasting, enabling them to better determine where transmission system improvements are needed.

Conversely, there is a need for regulators such as FERC, the Department of Justice (DOJ), and the state regulatory commissions to be vigilant against anticompetitive acts by market participants. For example, if a particular entity owns sufficient generation it may be possible for them to manipulate the market in such a way as to deliberately induce congestion in order to raise prices [19],[20]. The recent wave of mergers and proposed mergers in the United States requires that regulators have access to tools to assess the potential for this type of manipulation. FERC's need for such a tool is described in its Order 592 "Policy Statement on Utility Mergers" in December of 1996 [21], and its formal adoption of the Department of Justice/Federal Trade Commission (DOJ/FTC) Horizontal Merger Guidelines [22]. Both the DOJ and the FERC, in a recent proposed rulemaking, have explicitly stated a desire for computer models.

> The use of computer models -- specifically, computer programs used to simulate the electric power market -- has been raised in comments on the Policy Statement and also in specific cases. In comments on the Policy Statement, DOJ recommended using computer simulations to delineate markets and also noted that these simulations could be helpful in gauging the market power of the merged firm. The Commission believes that use of a properly structured computer model could account for important physical and economic effects in an analysis of mergers and may be a valuable tool to use in a horizontal screen analysis. For example, a computer model might prove particularly useful in identifying the suppliers in the geographic market that are capable of competing with the merged company. It could provide a framework to help ensure consistency in the treatment of the data used in identifying suppliers in a geographic market. [23]

1.5 Overview

This dissertation presents a new algorithm which allows a market participant to determine the bidding strategy for maximizing its individual welfare in a spot market. This algorithm must model the economics of the electricity spot market while also maintaining a full transmission system model. Without modeling the transmission system, the algorithm would not be able to reproduce the price volatility already seen in congested power systems today [1]. An overview of the spot market model and recent work in the area follows.

1.5.1 The spot market model

The starting point of an individual welfare maximization algorithm is the development of a model which represents the electricity market. This dissertation studies the behavior of the electric power pool which uses spot pricing. This market is modeled by using the optimal power flow (OPF). The OPF problem was formulated in 1962 [24] and has been an active area of research ever since. Because the OPF can be a very large, nonlinear mathematical programming problem, many numerical algorithms and techniques have been employed to help solve it [25]-[30]. An excellent literature survey of the different techniques is found in [31], while an overview of the challenges to solving the OPF is found in [32]. This dissertation builds on the OPF written in [25]. Chapter 2 introduces the concept of using an optimal power flow to model the behavior of an electric power pool.

Using an OPF, a spot price market can be simulated with all engineering constraints enforced. In this way, the impact of transmission constraints on the spot prices in the market can be directly assessed. Much of the theory describing a spot market for electricity using the OPF is discussed in [8]. Using the OPF as a software engine to simulate a spot market has been an

active area of research. A good overview of how a spot market is modeled using the OPF is provided in [33].

Spot pricing in power systems could also extend to reactive power pricing. Thus markets for real and reactive power are conceivable and have been recommended by some [34]. Reactive power prices are typically much smaller than the real power prices; however, they can be extremely volatile. For example, in both [35] and [36], reactive power spot prices are shown to vary by orders of magnitude when voltage limits are encountered in the power system. Also, capital investment for reactive power equipment such as capacitor banks is much greater than operating cost, so pricing must take into account this capital investment [35],[37]. The markets of today have not yet included spot pricing of reactive power. This dissertation does not concentrate on studying reactive power markets; however, a complete model of such a market is investigated, and supply and demand models for reactive power are introduced in Chapter 3.

Spot pricing ensures the efficient operation of the transmission system by providing price differences across the system which reflect the social cost of enforcing limits. The price differences can become quite large during times of high system demand resulting in price spikes in areas with a supply deficit. Work has been done investigating the interaction of transmission limits with the spot market in [38]-[40]. This dissertation will highlight this interaction throughout.

Throughout their history, electric utilities have concentrated on developing the economics of the supply side of the industry. Efforts have been made for decades to manage and minimize the costs of supplying electricity to customers. Because of this, the extension to a free market with supplier bidding has been conceptually straightforward. Recently however, markets have begun to incorporate behavior from the demand side through consumer bidding. An example in

Chapter 2 shows that this is necessary in order to achieve realistic market behavior. Chapter 3 shows that the OPF can easily be modified to include consumer bidding to capture the behavior of all market participants [41],[42]. A detailed explanation and a complete derivation of the incorporation of consumer models into the OPF algorithm is provided.

1.5.2 Maximizing individual welfare in a spot market

With a good market model, attention turns to determining how an individual can optimize its own outcome in the market. Work done in [43]-[45] concentrated on optimal bidding strategies in markets which use the last accepted bid method for determining dispatch and price. Genetic algorithms were applied to the problem in [45].

Game theoretic analysis is introduced as a possible method for maximizing individual welfare in a spot market in [46]-[48]. The introduction in [46]-[48] is useful and interesting, but in order to manage complexity, potential bids by each market participant are limited to three possibilities: bid low, bid medium, or bid high. A more general market model is presented in [49], which allows suppliers and consumers to submit a general bid curve to the market. In such a market, finding the individual welfare maximum presents a very difficult challenge. Extending the algorithm presented in [49] to larger systems does not look promising. Chapter 4 develops a new algorithm based on Newton's method for use in maximizing an individual's welfare. This algorithm is shown to be successful on several sample systems, and the prospects of scaling the algorithm up to systems of realistic size appear very good.

With the ability to model market participant behavior more generally, the investigation of game theoretic concepts such as market equilibrium points can be investigated as was done in [50]. Market equilibrium points were found in [50] by iteratively solving the individual welfare maximization problem for each market participant until bids became constant. This technique is

used in conjunction with the new individual welfare maximization algorithm developed in this dissertation and encouraging results are presented in Section 4.4.

The new individual welfare maximization technique developed in Chapter 4 is a calculus-based optimization routine. Results in Chapter 4, however, clearly demonstrate that maximizing the welfare of an individual is a highly nonconcave function with a potentially large number of local optima. These local optima correspond to the ability of a market participant to manipulate its bidding strategy around an engineering constraint in the system. Any calculus-based method will not be able to generally solve for a global maximum when more than one local maximum exists. As a result, the more global optimization approach of genetic algorithms is considered. Chapter 5 develops a genetic algorithm (GA) for use in aiding the solution of welfare maximization.

1.5.3 Contouring visualization

The development of new electricity market structures also necessitates the exchange of huge amounts of information among the participants in the market. Power systems typically involve information on tens of thousands of buses and transmission lines. Analyzing all this information has been a daunting task for experienced engineers for the last century. With more information and new people concerned with the operation of the electricity markets, new ways to process this information more quickly and easily are needed. As a result, this dissertation also develops several new techniques for the visualization of power system data based on the use of contours. Chapter 6 illustrates these advancements.

2. A MODEL OF BIDDING IN A POOL-BASED ELECTRICITY MARKET

This chapter introduces the electric power pool structure used throughout this dissertation. The modeling of this structure through the use of the optimal power flow (OPF) is discussed followed by several examples demonstrating the use of the OPF in modeling supplier bidding.

2.1 The Electric Power Pool Market Structure

The power pool structure is defined as a set of suppliers bidding for the right to provide energy service (MWh) to the consumers in the power pool. Suppliers are then paid according to the dispatch determined by the pool operator at the spot price for energy. The dispatch and spot prices are dependent on the system demand, transmission system structure, as well as the bids received from the suppliers. In order to keep the initial examples of this chapter consistent with the history of power system analysis, the market is initially confined to supplier bidding. The examples in this chapter will demonstrate the need to include consumer bidding behavior in the market.

A complete discussion of the theory of spot markets and this implementation of supplier and consumer bidding is reserved for discussion in Chapter 3. Here the topics are only introduced to motivate their more thorough analysis later.

2.2 The Optimal Power Flow

Over the last 30 years or so the optimal power flow (OPF) algorithm has been an active area of research. The OPF is defined as a static, nonlinear optimization problem in which certain control variables are adjusted to optimize an objective function, while satisfying physical and

operational constraints. Typically the objective function has been to either minimize the cost of generation, or to minimize system losses. Available controls have usually been power system devices, such as generator real and reactive power outputs, real power transactions between operating areas, transformer tap or phase positions, and switched shunt devices.

To provide some background, the traditional OPF with the objective of minimizing the total generation costs for the entire system is described. In order to compare these equations with developments later in the dissertation, maximizing the negative of the costs is presented instead of minimizing the costs.

$$\begin{aligned} \max_{\mathbf{s},\mathbf{x}} \quad & -C(\mathbf{s}) \\ & \mathbf{h}(\mathbf{x},\mathbf{s},\mathbf{d}) = \begin{bmatrix} \hat{\mathbf{h}}(\mathbf{x}) - \hat{\mathbf{s}} + \hat{\mathbf{d}} \\ \bar{\mathbf{h}}(\mathbf{x}) \end{bmatrix} = \mathbf{0} \\ \text{s.t.} \quad & \mathbf{g}(\mathbf{x},\mathbf{s},\mathbf{d}) = \begin{bmatrix} \mathbf{s}_{\min} - \mathbf{s} \\ \mathbf{s} - \mathbf{s}_{\max} \\ \bar{\mathbf{g}}(\mathbf{x}) \end{bmatrix} \le \mathbf{0} \end{aligned} \tag{2.1}$$

To solve this nonlinear program, form the Lagrange function for it:

$$\begin{aligned} \bar{L} &= -C(\mathbf{s}) + \boldsymbol{\lambda}_h^T \mathbf{h}(\mathbf{x},\mathbf{s},\mathbf{d}) + \boldsymbol{\lambda}_g^T \mathbf{g}(\mathbf{x},\mathbf{s},\mathbf{d}) \\ &= \begin{pmatrix} -C(\mathbf{s}) + \boldsymbol{\lambda}_{\hat{h}}^T [\hat{\mathbf{h}}(\mathbf{x}) - \hat{\mathbf{s}} + \hat{\mathbf{d}}] + \boldsymbol{\lambda}_{\bar{h}}^T [\bar{\mathbf{h}}(\mathbf{x})] \\ + \boldsymbol{\lambda}_{gs\min}^T [\mathbf{s}_{\min} - \mathbf{s}] + \boldsymbol{\lambda}_{gs\max}^T [\mathbf{s} - \mathbf{s}_{\max}] \\ + \boldsymbol{\lambda}_{\bar{g}}^T \bar{\mathbf{g}}(\mathbf{x}) \end{pmatrix} \end{aligned} \tag{2.2}$$

The problem can then be determined by solving for the necessary Kuhn-Tucker conditions [51].

Stationarity Conditions

$$\frac{\partial \overline{L}}{\partial \mathbf{x}} = \boldsymbol{\lambda}_h{}^T \frac{\partial \mathbf{h(x,s,d)}}{\partial \mathbf{x}} + \boldsymbol{\lambda}_g{}^T \frac{\partial \mathbf{g(x,s,d)}}{\partial \mathbf{x}} = \mathbf{0}$$

$$\frac{\partial \overline{L}}{\partial \mathbf{s}} = -\frac{\partial C(\mathbf{s})}{\partial \mathbf{s}} - \tilde{\boldsymbol{\lambda}}_{\hat{h}s} - \boldsymbol{\lambda}_{gs\min} + \boldsymbol{\lambda}_{gs\max} = \mathbf{0}$$

$$\frac{\partial \overline{L}}{\partial \boldsymbol{\lambda}_h} = \mathbf{h(x,s,d)} = \mathbf{0} \qquad (2.3)$$

Complementary Slackness Conditions

$$\boldsymbol{\lambda}_g^T \mathbf{g(x,s,d)} = \mathbf{0}$$

$$\boldsymbol{\lambda}_g \geq \mathbf{0} \quad ; \quad \mathbf{g(x,s,d)} \leq \mathbf{0}$$

The OPF problem has been solved using a variety of different techniques. Throughout this thesis, the Newton's method approach as in [25] and [28] is used. The software implementation in Chapters 2 and 3 are integrated into PowerWorld Simulator [52],[53].

2.3 A Market Model from the OPF

The Lagrange multipliers determined from the solution of the optimal power flow provide important economic information regarding the power system. A Lagrange multiplier can be interpreted as the derivative of the objective function with respect to enforcing the respective constraint. Therefore, the Lagrange multipliers associated with enforcing the power flow equations of the OPF can be interpreted as the marginal cost of providing energy service ($/MWh) to that bus in the power system. This is what lies at the heart of spot pricing theory [8] and allows the OPF to model the power pool.

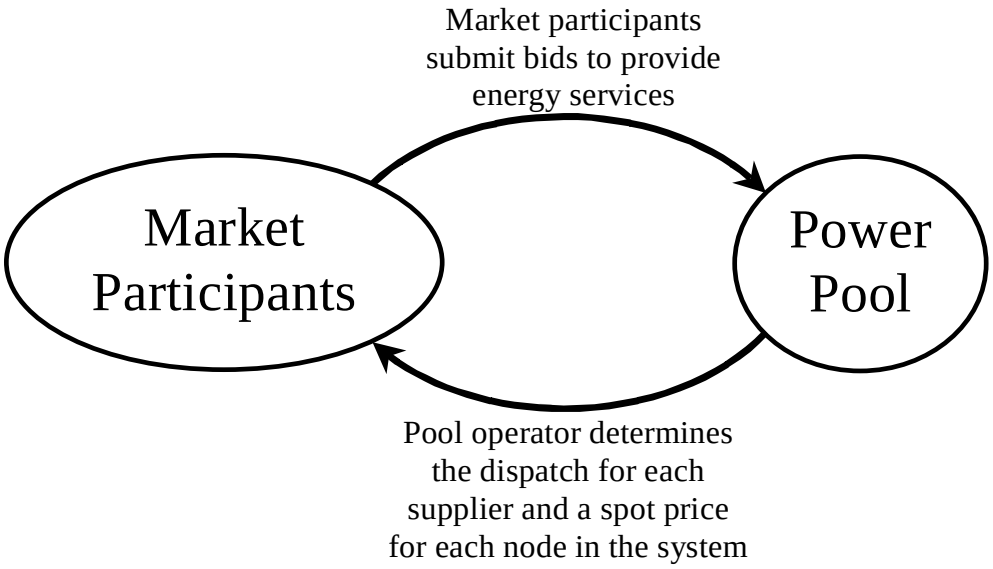

Figure 2.1 Power Pool Information Flow

As is illustrated in Figure 2.1, a power pool can be modeled in which suppliers submit bid curves that define amounts of energy (MW), along with respective prices ($/MWh). Chapter 3 will rigorously show these bids can be interpreted as being directly related to the marginal cost curves of the suppliers. The pool operator assumes the submitted bids are directly related to the *true* marginal cost curves of the suppliers and solves the OPF of minimizing the total generation costs of the generators in order to determine the generation dispatch as well as the spot prices for each node in the system. Each supplier then generates the amount of power specified by the pool operator and is paid according to its bid.

Using the ideas just put forth, an electricity market is constructed in which suppliers submit linear bid curves, such as those seen in Figure 2.2. Each supplier submits a minimum price p_{min} at which they will sell power along with a slope m_s defining the slope of the linear curve.[1] Using these bids, the pool operator (such as a power exchange or possibly an ISO) solves the OPF

[1]While only allowing single-segment linear bids may seem limiting, the analysis of the California power market done in [54] shows that over time supply bid curves appear to be two-segment linear curves. Two-segments could be added to this development in the future, but [54] shows that linear bids are reasonably accurate.

under the assumption that the participants are submitting their true marginal. The amount of dispatch received is then awarded according to the solution of this OPF.

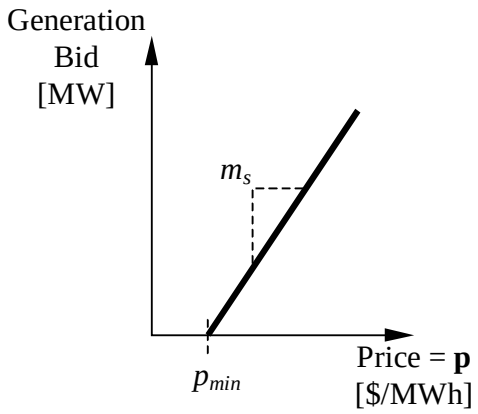

Figure 2.2 Linear Price-Dependent Supply Bids

2.4 Market Examples

When performing market analysis of the system, a market participant is interested in what its profit will be for various bidding strategies. This profit will depend not only on its bids, but also on the bids of the other participants in the market. In order to analyze the electricity market, the individual must make an estimate of the bids for each of the suppliers which it does not control. The individual then must determine the set of bids for the suppliers it controls which are an optimal response to the competitors' bids.

2.4.1 Example market model for a four-supplier lossless system

In order to demonstrate the market model, the six-bus, four-generator system shown in Figure 2.3 was used. The OPF solution for the pool when all generators bid their true marginal cost is shown in Figure 2.3. Note that this is a lossless system. As a result, the spot prices throughout the system are equal, as long as no transmission constraints are reached.

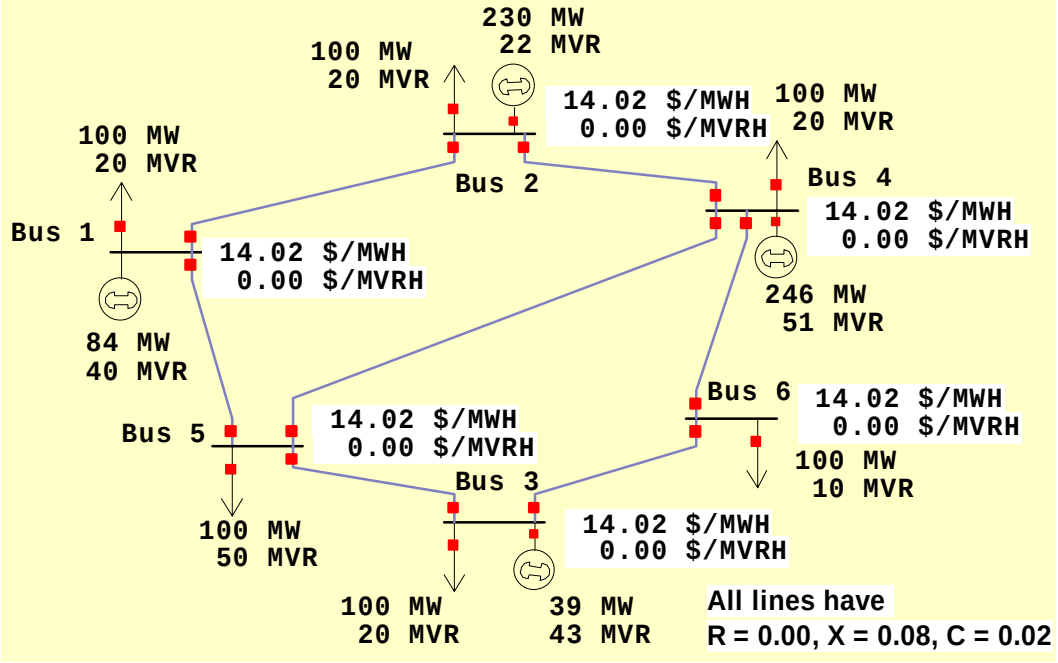

Figure 2.3 Six-Bus System with Four Generators

The cost curves for the generators shown in Figure 2.3 are

$$C(P_{G1}) = 12P_{G1} + 0.012P_{G1}^2; \quad C(P_{G2}) = 9.6P_{G2} + 0.0096P_{G2}^2$$
$$C(P_{G3}) = 13P_{G3} + 0.013P_{G3}^2; \quad C(P_{G4}) = 9.4P_{G4} + 0.0094P_{G4}^2.$$

Units on these equations are in dollars per hour.

Defining the cost curves to be of the form $C(P) = bP + cP^2$, it will be shown in Chapter 3 that the true marginal cost bid for a generator is of the form

$$s(p) = \frac{1}{2c}(p - b) = m_s(p - p_{\min}) \text{ [MW]} \tag{2.4}$$

where p is the spot price the supplier receives in the market and s is the generator dispatch. This yields the following true marginal cost bids for each generator:

$$s_1(p) = \frac{1}{2(0.0120)}(p - 12) = 41.67(p - 12); \qquad s_2(p) = \frac{1}{2(0.0096)}(p - 9.6) = 52.08(p - 9.6)$$

$$s_3(p) = \frac{1}{2(0.0130)}(p - 13) = 38.46(p - 13); \qquad s_4(p) = \frac{1}{2(0.0094)}(p - 9.4) = 53.19(p - 9.4)$$

With these bids as a base, to test the market model, bids are chosen as some percentage over or under *true* marginal cost. In order to bid *k* times higher than the true marginal cost, the supplier must submit a new bid ($\overline{m}_s$, $\overline{p}_{\min}$) which satisfies $\overline{m}_s = \frac{m_s}{k}$ and $\overline{p}_{\min} = k * p_{\min}$. Figure 2.4 shows a bid that is *k* times higher than the true marginal cost bid.

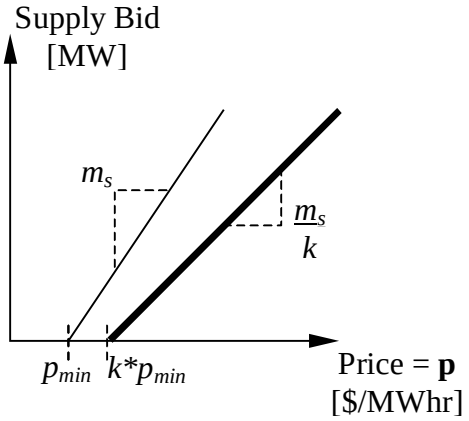

Figure 2.4 Bidding *k* Times Higher Than Marginal Cost

To the central operator who solves the OPF for maximization of social welfare, this bid is treated as though the cost of the supplier is as shown in Equation (2.5).

$$C(P) = k(bP + cP^2) \tag{2.5}$$

Initially, the optimal bid for each supplier is found under the assumption that other suppliers bid their true marginal cost. Only the individual supplier is allowed to change its bid. In a perfectly competitive market, the best response for each supplier is to bid its marginal cost. This is a well-known economic principle which can be proven very simply. Define supplier profit as revenue minus costs, written $\Pi = sp - C(s)$. To determine the maximum of the profit function, set its derivative with respect to *s* equal to zero: $\frac{\partial \Pi}{\partial s} = p + \frac{\partial p}{\partial s} s - \frac{\partial C(s)}{\partial s} = 0$. The supplier can not affect the price of the market because it is perfectly competitive, thus $\frac{\partial p}{\partial s} = 0$. Therefore, the

necessary condition for maximizing profit is $p = \frac{\partial C(s)}{\partial s}$, meaning the supplier should submit a bid that corresponds to its marginal cost. As a result, it might be expected that the optimal bid for each of the suppliers in our system would be to continue bidding marginal cost. This is tested and results are shown in Table 2.1.

Table 2.1 Profit for each Supplier in the Four-Supplier Market (Assuming Others Bid Marginal)

Bid % over Marginal Cost	Bus 1 Profit	Bus 2 Profit	Bus 3 Profit	Bus 4 Profit
0% (k = 1.00)	85.31	509.57	20.15	568.53
1% (k = 1.01)	87.55	518.11	20.92	577.89
2% (k = 1.02)	89.03	525.64	**20.96**	586.15
3% (k = 1.03)	89.75	532.16	20.39	593.44
4% (k = 1.04)	**89.76**	537.73	19.15	599.75
5% (k = 1.05)	89.07	542.38	17.28	605.11
6% (k = 1.06)	87.75	546.17	14.83	609.57
7% (k = 1.07)	85.79	549.10	11.82	613.18
8% (k = 1.08)	83.24	551.23	8.28	615.93
9% (k = 1.09)	80.12	552.58	4.22	617.88
10% (k = 1.10)	76.46	**553.18**	0.00	619.07
11% (k = 1.11)	72.15	553.08	0.00	**619.53**
12% (k = 1.12)	67.58	552.25	0.00	619.25
13% (k = 1.13)	62.44	550.80	0.00	618.31
14% (k = 1.14)	56.82	548.69	0.00	616.71
15% (k = 1.15)	50.78	545.98	0.00	614.48
16% (k = 1.16)	44.31	542.68	0.00	611.62
17% (k = 1.17)	37.45	538.81	0.00	608.21
18% (k = 1.18)	30.22	534.41	0.00	604.24
19% (k = 1.19)	22.61	529.48	0.00	599.71

Note that each column of Table 2.1 represents a variation only in the bid of the respective supplier. For instance, the bus 2 profit column at the 6% over marginal cost row means that the supplier at bus 2 is bidding 6% over marginal cost while the suppliers at buses 1, 3, and 4 are bidding exactly at marginal cost. The values shown are the profit for the respective suppliers in dollars per hour. Profit is the difference between revenue and cost. Revenue is calculated by

multiplying the MW output of the supplier by the spot price. Cost is calculated by evaluating the true cost function at the MW output level.

From the values in Table 2.1, the best responses for each supplier, assuming the others bid true marginal cost, are

Bus 1: Bid 4% over true marginal cost Bus 2: Bid 10% over true marginal cost
Bus 3: Bid 2% over true marginal cost Bus 4: Bid 11% over true marginal cost

Economic theory said that the best response would be bidding true marginal cost, but Table 2.1 does not show this. What do these results mean? They mean that the individual suppliers in this market do have some market power, violating an underlying assumption of competitive markets. Each supplier's bid is affecting the market price because there are so few suppliers available. The results in Table 2.2 show this effect for the supplier at bus 4. As it raises its bid, the pool price increases.

Table 2.2 Effect of Supplier Bid Increase on the Pool Price

Bid % over Marginal Cost	Pool Price	Bus 4 Profit
0% (k = 1.00)	14.02	568.53
1% (k = 1.01)	14.06	577.89
2% (k = 1.02)	14.10	586.15
3% (k = 1.03)	14.14	593.44
4% (k = 1.04)	14.18	599.75
5% (k = 1.05)	14.22	605.11
6% (k = 1.06)	14.25	609.57
7% (k = 1.07)	14.29	613.18
8% (k = 1.08)	14.33	615.93
9% (k = 1.09)	14.37	617.88
10% (k = 1.10)	14.40	619.07
11% (k = 1.11)	14.43	**619.53**
12% (k = 1.12)	14.47	619.25
13% (k = 1.13)	14.50	618.31
14% (k = 1.14)	14.54	616.71
15% (k = 1.15)	14.57	614.48
16% (k = 1.16)	14.60	611.62
17% (k = 1.17)	14.63	608.21
18% (k = 1.18)	14.66	604.24

This ability to directly affect the pool price is what gives the suppliers in the market some measure of market power and encourages them to bid higher than true marginal cost.

2.4.2 Demonstration of market power in a 54-supplier market

To study this problem on a slightly larger system, the IEEE 118-bus, 54-generator system is augmented to include generation cost curves. A market is then simulated which includes all 54 generators in the case. This system, shown in Figure 2.5, has a total load of 3668.0 MW.

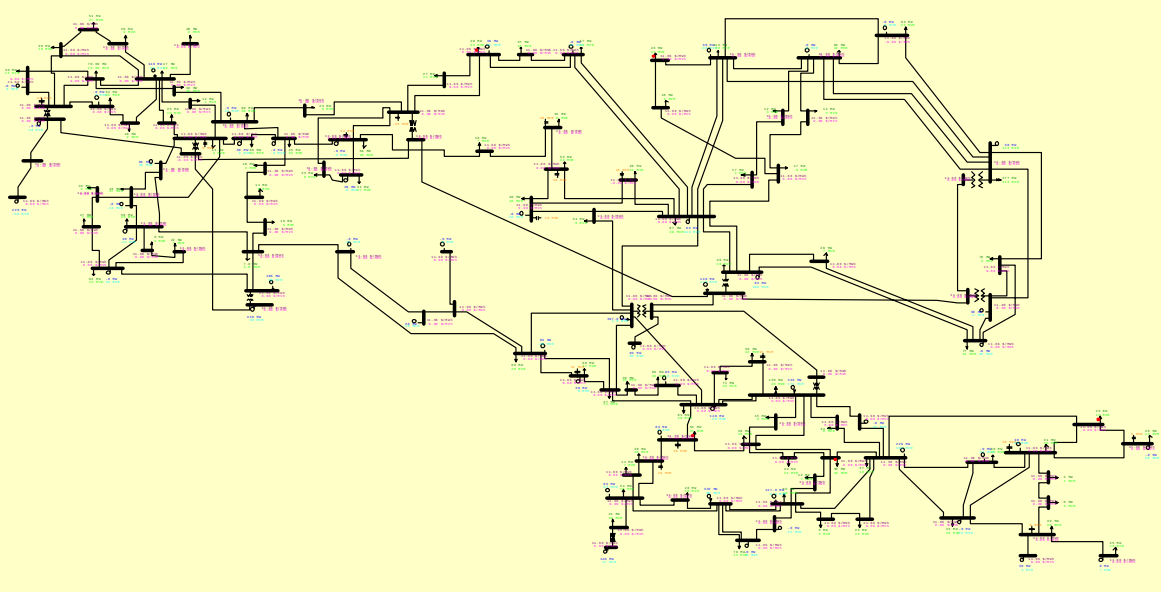

Figure 2.5 IEEE 118-Bus Case

Here, the large number of generators would likely inhibit the ability of any one generator to exercise market power. This is tested in the same manner done for the four-supplier system of Section 2.4.1. All generators have cost curves defined by $C(P) = bP + cP^2$ and true marginal cost bids defined by $s(p) = 1/c*(p-b) = m_s(p - p_{\min})$. Several representative generators, whose constant values are show in Table 2.3, are chosen for study.

Table 2.3 True Cost Curves and True Marginal Bid Curves

Supplier Bus	b	c	p_{min} (b)	m_s (0.5/c)	MW output if all Marginal Bids
25	8.5	0.0085	8.5	58.82	185.92
32	11.0	0.0110	11.0	45.45	30.03
49	10.0	0.0100	10.0	50.00	83.03
69	6.5	0.0065	6.5	76.92	396.98
77	9.0	0.0090	9.0	55.56	147.81
89	7.0	0.0070	7.0	71.43	332.90

The last column in Table 2.3 shows the amount of power dispatched by the OPF algorithm when all 54 generators submit their true marginal cost bids. Note that the generator at bus 69 has the highest MW output, and thus will possibly have the greatest ability to profitably bid above marginal cost.

Tests are run as done in Section 2.4.1 in order to determine each supplier's best response under the assumption that all the other suppliers are bidding at true marginal cost. The results of these simulations are shown in Table 2.4.

Table 2.4 Profit for Suppliers in the 118-Bus, 54-Supplier Market (Assuming Others Bid Marginal)

Base MW	397.0	332.9	185.9	147.8	83.0	30.0
Bid % over Marginal Cost	Bus 69 Profit	Bus 89 Profit	Bus 25 Profit	Bus 77 Profit	Bus 49 Profit	Bus 32 Profit
-2% (k = 0.98)	1017.7	770.3	193.9	290.6	66.93	8.44
-1% (k = 0.99)	1021.6	773.6	195.7	292.6	68.30	9.51
0% (k = 1.00)	1024.3	775.8	196.6	293.8	**68.94**	**9.92**
1% (k = 1.01)	1026.0	777.0	**196.9**	**294.2**	68.92	9.71
2% (k = 1.02)	**1026.6**	**777.2**	196.3	293.8	68.22	8.92
3% (k = 1.03)	1026.2	776.6	195.1	292.7	66.92	7.58
4% (k = 1.04)	1024.9	775.1	193.3	290.9	65.05	5.72
5% (k = 1.05)	1022.8	772.8	190.8	288.4	62.63	3.36
6% (k = 1.06)	1019.8	769.7	187.8	285.4	59.70	0.55
7% (k = 1.07)	1016.1	766.0	184.3	281.8	56.27	0.00
8% (k = 1.08)	1011.6	761.5	180.1	277.5	52.41	0.00
9% (k = 1.09)	1006.4	756.5	175.6	272.9	48.11	0.00
10% (k = 1.10)	1000.6	750.8	170.6	267.7	43.40	0.00

From Table 2.4, it is apparent that none of the suppliers have an incentive to bid substantially above true marginal cost. The generators with the largest market share have at most a small incentive, at only 2% over marginal cost. This is substantially below the 10% and 11% over, as in the six-bus, four-supplier market studied previously. This shows that larger numbers of competitors reduce market power. While this is an obvious result, it does show that this market model is valuable in modeling the behavior of the market.

Thus far, each supplier in our market has been treated as a separate individual. In the market, however, an individual company will control the bidding of several generators. Now consider the case in which the individual controls more than one generator. When all bidders submit their true marginal cost curves, the suppliers at bus 69 and 89 serve 397.0 MW and 332.9 MW, respectively. This is 10.8% and 9.1% of the total 3668.0-MW demand. Table 2.4 shows that both maximize their profits by bidding 2% over their true marginal cost. However, if they merge to form a single individual company, an even greater market advantage may be achieved. Simulations are run to determine if this is true and the results are shown in Table 2.5.

From Table 2.5 the individual's best response is for the bus 69 supplier and the bus 89 supplier to bid at 4% over true marginal costs. Comparing this scenario to the analysis when the two suppliers do not cooperate, it is seen that the bus 69 supplier's profit increases from 1026.6 to 1032.7, and the bus 89 supplier's profit increases from 777.2 to 782.1. This is an increase of 0.6% for each supplier. This analysis does indeed demonstrate that the combination of bus 69 and bus 89 into one individual increases the market power for each of them. Note that in this scenario, the combined individual still only controls about 20% of the generation.

Table 2.5 Profits for Suppliers at Buses 69 and 89 when One Individual Controls Their Bids

Bid % over Marginal Cost	Bus 89 **0%** over	Bus 89 **1%** over	Bus 89 **2%** over	Bus 89 **3%** over	Bus 89 **4%** over	Bus 89 **5%** over	Bus 89 **6%** over
Bus 69 **0%** over	1024.3 +775.8 1800.1	1026.3 +777.0 1803.3	1028.3 **+777.2** 1805.5	1030.2 +776.6 1806.8	1032.1 +775.1 1807.2	1033.9 +772.8 1806.7	1035.8 +769.7 1805.5
Bus 69 **1%** over	1026.0 +777.6 1803.5	1027.9 +778.8 1806.7	1029.9 +779.0 1809.0	1031.8 +778.4 1810.2	1033.7 +776.9 1810.6	1035.7 +774.7 1810.3	1037.4 +771.5 1809.0
Bus 69 **2%** over	**1026.6** +779.4 1805.9	1028.6 +780.6 1809.1	1030.5 +780.8 1811.3	1032.5 +780.2 1812.6	1034.4 +778.7 1813.0	1036.2 +776.4 1812.6	1038.0 +773.3 1811.4
Bus 69 **3%** over	1026.2 +781.1 1807.3	1028.2 +782.3 1810.5	1030.2 +782.5 1812.7	1032.1 +781.9 1814.1	1034.0 +780.4 1814.4	1035.9 +778.1 1814.0	1037.7 +775.1 1812.7
Bus 69 **4%** over	1024.9 +782.8 1807.7	1026.9 +784.0 1810.9	1028.9 +784.3 1813.1	1030.9 +783.7 1814.6	**1032.7** **+782.1** **1814.8**	1034.6 +779.8 1814.4	1036.4 +776.8 1813.2
Bus 69 **5%** over	1022.8 +784.5 1807.2	1024.8 +785.7 1810.5	1026.8 +785.9 1812.7	1028.7 +785.3 1814.0	1030.6 +783.8 1814.4	1032.4 +781.5 1813.9	1034.3 +778.5 1812.7
Bus 69 **6%** over	1019.8 +786.1 1805.9	1021.8 +787.3 1809.1	1023.8 +787.6 1811.4	1025.7 +786.9 1812.7	1027.6 +785.5 1813.1	1029.5 +783.2 1812.6	1031.3 +780.1 1811.4

Note: Each grid contains three numbers. The first number is the profit for bus 69, the second is the profit for bus 89, and the third is sum of the two profits.

2.4.3 Effect of transmission constraints on the market model

Thus far enforcement of transmission line constraints has not been considered in the market examples. Including these may result in other types of market interactions which thus far have not been seen. In order to investigate, the previous six-bus, four-supplier system was used with the thermal limit of each line defined to be 100 MVA. This is shown in Figure 2.6.

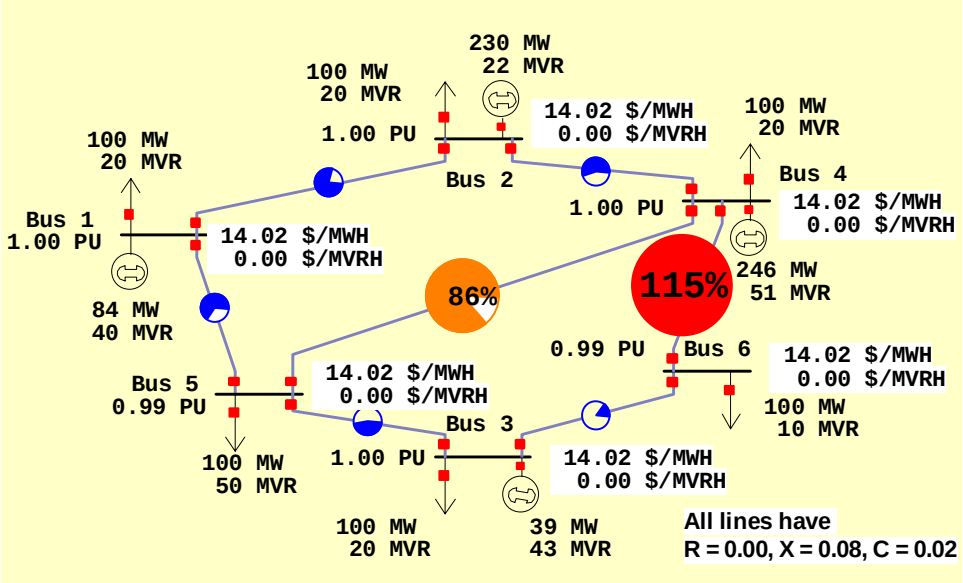

Figure 2.6 Six-Bus System with 100-MVA Limit on Each Line

Figure 2.6 is the same as Figure 2.3, except pie charts have been added to each line in Figure 2.6. These pie charts represent the percent line loading for each line. Figure 2.6 shows some lines are heavily loaded and that the line from bus 4 to bus 6 is overloaded at 115% of its limit. It is apparent that enforcing these limits will change the dispatch of the pool and thus the bidding strategies of all participants. As a reference point, the solution to the OPF enforcing line constraints with all suppliers bidding their true marginal cost is shown in Figure 2.7.

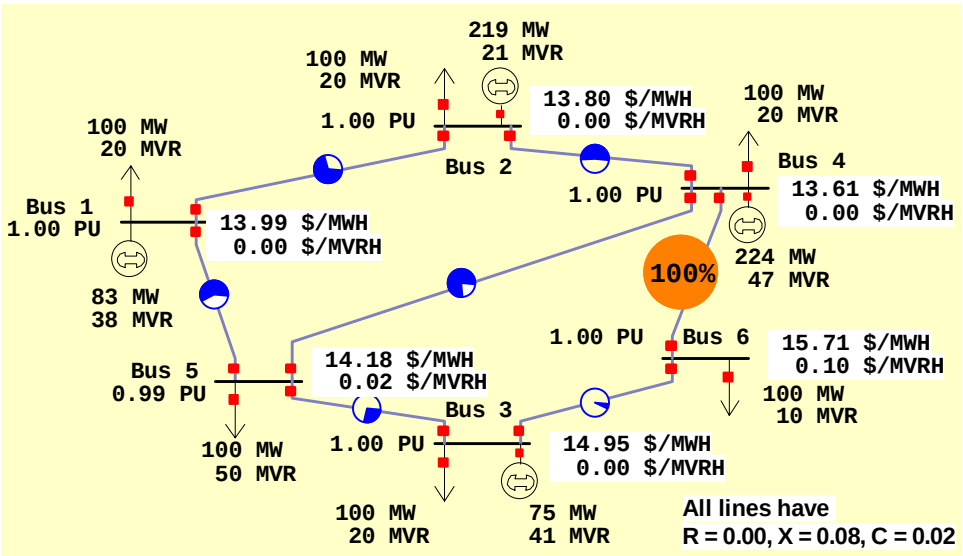

Figure 2.7 Six-Bus OPF Solution with Line Constraints Enforced

Enforcement of the transmission line constraint has resulted in a redispatch of the generation in the system in order to remove the line constraint. Also the presence of congestion has altered the bus marginal costs. Note that the bus marginal costs are also called locational marginal prices or LMPs [9]. Comparing Figure 2.6 and Figure 2.7 shows that the supplier at bus 3 has been dispatched at a greater amount of power while the suppliers at buses 2 and 4 have been backed off. Because the dispatch and spot prices have changed, the profits received by the bidders have also changed. These results are summarized in Table 2.6.

Table 2.6 Changes in Dispatch and Profits Due to Line Constraints

	Not Enforcing Limits All True Marginal Bids		Enforcing Limits All True Marginal Bids	
	MW Dispatch	Profit	MW Dispatch	Profit
Bus 1	84	85.31	83	82.33
Bus 2	230	509.57	219	458.53
Bus 3	39	20.15	75	73.10
Bus 4	246	568.53	224	470.3
		Sum = 1183.56		Sum = 1084.26

The best response of each supplier to a bid of true marginal cost by all the other suppliers is determined. Each supplier varies its bid from the true marginal bid up to 80% higher than the true marginal bid. The results for each supplier are summarized in Figure 2.8.

There are several interesting phenomena seen in Figure 2.8. The first and most striking is that the profit for the supplier at bus 3 increases without bound as its bid price is raised. This is occurring because the transmission line from bus 4 to 6 is very heavily loaded in this system. As a result, the supplier at bus 3 is required to serve some of the demand at bus 6 in order to reduce the line loading. In effect, the supplier at bus 3 has complete market power over some of the demand at bus 6 and can therefore charge as high a price as desired since some power will always be dispatched from the bus 3 supply.

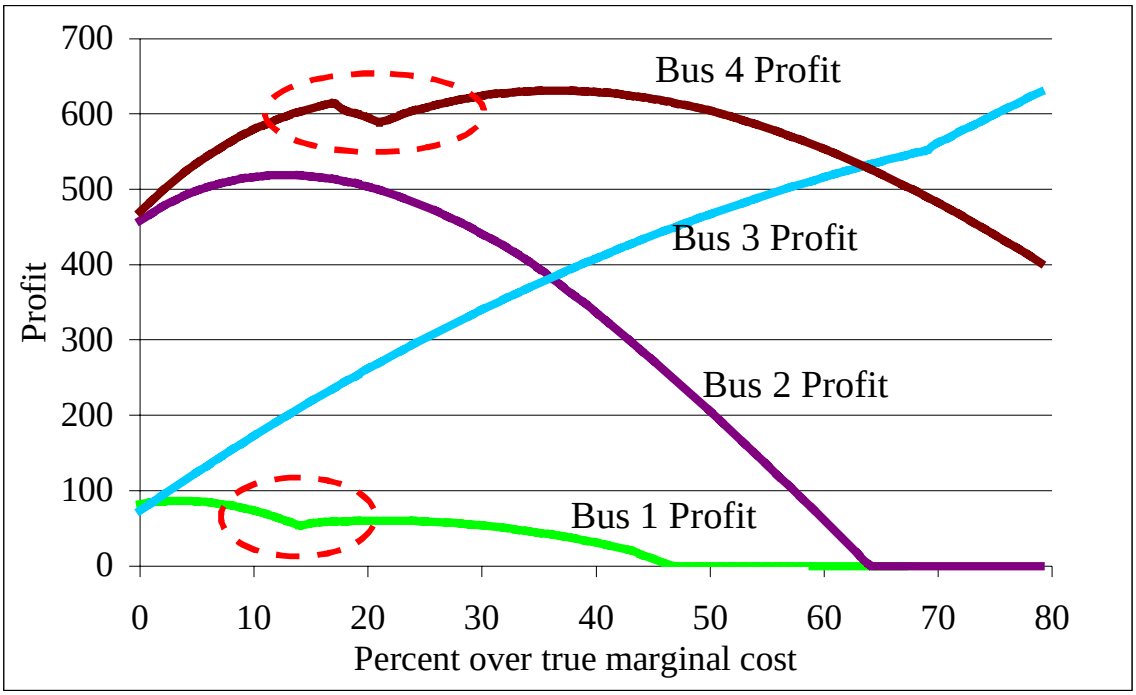

Figure 2.8 Profits versus Percent Over True Marginal Bid

Note, however, that the inclusion of consumer side bidding in the market would quickly remove this phenomenon. With consumer bidding, presumably the demand would decrease as the bids by the suppliers continued to increase. This localized market power is not unseen in real markets. The United States Federal Energy Regulatory Commission (FERC) dismissed a proposed merger in 1995 partly due to their concern

> …about the possibility that the combination of such transmission constraints and strategically located generation facilities owned by the wholesale seller may result in market power in more localized markets. [55]

Another interesting characteristic of the simulation appears in the results for bus 1 and 4. Both graphs show sudden changes in the direction of the profit curve in the areas circled in Figure 2.8. This is caused by transmission line limits. To examine further, the percent loading for the line from bus 2 to 4 and the line from bus 4 to 6 are determined at various bid levels of the supplier at bus 4. These values along with the revenue, cost, and profit for the supplier at bus 4 are shown in Table 2.7. A plot of these values is seen in Figure 2.9.

Table 2.7 Profits for Bus 4 with Line Limits Enforced

Bid % over Marginal Cost	Line Loading		Bus 4 Price	Bus 4 MW	Revenue	Cost	Profit
	Bus 2-4	Bus 4-6					
12%	80%	100%	14.36	182	2613.5	2022.2	591.4
13%	83%	100%	14.42	179	2581.2	1983.8	597.4
14%	85%	100%	14.48	176	2548.5	1945.6	602.9
15%	88%	100%	14.54	173	2515.4	1907.5	607.9
16%	90%	100%	14.60	169	2467.4	1857.1	610.3
17%	92%	100%	14.66	166	2433.6	1819.4	614.1
18%	95%	100%	14.71	163	2397.7	1781.9	615.8
19%	96%	97%	14.70	157	2307.9	1707.5	600.4
20%	98%	96%	14.73	153	2253.7	1658.2	595.4
21%	99.5%	96%	14.76	149	2199.2	1609.3	590.0
22%	100%	94%	14.83	147	2180.0	1584.9	595.1
23%	100%	93%	14.90	145	2160.5	1560.6	599.9
24%	100%	92%	14.98	142	2127.2	1524.3	602.8
25%	100%	91%	15.05	140	2107.0	1500.2	606.8
26%	100%	90%	15.12	138	2086.6	1476.2	610.3

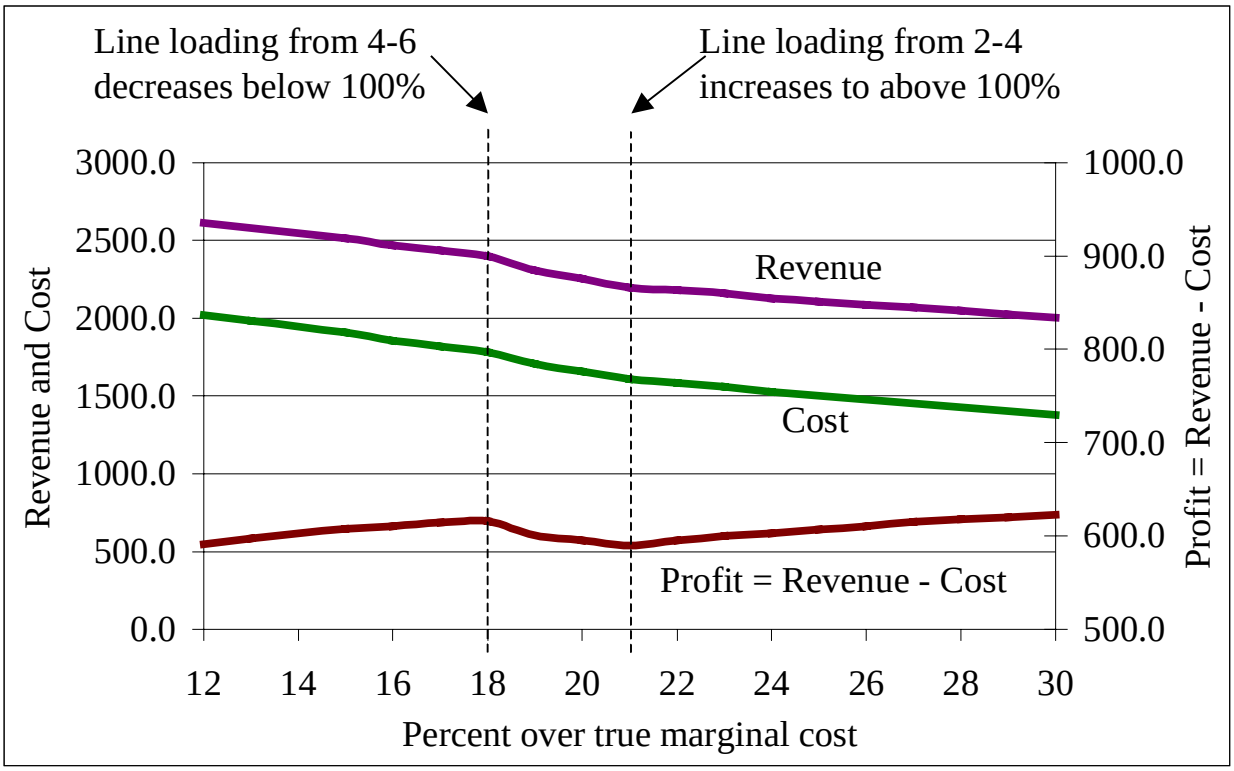

Figure 2.9 Revenues, Costs, and Profit versus Bid While Enforcing Line Thermal Limits

Figure 2.9 shows that for bids from 0% to 18% over true marginal cost, bus 4 enjoys an increasing amount of profit. However, moving from 18% to 19% causes a drop in profit. This is because the transmission line from bus 4 to bus 6, which had been overloaded, has now dropped down below the 100% loading level. This resulted in a reduction in the spot price received by the supplier and thus a reduction in profit. As the bid continues to increase, however, when it moves from 21% to 22% over true marginal cost the profit curve suddenly begins to increase again. This is because the line from bus 2 to bus 4 is now overloaded, resulting in a steeper increase in the spot prices.

Analysis done for the profit curve of bus 1 showed that a similar cause was at the heart of the kink in its profit curve.

3. INCORPORATION OF CONSUMER MODELS INTO AN OPF [42]

The OPF was introduced in Chapter 2 without discussing the implementation of consumer load as a control variable. Figure 2.8 clearly demonstrates the need for including consumer load in the OPF. Not including the consumer can result in unbounded profit for generators which have a captive demand.

In the past, consumer load has usually not been an explicit control device, except in the extreme case of "load shedding" in which the load is involuntarily disconnected. For the most part, the absence of load as a control in the OPF has been due to the inability of the operating utility to directly or indirectly control the load. The present-day flat and time-of-use rate structures have provided no opportunity for price-based control of most loads, with interruptible contracts and direct load management being two possible exceptions.

However, over the last 10-15 years there has been a growing movement towards providing consumers as well as suppliers with more price feedback through an electricity spot market. Much of the theory for such a market is described in [8], with the definition of a spot price given as one in which consumers are charged the marginal cost of providing electricity to their point of service (that is, their node or bus). Many papers have addressed the issues of power system spot markets [33]-[40]. A key advantage of nodal spot prices is that they provide a more economic approach to pricing with a result of improved transmission efficiency. In such a market, consumer load and supplier generation is assumed to vary in response to changing prices according to its demand curve. That is, generation and load become price-dependent and hence potential OPF controls.

The inclusion of supplier generation as an OPF control has been done since the inception of the OPF. This chapter incorporates a consumer model as a price-dependent load in the OPF. While the inclusion of such price-dependent loads had been done [33],[41], this author presented an original formal argument for their inclusion in [42]. This formal argument is presented again here. The ease of adding this price-dependent consumer model to a traditional OPF is also demonstrated. By *traditional OPF*, it is meant an OPF that minimizes the total supplier costs.

3.1 Maximizing Social Welfare Using the OPF

The traditional OPF only considers the supplier costs in the market. In order to include the consumer in the market model, the concept of *consumer benefit* must be introduced. Consumer benefit represents the value the consumer gains from using a product. Mathematically, consumer benefit is written as a function of demand $B(d)$. It is analogous to cost for the supplier, but with a negative sign. Once consumer benefit is defined, *social welfare* is defined as the total consumer benefits minus the total supplier costs: $B(\mathbf{d}) - C(\mathbf{s})$.

In order to maximize social welfare within a power system, the objective function for the traditional OPF described in Section 2.2 need only be modified to include a consumer benefit function $B(\mathbf{d})$. This function models the benefit that the consumer gains by using the real power and reactive power that they receive.

$$\begin{aligned} \max_{\mathbf{x,s,d}} \quad & B(\mathbf{d}) - C(\mathbf{s}) \\ & \mathbf{h(x,s,d)} = \begin{bmatrix} \hat{\mathbf{h}}(\mathbf{x}) - \hat{\mathbf{s}} + \hat{\mathbf{d}} \\ \underline{\mathbf{h}}(\mathbf{x}) \end{bmatrix} = \mathbf{0} \\ \text{s.t.} \quad & \mathbf{g(x,s,d)} = \begin{bmatrix} \mathbf{s}_{\min} - \mathbf{s} \\ \mathbf{s} - \mathbf{s}_{\max} \\ \mathbf{d}_{\min} - \mathbf{d} \\ \mathbf{d} - \mathbf{d}_{\max} \\ \overline{\mathbf{g}}(\mathbf{x}) \end{bmatrix} \le \mathbf{0} \end{aligned} \tag{3.1}$$

To solve this, form a Lagrange function as follows:

$$
\begin{aligned}
L &= B(\mathbf{d}) - C(\mathbf{s}) + \boldsymbol{\lambda}_h^T \mathbf{h}(\mathbf{x},\mathbf{s},\mathbf{d}) + \boldsymbol{\lambda}_g^T \mathbf{g}(\mathbf{x},\mathbf{s},\mathbf{d}) \\
&= \begin{pmatrix} B(\mathbf{d}) - C(\mathbf{s}) + \boldsymbol{\lambda}_{\hat{h}}^T [\hat{\mathbf{h}}(\mathbf{x}) - \hat{\mathbf{s}} + \hat{\mathbf{d}}] + \boldsymbol{\lambda}_{\bar{h}}^T [\bar{\mathbf{h}}(\mathbf{x})] \\ + \boldsymbol{\lambda}_{gs\min}^T [\mathbf{s}_{\min} - \mathbf{s}] + \boldsymbol{\lambda}_{gs\max}^T [\mathbf{s} - \mathbf{s}_{\max}] \\ + \boldsymbol{\lambda}_{gd\min}^T [\mathbf{d}_{\min} - \mathbf{d}] + \boldsymbol{\lambda}_{gd\max}^T [\mathbf{d} - \mathbf{d}_{\max}] + \boldsymbol{\lambda}_{\bar{g}}^T \bar{\mathbf{g}}(\mathbf{x}) \end{pmatrix}
\end{aligned}
\tag{3.2}
$$

The maximization problem can then be determined by solving for the necessary Kuhn-Tucker conditions:

$$
\begin{aligned}
&\frac{\partial L}{\partial \mathbf{x}} = \boldsymbol{\lambda}_h{}^T \frac{\partial \mathbf{h}(\mathbf{x},\mathbf{s},\mathbf{d})}{\partial \mathbf{x}} + \boldsymbol{\lambda}_g{}^T \frac{\partial \mathbf{g}(\mathbf{x},\mathbf{s},\mathbf{d})}{\partial \mathbf{x}} = \mathbf{0} \\
&\frac{\partial L}{\partial \mathbf{s}} = -\frac{\partial C(\mathbf{s})}{\partial \mathbf{s}} - \tilde{\boldsymbol{\lambda}}_{\hat{h}s} - \boldsymbol{\lambda}_{gs\min} + \boldsymbol{\lambda}_{gs\max} = \mathbf{0} \\
&\frac{\partial L}{\partial \mathbf{d}} = \frac{\partial B(\mathbf{d})}{\partial \mathbf{d}} + \tilde{\boldsymbol{\lambda}}_{\hat{h}d} - \boldsymbol{\lambda}_{gd\min} + \boldsymbol{\lambda}_{gd\max} = \mathbf{0} \\
&\frac{\partial L}{\partial \boldsymbol{\lambda}_h} = \mathbf{h}(\mathbf{x},\mathbf{s},\mathbf{d}) = \mathbf{0} \\
&\boldsymbol{\lambda}_g^T \mathbf{g}(\mathbf{x},\mathbf{s},\mathbf{d}) = \mathbf{0} \\
&\mathbf{g}(\mathbf{x},\mathbf{s},\mathbf{d}) \le \mathbf{0} \quad ; \quad \boldsymbol{\lambda}_g \ge \mathbf{0}
\end{aligned}
\tag{3.3}
$$

The solution to Equations (3.3) would then constitute a maximization of the social welfare for a power market.

3.2 Modeling Consumers as Price-Dependent Loads

Because many people already have an optimal power flow algorithm with the objective of minimizing generation costs in the system, it is of interest to incorporate the maximization of social welfare into this OPF in the simplest manner possible. To do this, consider the difference between the necessary conditions described in Equation (2.3) with those of Equation (3.3). The only difference is the condition

$$
\frac{\partial B(\mathbf{d})}{\partial \mathbf{d}} = -\tilde{\boldsymbol{\lambda}}_{\hat{h}d} + \boldsymbol{\lambda}_{gd\min} - \boldsymbol{\lambda}_{gd\max} \tag{3.4}
$$

Instead of enforcing this condition, consider defining the function $\mathbf{D}(\mathbf{p}_d)$ as the functional inverse of $\frac{\partial B(\mathbf{d})}{\partial \mathbf{d}}$, meaning that for all $\mathbf{p}_d$ and $\mathbf{d}$ the following hold:

$$\frac{\partial B(\mathbf{D}(\mathbf{p}_d))}{\partial \mathbf{d}} = \mathbf{p}_d \quad \text{and} \quad \mathbf{D}\left(\frac{\partial B(\mathbf{d})}{\partial \mathbf{d}}\right) = \mathbf{d} \tag{3.5}$$

After studying Equation (3.5), one realizes that enforcing the condition of Equation (3.4) is equivalent to enforcing the condition

$$\mathbf{d} = \left(\frac{\partial B(\mathbf{d})}{\partial \mathbf{d}}\right)^{-1} = \mathbf{D}(-\tilde{\boldsymbol{\lambda}}_{\hat{h}d} + \boldsymbol{\lambda}_{gd\,\min} - \boldsymbol{\lambda}_{gd\,\max}) \tag{3.6}$$

Equation (3.6) is what is called the price-dependent load model.

Therefore, in order to solve the maximization of social welfare, simply take the traditional OPF, which enforces the conditions of minimizing costs of Equation (2.3), and add to it the condition of Equation (3.6). In order to further simplify this, substitute Equation (3.6) back into Equations (2.3) anywhere **d** appears. This results in the necessary conditions

$$\begin{aligned}
\left(\begin{array}{l}
\boldsymbol{\lambda}_h{}^T \dfrac{\partial \mathbf{h}(\mathbf{x},\mathbf{s},\mathbf{D}(-\tilde{\boldsymbol{\lambda}}_{\hat{h}d} + \boldsymbol{\lambda}_{gd\,\min} - \boldsymbol{\lambda}_{gd\,\max}))}{\partial \mathbf{x}} \\
+ \boldsymbol{\lambda}_g{}^T \dfrac{\partial \mathbf{g}(\mathbf{x},\mathbf{s},\mathbf{D}(-\tilde{\boldsymbol{\lambda}}_{\hat{h}d} + \boldsymbol{\lambda}_{gd\,\min} - \boldsymbol{\lambda}_{gd\,\max}))}{\partial \mathbf{x}}
\end{array}\right) &= \mathbf{0} \\
-\frac{\partial C(\mathbf{s})}{\partial \mathbf{s}} - \tilde{\boldsymbol{\lambda}}_{\hat{h}s} - \boldsymbol{\lambda}_{gs\,\min} + \boldsymbol{\lambda}_{gs\,\max} &= \mathbf{0} \\
\mathbf{h}(\mathbf{x},\mathbf{s},\mathbf{D}(-\tilde{\boldsymbol{\lambda}}_{\hat{h}d} + \boldsymbol{\lambda}_{gd\,\min} - \boldsymbol{\lambda}_{gd\,\max})) &= \mathbf{0} \\
\boldsymbol{\lambda}_g{}^T \mathbf{g}(\mathbf{x},\mathbf{s},\mathbf{D}(-\tilde{\boldsymbol{\lambda}}_{\hat{h}d} + \boldsymbol{\lambda}_{gd\,\min} - \boldsymbol{\lambda}_{gd\,\max})) &= \mathbf{0} \\
\mathbf{g}(\mathbf{x},\mathbf{s},\mathbf{D}(-\tilde{\boldsymbol{\lambda}}_{\hat{h}d} + \boldsymbol{\lambda}_{gd\,\min} - \boldsymbol{\lambda}_{gd\,\max})) &\le \mathbf{0} \\
\boldsymbol{\lambda}_g &\ge \mathbf{0}
\end{aligned} \tag{3.7}$$

3.3 Modeling Suppliers as Price-Dependent Generators

Consider the necessary equations for our alternate approach shown in Equation (3.7). Consider the function S(**p**) which is the functional inverse of $\frac{\partial C(\mathbf{s})}{\partial \mathbf{s}}$. In other words, $\mathbf{p}_s - \frac{\partial C}{\partial \mathbf{s}}(\mathbf{S}(\mathbf{p}_s)) = 0 \quad \forall \mathbf{p}_s$. Then enforcing the condition $-\frac{\partial C(\mathbf{s})}{\partial \mathbf{s}} - \tilde{\boldsymbol{\lambda}}_{\hat{h}s} - \boldsymbol{\lambda}_{gs\min} + \boldsymbol{\lambda}_{gs\max} = \mathbf{0}$ is the same as enforcing the condition $\mathbf{s} = \mathbf{S}(\tilde{\boldsymbol{\lambda}}_{\hat{h}s} + \boldsymbol{\lambda}_{gs\min} - \boldsymbol{\lambda}_{gs\max})$.

Therefore, the necessary conditions may be rewritten as

$$\begin{aligned}
&\begin{pmatrix} \boldsymbol{\lambda}_h{}^T \dfrac{\partial \mathbf{h}(\mathbf{x},\mathbf{s},\mathbf{D}(-\tilde{\boldsymbol{\lambda}}_{\hat{h}d} + \boldsymbol{\lambda}_{gd\min} - \boldsymbol{\lambda}_{gd\max}))}{\partial \mathbf{x}} \\ + \boldsymbol{\lambda}_g{}^T \dfrac{\partial \mathbf{g}(\mathbf{x},\mathbf{s},\mathbf{D}(-\tilde{\boldsymbol{\lambda}}_{\hat{h}d} + \boldsymbol{\lambda}_{gd\min} - \boldsymbol{\lambda}_{gd\max}))}{\partial \mathbf{x}} \end{pmatrix} = \mathbf{0} \\
&\mathbf{s} - \mathbf{S}(\tilde{\boldsymbol{\lambda}}_{\hat{h}s} + \boldsymbol{\lambda}_{gs\min} - \boldsymbol{\lambda}_{gs\max}) = \mathbf{0} \\
&\mathbf{h}(\mathbf{x},\mathbf{s},\mathbf{D}(-\tilde{\boldsymbol{\lambda}}_{\hat{h}d} + \boldsymbol{\lambda}_{gd\min} - \boldsymbol{\lambda}_{gd\max})) = \mathbf{0} \\
&\boldsymbol{\lambda}_g{}^T \mathbf{g}(\mathbf{x},\mathbf{s},\mathbf{D}(-\tilde{\boldsymbol{\lambda}}_{\hat{h}d} + \boldsymbol{\lambda}_{gd\min} - \boldsymbol{\lambda}_{gd\max})) = \mathbf{0} \\
&\mathbf{g}(\mathbf{x},\mathbf{s},\mathbf{D}(-\tilde{\boldsymbol{\lambda}}_{\hat{h}d} + \boldsymbol{\lambda}_{gd\min} - \boldsymbol{\lambda}_{gd\max})) \le \mathbf{0} \\
&\boldsymbol{\lambda}_g \ge \mathbf{0}
\end{aligned} \tag{3.8}$$

which can be simplified to

$$\begin{aligned}
&\begin{pmatrix} \boldsymbol{\lambda}_h{}^T \dfrac{\partial \mathbf{h}\left(\mathbf{x},\mathbf{S}(\tilde{\boldsymbol{\lambda}}_{\hat{h}s} + \boldsymbol{\lambda}_{gs\min} - \boldsymbol{\lambda}_{gs\max}),\mathbf{D}(-\tilde{\boldsymbol{\lambda}}_{\hat{h}d} + \boldsymbol{\lambda}_{gd\min} - \boldsymbol{\lambda}_{gd\max})\right)}{\partial \mathbf{x}} \\ + \boldsymbol{\lambda}_g{}^T \dfrac{\partial \mathbf{g}\left(\mathbf{x},\mathbf{S}(\tilde{\boldsymbol{\lambda}}_{\hat{h}s} + \boldsymbol{\lambda}_{gs\min} - \boldsymbol{\lambda}_{gs\max}),\mathbf{D}(-\tilde{\boldsymbol{\lambda}}_{\hat{h}d} + \boldsymbol{\lambda}_{gd\min} - \boldsymbol{\lambda}_{gd\max})\right)}{\partial \mathbf{x}} \end{pmatrix} = \mathbf{0} \\
&\mathbf{h}\left(\mathbf{x},\mathbf{S}(\tilde{\boldsymbol{\lambda}}_{\hat{h}s} + \boldsymbol{\lambda}_{gs\min} - \boldsymbol{\lambda}_{gs\max}),\mathbf{D}(-\tilde{\boldsymbol{\lambda}}_{\hat{h}d} + \boldsymbol{\lambda}_{gd\min} - \boldsymbol{\lambda}_{gd\max})\right) = \mathbf{0} \\
&\boldsymbol{\lambda}_g{}^T \mathbf{g}\left(\mathbf{x},\mathbf{S}(\tilde{\boldsymbol{\lambda}}_{\hat{h}s} + \boldsymbol{\lambda}_{gs\min} - \boldsymbol{\lambda}_{gs\max}),\mathbf{D}(-\tilde{\boldsymbol{\lambda}}_{\hat{h}d} + \boldsymbol{\lambda}_{gd\min} - \boldsymbol{\lambda}_{gd\max})\right) = \mathbf{0} \\
&\mathbf{g}(\mathbf{x},\mathbf{S}(\tilde{\boldsymbol{\lambda}}_{\hat{h}s} + \boldsymbol{\lambda}_{gs\min} - \boldsymbol{\lambda}_{gs\max}),\mathbf{D}(-\tilde{\boldsymbol{\lambda}}_{\hat{h}d} + \boldsymbol{\lambda}_{gd\min} - \boldsymbol{\lambda}_{gd\max})) \le \mathbf{0} \\
&\boldsymbol{\lambda}_g \ge \mathbf{0}
\end{aligned} \tag{3.9}$$

In this formulation, the social optimum for a market may be determined by accepting price-dependent load and generation curves from prospective consumers and suppliers. Typically, these price-dependent curves are called bids.

3.4 Example Player Models

As shown in the previous sections, the price-dependent load model is based on the existence of a consumer benefit function $B(\mathbf{d})$, where $\mathbf{d}$ includes both the real and reactive power demand: $\mathbf{d} = \begin{bmatrix} \mathbf{d}_p^T & \mathbf{d}_q^T \end{bmatrix}^T$. Similarly, the existence of the price-dependent generation model is based on the existence of a supplier cost function $C(\mathbf{s})$, where $\mathbf{s}$ includes both the real and reactive power supply. This section shows example benefit and cost functions with their respective price-dependent load and generation models.

3.4.1 A price-dependent real power load as a model of a consumer

The consumer demand in our development is a function of the price paid at the node $\mathbf{d} = \mathbf{D}(\mathbf{p})$. This demand function is the inverse of $\frac{\partial B(\mathbf{d})}{\partial \mathbf{d}}$. For a more intuitive feel of what this means, consider the sample plot of consumer benefit for real power and its derivative shown in Figure 3.1.

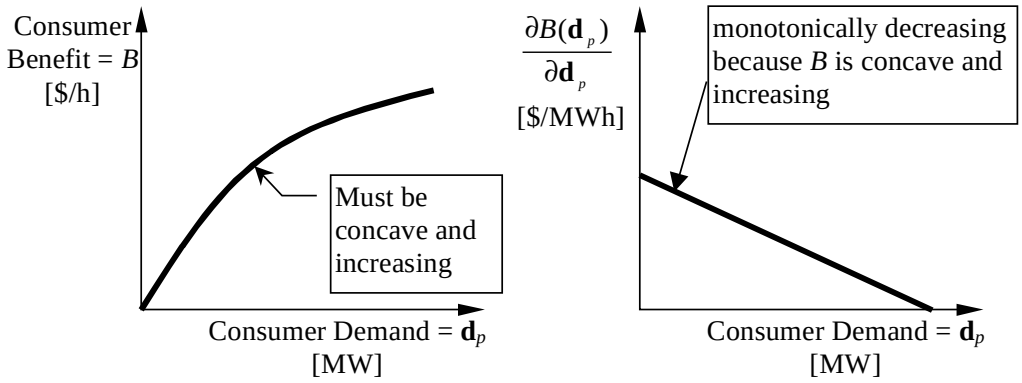

Figure 3.1 Consumer Benefit and Derivative of Benefit

It is important to assume that the consumer benefit function *B*, is concave and increasing in order to help ensure only one social welfare maximum exists (ignoring the convexity of the constraints). These are good assumptions, however. Presumably, the consumer always gains some benefit from more consumption; therefore, the benefit increases. Even if the consumer does not personally gain more benefit, he will be able to resell the power in the market. The concavity assumption is valid because an intelligent consumer will always give energy to her most beneficial processes first, thereby making the marginal benefit for lower consumption larger.

At the optimal solution from the social welfare perspective, $\frac{\partial B(\mathbf{d})}{\partial \mathbf{d}}$ will be the price for each consumer. Thus by taking the inverse of $\frac{\partial B(\mathbf{d})}{\partial \mathbf{d}}$, the consumer demand function for real power will be as shown in Figure 3.2.

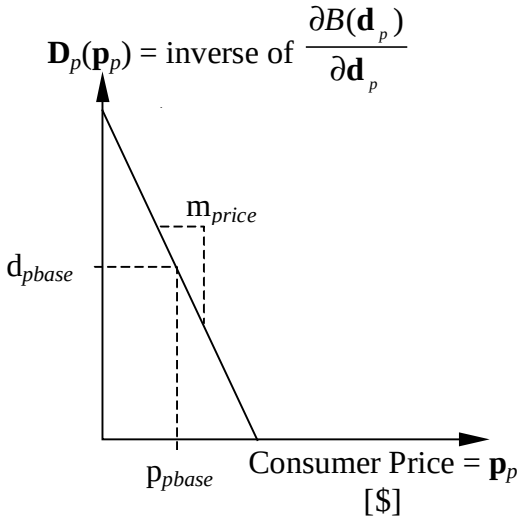

Figure 3.2 Consumer Demand for Real Power

This consumer demand function is what must be used in Equation (3.6) in order to produce the social welfare maximum. The point (p_{base}, d_{base}) and the slope m_{price} will specify the line. Therefore, the consumer demand function will be

$$\mathbf{D}_p(\mathbf{p}_p) = (\mathbf{d}_{pbase} + \mathbf{M}_{price}\mathbf{p}_{pbase}) - \mathbf{M}_{price}\mathbf{p}_p \tag{3.10}$$

where $\mathbf{M}_{price}$ is a diagonal matrix with entries m_{price}. Ignoring reactive power consumption completely, this demand function corresponds to a quadratic consumer benefit function for real power:

$$B_p(\mathbf{d}_p) = \mathbf{d}_p^T\left(\mathbf{M}_{price}^{-1}\mathbf{d}_{pbase} + \mathbf{p}_{pbase}\right) - \frac{1}{2}\mathbf{d}_p^T\mathbf{M}_{price}^{-1}\mathbf{d}_p \tag{3.11}$$

To model only a real power market without the reactive power market, then simply ignore the price dependence of reactive power demand and assume that the load always maintains constant power factor. This results in the following price-dependent load for the consumer model at each node:

$$\begin{aligned} d_p &= (d_{pbase} + m_p p_{pbase}) - m_p p_p \\ d_q &= \gamma d_p \end{aligned} \tag{3.12}$$

3.4.2 A price-dependent real power generation as a model of a supplier

In order to model the supplier costs, a quadratic function of the real power generation is used. This is a common practice in electric power system analysis. Just as a quadratic model for benefit shown in Equation (3.11) corresponds to a linear price-dependent load of Equation (3.10) so does a quadratic model for cost correspond to a linear price-dependent generation. This is depicted in Figure 3.3.

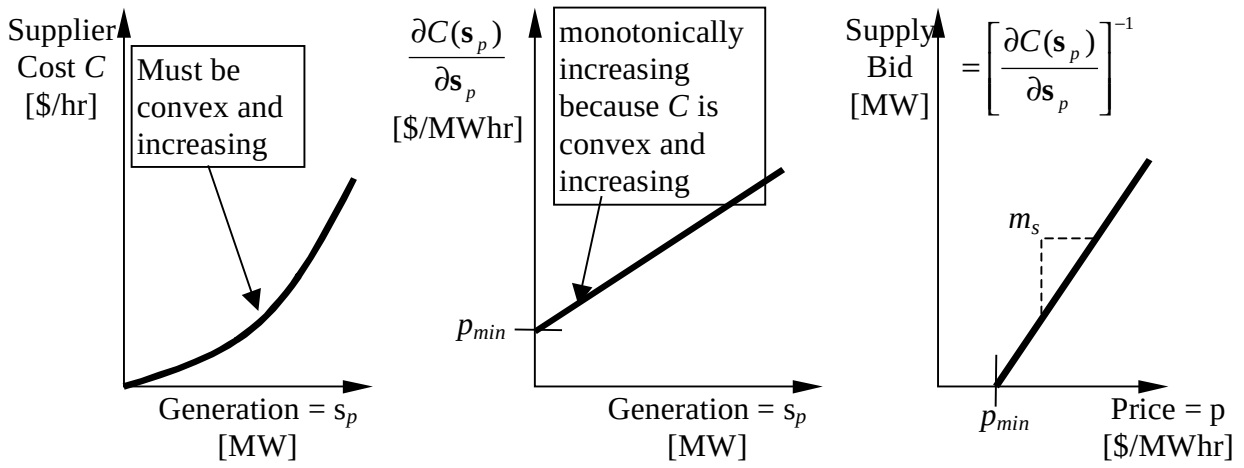

Figure 3.3 From a Quadratic Cost to a Linear Supply Curve

3.4.3 Incorporation of the benefit of reactive power into the consumer model

While many are comfortable with the idea of a spot market for real power, the viability of a spot market for reactive power remains cloudy. In [34], the creation of a full spot market for reactive power is put forth. This helps create an efficient market for allocating the operational costs of the reactive power supply, but it does not overcome two large issues in the reactive power market: the capital cost of reactive power equipment (such as capacitor banks and LTCs) are large compared to operational costs, and reactive power spot prices are extremely volatile. For example, in both [35] and [36], reactive power spot prices are shown to vary by orders of magnitude when voltage limits are encountered in the power system. In order to overcome these issues, both [35] and [37] propose the development of pricing schemes which take into account the capital investment required to install reactive power equipment along with alternatives which try to overcome some of the price volatility in reactive power spot prices.

Although there is still some debate regarding the viability of reactive power spot prices, a portion of any pricing scheme will likely be based on the spot pricing approach. This section investigates how to incorporate this idea into the price-dependent load model.

In order to determine a reasonable price-dependent reactive power load, it is necessary to determine a benefit function that befits the benefits gained by reactive power consumption. This reactive benefit function should not follow the same mold as the real power benefit equation because reactive power acts more as a service enabling the consumption of real power.

Using this point of view, consider the benefit of the reactive power as the avoidance of moving the reactive power from some desired level for a given power consumption. Define a desired reactive power demand as a function of the real power demand: $d_{qdesired} = f(d_p)$. This desired reactive demand will be the demand which the load will naturally require at the given load level. Also assume that the magnitude of the function increases with d_p. Now consider a concave function $k(x)$, which has a maximum value of zero at zero such as in Figure 3.4.

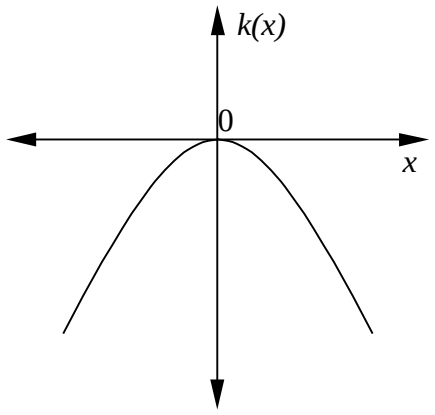

Figure 3.4 Concave $k(x)$

Then using $d_{qdesired} = f(d_p)$ along with the function $k(x)$ and a constant B_{qo}, construct the reactive power benefit function for an individual load as

$$B_q(d_p, d_q) = B_{qo}k\left(d_q - f(d_p)\right) \tag{3.13}$$

Due to the properties specified for $k(x)$, this benefit has a maximum value of zero, which is achieved when the reactive power demand is equal to the desired reactive demand $f(d_p)$. The benefit decreases on both sides of this value because the consumer must provide their own

reactive power support using power electronics, capacitor/inductor support, etc. One can envision a system load with a filtering device such as that seen in Figure 3.5.

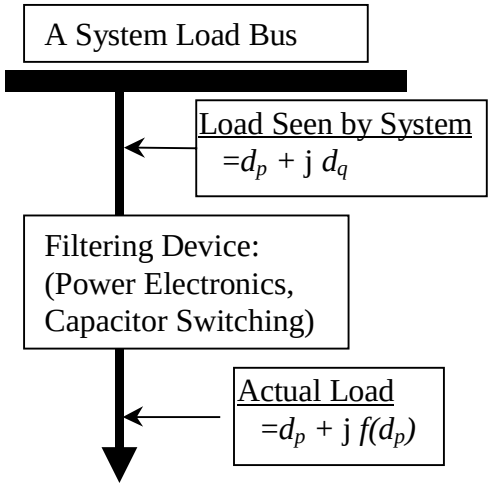

Figure 3.5 A Load Model with Reactive Control

The model here assumes that the cost of operating this filtering device is equal to zero when it is performing no filtering, i.e., when $d_q = f(d_p)$, and increases according to $k(x)$ as it moves away from that point.

Incorporating Equation (3.13) into the total consumer benefit results in a function of both the real and reactive demand:

$$B(\mathbf{d}_p, \mathbf{d}_q) = \sum_{\text{all consumers}} \left(B_p(d_p) + B_q(d_p, d_q) \right) \tag{3.14}$$

The consumer demand function can then be calculated from Equation (3.14) by determining the functional inverse of the derivative of this consumer benefit function.

As an example, consider using the quadratic real power benefit function for each consumer of the form $B_p(d_p) = ad_p - bd_p^2$. This is the same form as Equation (3.11). For the reactive power benefit function, use $d_{qdesired} = f(d_p) = \gamma d_p$ and $k(x) = -x^2$. This corresponds to a constant power factor load where $\gamma = \sqrt{1 - \text{pf}^2} \,/\, \text{pf}$, and the cost of compensating for reactive

power by the consumer increases quadratically as it moves away from constant power factor. Thus, the consumer benefit function is

$$\begin{aligned} B(d_p, d_q) &= ad_p - bd_p^2 - B_{qo}\left[d_q - \gamma d_p\right]^2 \\ &= ad_p + (-b - B_{qo}\gamma^2)d_p^2 - B_{qo}d_q^2 + 2B_{qo}\gamma d_p d_q \end{aligned} \tag{3.15}$$

It should be noted that Equation (3.15) is simply the summation of two concave functions and is therefore itself concave.

At this point, it is of interest to determine the consumer demand functions that result by calculating the functional inverse of the derivative of the consumer demand function. The derivative with respect to the real power demand is

$$\begin{aligned} \frac{\partial B(d_p, d_q)}{\partial d_p} &= \frac{\partial B_p(d_p)}{\partial d_p} + \frac{\partial B_q(d_p, d_q)}{\partial d_p} \\ &= \left[a - 2bd_p\right] + \left[2B_{qo}\gamma(-\gamma d_p + d_q)\right] \end{aligned} \tag{3.16}$$

In looking at the derivative of the consumer benefit function with respect to real power demand, it is normally expected that this derivative will always be positive because some marginal benefit is expected from increased consumption. However, because of the model that is being proposed, this will not always be true.

If $\frac{\partial B_p(d_p)}{\partial d_p}$ is negative, then $\frac{\partial B(d_p, d_q)}{\partial d_p}$ may be negative. This is an artifact of using the model outside the range intended. The benefit model for real power should be concave and increasing. The quadratic function is concave, but will begin decreasing once a maximum point is reached. It is therefore important that the real power load for a consumer is limited to the range in which the function $a - 2bd_p$ is positive; otherwise, the consumer gets more benefit by decreasing power consumption regardless of any other costs. This would not make sense as the consumer could always resell the power and thereby get some use.

The other possibility is that $\frac{\partial B_q(d_p, d_q)}{\partial d_p}$ is negative and begins to dominate the first term. This is not unrealistic. It would merely mean that further increases in real power would result in large costs for reactive power consumption and therefore reduce the consumer benefit.

Now consider taking the derivative with respect to reactive power demand:

$$\frac{\partial B(d_p, d_q)}{\partial d_q} = 2B_{qo}(-d_q + \gamma d_p) \tag{3.17}$$

Equation (3.17) shows that in order to increase benefit, the reactive power demand is always pushed toward the desired level γd_p.

In order to determine the consumer demand function, equate Equations (3.16) and (3.17) to the price of real and reactive power, respectively.

$$\frac{\partial B(d_p, d_q)}{\partial \mathbf{d}} = \begin{bmatrix} a \\ 0 \end{bmatrix} + \begin{bmatrix} -2b - 2B_{qo}\gamma^2 & 2B_{qo}\gamma \\ 2B_{qo}\gamma & -2B_{qo} \end{bmatrix} \begin{bmatrix} d_p \\ d_q \end{bmatrix} = \begin{bmatrix} p_p \\ p_q \end{bmatrix} \tag{3.18}$$

Then solve for real and reactive demand in terms of these prices, i.e., determine the functional inverse:

$$\mathbf{D(p)} = \begin{bmatrix} -\frac{1}{2b}(p_p + \gamma p_q) + \frac{a}{2b} \\ \gamma\left(-\frac{1}{2b}(p_p + \gamma p_q) + \frac{a}{2b}\right) - \frac{1}{2B_{qo}} p_q \end{bmatrix} \tag{3.19}$$

$$\text{Note: } d_q = \gamma d_p - \frac{1}{2B_{qo}} p_q$$

It is helpful to rewrite this additional equation in a more meaningful way. Equation (3.19) can be re-written as

$$\mathbf{D(p)} = \begin{bmatrix} d_{pbase} + m_p p_{pbase} \\ d_{qbase} + \gamma m_p p_{pbase} \end{bmatrix} - \begin{bmatrix} m_p & \gamma m_p \\ \gamma m_p & \left(\gamma^2 m_p + \frac{d_{qbase}}{2B_{qo}}\right) \end{bmatrix} \begin{bmatrix} p_p \\ p_q \end{bmatrix} \tag{3.20}$$

with the following definitions:

$$m_p = \frac{1}{2b} \qquad \gamma = \frac{d_{qbase}}{d_{pbase}} \qquad B_{qo} = \frac{\overline{B_{qo}}}{d_{qbase}}$$

and one demand point of $d_p = d_{pbase}$ and $d_q = d_{qbase}$

at prices $p_p = p_{pbase}$ and $p_q = 0$ given.

Equation (3.20) can also be written in the form

$$\begin{aligned} d_p &= \left(d_{pbase} + m_p p_{pbase}\right) - m_p (p_p + \gamma p_q) \\ d_q &= \gamma d_p - \frac{d_{qbase}}{2\overline{B_{qo}}} p_q \end{aligned} \tag{3.21}$$

Now, at each demand bus specify a value of m_p, p_{pbase}, $\overline{B_{qo}}$, d_{pbase}, and d_{qbase} and substitute

$$\begin{aligned} \mathbf{D}_{busk}\left(\begin{bmatrix} \lambda_{\hat{h}dp} + \lambda_{gdp\min} - \lambda_{gdp\max} \\ \lambda_{\hat{h}dq} + \lambda_{gdq\min} - \lambda_{gdq\max} \end{bmatrix}\right) &= \begin{bmatrix} d_{pbase} + m_p p_{pbase} \\ d_{qbase} + \gamma m_p p_{pbase} \end{bmatrix} \\ &- \begin{bmatrix} m_p & \gamma m_p \\ \gamma m_p & \left(\gamma^2 m_p + \frac{d_{qbase}}{2\overline{B_{qo}}}\right) \end{bmatrix} \begin{bmatrix} \lambda_{\hat{h}dp} + \lambda_{gdp\min} - \lambda_{gdp\max} \\ \lambda_{\hat{h}dq} + \lambda_{gdq\min} - \lambda_{gdq\max} \end{bmatrix} \end{aligned} \tag{3.22}$$

into the optimal power flow necessary conditions shown in Equation (3.7). This will result in the social welfare maximum for the economic consumer model that has been described.

3.5 Implementation of Real and Reactive Price-Dependent Loads into the OPF

This section will study how the price-dependent demand incorporated into the necessary conditions of Equation (3.7) affects the calculations of the Newton's method algorithm.

It is first noted that after taking derivatives of **h** and **g** with respect to **x**, no dependence on **s** or **d** is found (as long as **s** and **d** are not functions of **x**, which we will assume in this thesis). Note: in the future, it may make sense to write the consumer benefit as a function of voltage, which would make **d** dependent on **x**. For now, however, the choice of the consumer demand

function has no effect on the first equation. The only influence comes in the third and fourth equations. The consumer demand function has only changed the demand function from a constant to one dependent on the Lagrange multipliers $\tilde{\boldsymbol{\lambda}}_{\hat{h}d}$, $\boldsymbol{\lambda}_{gd\min}$ and $\boldsymbol{\lambda}_{gd\max}$. This will not impede the OPF algorithm as it will only require a simple function evaluation.

In using Newton's method to solve these nonlinear equations, derivatives of the equations must be determined in order to calculate a Hessian matrix. In order to evaluate how the consumer demand function will affect these equations, take the derivatives of the third and fourth equations with respect to $\tilde{\boldsymbol{\lambda}}_{\hat{h}d}$, $\boldsymbol{\lambda}_{gd\min}$ and $\boldsymbol{\lambda}_{gd\max}$:

$$\frac{\partial \mathbf{h(x,s,D)}}{\partial \tilde{\boldsymbol{\lambda}}_{\hat{h}d}} = \frac{\partial \begin{bmatrix} \hat{\mathbf{h}}(\mathbf{x}) - \hat{\mathbf{s}} + \hat{\mathbf{d}}) \\ \bar{\mathbf{h}}(\mathbf{x}) \end{bmatrix}}{\partial \mathbf{d}} \frac{\partial \mathbf{D}}{\partial \tilde{\boldsymbol{\lambda}}_{\hat{h}d}} = -[\hat{\mathbf{I}}_{PQ}][-\hat{\mathbf{M}}_{PQprice}]$$

$$\frac{\partial \mathbf{h(x,s,D)}}{\partial \boldsymbol{\lambda}_{gd\min}} = \frac{\partial \begin{bmatrix} \hat{\mathbf{h}}(\mathbf{x}) - \hat{\mathbf{s}} + \hat{\mathbf{d}}) \\ \bar{\mathbf{h}}(\mathbf{x}) \end{bmatrix}}{\partial \mathbf{d}} \frac{\partial \mathbf{D}}{\partial \boldsymbol{\lambda}_{gd\min}} = +[\hat{\mathbf{I}}_{PQ}][-\tilde{\mathbf{M}}_{PQprice}]$$

$$\frac{\partial \mathbf{h(x,s,D)}}{\partial \boldsymbol{\lambda}_{gd\max}} = \frac{\partial \begin{bmatrix} \hat{\mathbf{h}}(\mathbf{x}) - \hat{\mathbf{s}} + \hat{\mathbf{d}}) \\ \bar{\mathbf{h}}(\mathbf{x}) \end{bmatrix}}{\partial \mathbf{d}} \frac{\partial \mathbf{D}}{\partial \boldsymbol{\lambda}_{gd\max}} = -[\hat{\mathbf{I}}_{PQ}][-\overline{\mathbf{M}}_{PQprice}]$$

$$\frac{\partial \mathbf{g(x,s,D)}}{\partial \tilde{\boldsymbol{\lambda}}_{\hat{h}d}} = \frac{\partial \begin{bmatrix} \mathbf{s}_{\min} - \mathbf{s} \\ \mathbf{s} - \mathbf{s}_{\max} \\ \mathbf{d}_{\min} - \mathbf{d} \\ \mathbf{d} - \mathbf{d}_{\max} \\ \bar{\mathbf{g}}(\mathbf{x}) \end{bmatrix}}{\partial \mathbf{D}} \frac{\partial \mathbf{D}}{\partial \tilde{\boldsymbol{\lambda}}_{\hat{h}d}} = +[\tilde{\mathbf{I}}_{PQ}][-\hat{\mathbf{M}}_{PQprice}]$$

$$\frac{\partial \mathbf{g(x,s,D)}}{\partial \boldsymbol{\lambda}_{gd\min}} = +[\tilde{\mathbf{I}}_{PQ}][\tilde{\mathbf{M}}_{PQprice}]$$

$$\frac{\partial \mathbf{g(x,s,D)}}{\partial \boldsymbol{\lambda}_{gd\max}} = +[\tilde{\mathbf{I}}_{PQ}][-\overline{\mathbf{M}}_{PQprice}]$$

where the variables are defined as

$$\hat{\mathbf{I}}_{PQ} = \begin{matrix}\text{matrix with diagonal entries of 1 corresponding} \\ \text{to consumer demand variables } \mathbf{d}\end{matrix}$$

$$\tilde{\mathbf{I}}_{PQ} = \begin{matrix}\text{matrix with diagonal entries of 1 corresponding} \\ \text{to consumer demands } \mathbf{d} \text{ which are at a limit}\end{matrix}$$

$$\hat{\mathbf{M}}_{PQ\,price} = \begin{matrix}\text{a block diagonal matrix with } 2\times 2 \text{ entries of} \\ \begin{bmatrix} m_p & \gamma m_p \\ \gamma m_p & \left(\gamma^2 m_p + \dfrac{d_{qbase}}{2\overline{B}_{qo}}\right)\end{bmatrix} \text{corresponding to} \\ \text{variables } \mathbf{d}\end{matrix}$$

$$\tilde{\mathbf{M}}_{PQprice} = \begin{matrix}\text{a block diagonal matrix with } 2\times 2 \text{ entries of} \\ \begin{bmatrix} m_p & \gamma m_p \\ \gamma m_p & \left(\gamma^2 m_p + \dfrac{d_{qbase}}{2\overline{B}_{qo}}\right)\end{bmatrix} \text{corresponding to} \\ \text{variables } \boldsymbol{\lambda}_{gd\,\min} \\ \text{related to } \mathbf{d}\end{matrix}$$

$$\overline{\mathbf{M}}_{PQprice} = \begin{matrix}\text{a block diagonal matrix with } 2\times 2 \text{ entries of} \\ \begin{bmatrix} m_p & \gamma m_p \\ \gamma m_p & \left(\gamma^2 m_p + \dfrac{d_{qbase}}{2\overline{B}_{qo}}\right)\end{bmatrix} \text{corresponding to} \\ \text{variables } \boldsymbol{\lambda}_{gd\,\max} \\ \text{related to } \mathbf{d}\end{matrix}$$

The key point to recognize is that the effect of the additional price-dependent equations on the Hessian matrix is limited to small 2 x 2 block diagonal entries. From Equation (7) of reference [28], the Hessian matrix for the coupled OPF formulation is shown to have the structure

$$\mathbf{W} = \left[\begin{array}{c|c} \mathbf{H} & -\mathbf{J}^{\mathbf{T}} \\ \hline -\mathbf{J} & \mathbf{0} \end{array}\right] \tag{3.23}$$

The block diagonal entries which are added to the Hessian by the price-dependent loads will be in the zero matrix in the lower right partition. Because some entries are added on the off-diagonals in this zero matrix, it is possible that some degradation of sparsity may occur; however, it will be minor. If one is only interested in simulating the real power market using the

price-dependent load of Equation (3.12), the 2 x 2 block diagonals will be replaced by elements purely on the diagonal. This will result in no degradation of sparsity.

Although some minor degradation of sparsity is possible, overall, it is expected that the price-dependent load will help with convergence of the OPF. This is because the loads in the system will tend to decrease if the system moves close to a limit due to the system prices increasing.

As a demonstration of how these models affect the Hessian matrix, study Figure 3.6 and Figure 3.7. They show Hessian matrices for the IEEE 118-bus system with cost data created following the premise that larger units are generally cheaper units. Figure 3.6 shows the Hessian matrix for the objective of minimizing total generation costs. Notice the large zero partition in the lower right. Figure 3.7 shows the Hessian matrix with price-dependent real power loads included. Notice that new elements are only added along the diagonal of the zero partition. Also note that with both real and reactive price-dependent loads included, 2 x 2 blocks would appear along the diagonal of the Hessian matrix.

This shows that one can make simple modifications to an existing OPF algorithm that minimizes generation costs in order to solve the maximization of the social welfare objective of the OPF. This modification is both simple and intuitive and leads to the possibility of simulating a real and reactive power market by asking consumers to submit price-dependent load curves while suppliers submit price-dependent generation curves. In this manner a two-sided power market can be modeled.

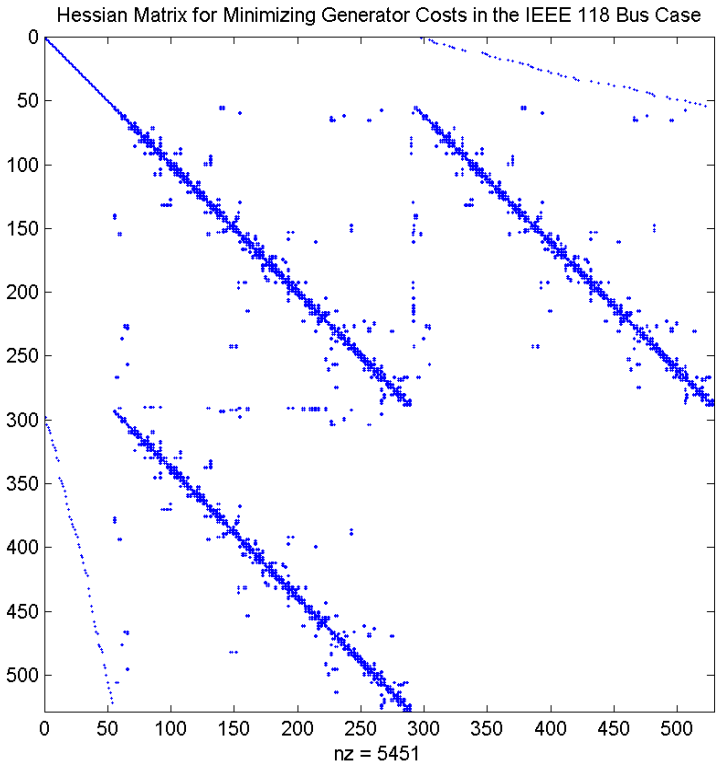

Figure 3.6 Hessian for Minimizing Costs

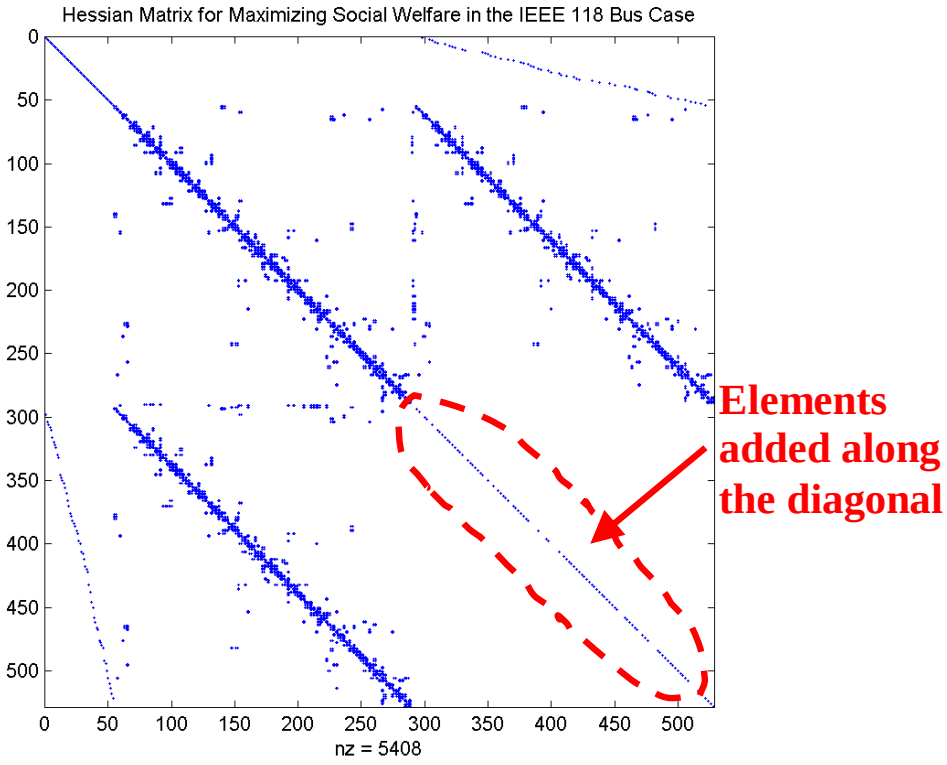

Figure 3.7 Hessian Matrix for IEEE 118-Bus System with Price-Dependent Real Power Loads

4. INDIVIDUAL PLAYER OPTIMIZATION IN ELECTRICITY MARKETS

The previous chapters have thoroughly covered the market model for an electric power pool. In the examples of Chapter 2, an individual's optimal bid was determined by solving the market model for several different bids and then comparing results to determine the best bid among those tested. This chapter will look at solving the maximization of a player's profit in a single optimization problem. It will require solving profit maximization with the constraint being the OPF problem. This presents a nested optimization problem in which players try to maximize their profit under the constraint that their dispatch and price are determined by the OPF. This chapter presents a new efficient numerical technique, using price and dispatch sensitivity information available from the OPF solution, to determine how a player should vary its bid portfolio in order to maximize its overall profit. The chapter will further demonstrate the determination of Nash equilibrium when all players are trying to maximize their profit in this manner.

4.1 Individual Welfare Maximization Problem

The market setup from Chapter 2 essentially defines the market rules for our system. Again, the variation in bidding will be limited to the variation of a single parameter *k* for each consumer or supplier as shown in Figure 4.1. This parameter will vary the bid around the true marginal curve of the supplier or consumer. The supply curve that reflects true marginal cost is defined as the linear function $p(s) = \frac{1}{m_s} s + p_{\min}$, while for the consumer, a true marginal curve is defined as $p(d) = -\frac{1}{m_d} d + p_{\max}$.

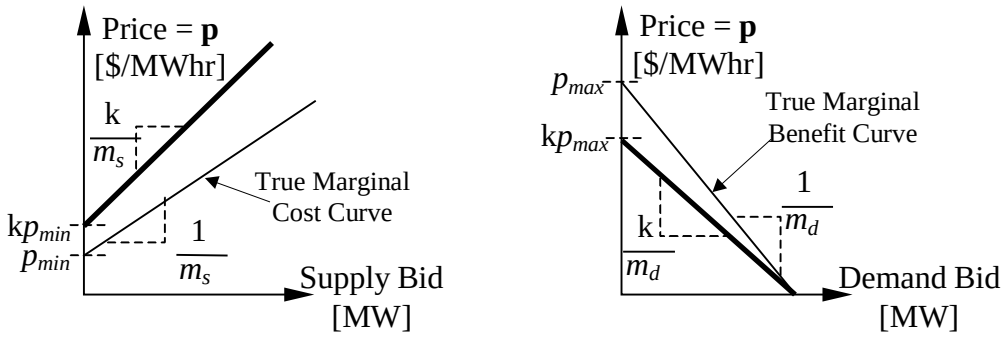

Figure 4.1 Bidding Variation for Supply and Demand

While this limits market behavior, it will be shown in Section 4.5 that from an individual's viewpoint, the shape of this curve is not important for a single market solution. Note that modifying a bid in this manner is the same as multiplying the cost or benefit function used in the OPF by k: $C(s) = k(bs + cs^2)$ and $B(d) = k(bd - cd^2)$.

Here it is assumed that each individual seeks to maximize its personal welfare. A single consumer's welfare is defined as the amount of benefit received from using the power, minus the expenses incurred in purchasing the power. Similarly, a single supplier's welfare is defined as the amount of revenue received from selling the power, minus the cost of supplying the power. An individual wants to maximize the total welfare of all the consumers and suppliers that it controls.

$$\begin{aligned} f(\mathbf{s},\mathbf{d},\boldsymbol{\lambda}) &= \sum_{\substack{\text{i=controlled}\\ \text{demands}}} [\underbrace{B_i(d_i)}_{\text{Benefits}} - \underbrace{\lambda_i \mathrm{d_i}}_{\text{Expenses}}] + \sum_{\substack{\text{controlled}\\ \text{supplies}}} [-\underbrace{C_i(s_i)}_{\text{Costs}} + \underbrace{\lambda_i \mathrm{s_i}}_{\text{Revenues}}] \\ &= \underbrace{\left(-\mathbf{d}^T\mathbf{C_d}\mathbf{d} + \mathbf{B_d}^T\mathbf{d}\right)}_{\text{Benefits}} - \underbrace{\left(\boldsymbol{\lambda}^T\mathbf{d}\right)}_{\text{Expenses}} - \underbrace{\left(\mathbf{s}^T\mathbf{C_s}\mathbf{s} + \mathbf{B_s}^T\mathbf{s}\right)}_{\text{Costs}} + \underbrace{\left(\boldsymbol{\lambda}^T\mathbf{s}\right)}_{\text{Revenues}} \end{aligned} \tag{4.1}$$

where $\mathbf{C_d}$ and $\mathbf{C_s}$: are diagonal matrices of quadratic coefficients for supply cost and demand benefit functions

$\mathbf{B_d}$ and $\mathbf{B_s}$: are vectors of linear coefficients for supply cost and demand benefit functions

Note that an individual's welfare $f(\mathbf{s},\mathbf{d},\lambda)$ is not an explicit function of its bid variable k. However, f is an implied function of k since $\mathbf{s}$, $\mathbf{d}$, and λ are all determined by an OPF solution which is a function of k. Thus s, d, and λ are all implicit functions of the bids k.

Assuming the individual has some estimate of what other individuals in the market are going to bid, the individual's goal is to maximize its welfare by choosing a bid which is the best response to the other individuals' bids. As a result, the maximization of an individual's welfare forms a nested optimization problem where the individual maximizes its welfare subject to an OPF solution which maximizes social welfare based on all bids in the market. That is,

$$\begin{aligned} \max_{\mathbf{k}} \quad & f(\mathbf{s},\mathbf{d},\lambda) \\ \text{s.t.} \quad & (\mathbf{s},\mathbf{d},\lambda) \text{ are determined by} \\ & \left(\begin{array}{ll} \max\limits_{\mathbf{x},\mathbf{s},\mathbf{d}} & B_{ind}(\mathbf{d},\mathbf{k}) - C_{ind}(\mathbf{s},\mathbf{k}) + B_{comp}(\mathbf{d}) - C_{comp}(\mathbf{s}) \\ & \mathbf{h(x,s,d) = 0} \\ \text{s.t.} & \mathbf{g(x,s,d) \le 0} \end{array} \right) \end{aligned} \tag{4.2}$$

where $B_{ind}(\mathbf{d},\mathbf{k})$ and $C_{ind}(\mathbf{s},\mathbf{k})$ are the benefit and cost functions of the consumers and suppliers that the individual controls, and $B_{comp}(\mathbf{d})$ and $C_{comp}(\mathbf{s})$ are the estimates of the benefit and cost functions that the individual's competitors will submit as bids. Thus, the total societal benefit used by the OPF market model is $B(\mathbf{d}) = B_{ind}(\mathbf{d},\mathbf{k}) + B_{comp}(\mathbf{d})$, and the total societal cost used is $C(\mathbf{s},\mathbf{k}) = C_{ind}(\mathbf{s},\mathbf{k}) + C_{comp}(\mathbf{s})$.

4.2 Solution of Individual Welfare Maximization by the Direct Application of Kuhn-Tucker Conditions

One approach to solving Equation (4.2) is to represent the OPF maximization subproblem by the Kuhn-Tucker necessary conditions as done in [49]. Thus the nested optimization problem may be recast as a standard optimization problem:

$$
\begin{aligned}
\max_{\mathbf{k}} \quad & f(\mathbf{s},\mathbf{d},\lambda) \\
& -\frac{\partial C}{\partial \mathbf{s}} + \boldsymbol{\lambda}_{\mathrm{h}}^{\mathrm{T}} \frac{\partial \mathbf{h}}{\partial \mathbf{s}} + \boldsymbol{\lambda}_{\mathrm{g}}^{\mathrm{T}} \frac{\partial \mathbf{g}}{\partial \mathbf{s}} = \mathbf{0} \\
\text{s.t.} \quad & \frac{\partial B}{\partial \mathbf{d}} + \boldsymbol{\lambda}_{\mathrm{h}}^{\mathrm{T}} \frac{\partial \mathbf{h}}{\partial \mathbf{d}} + \boldsymbol{\lambda}_{\mathrm{g}}^{\mathrm{T}} \frac{\partial \mathbf{g}}{\partial \mathbf{d}} = \mathbf{0} \\
& + \boldsymbol{\lambda}_{\mathrm{h}}^{\mathrm{T}} \frac{\partial \mathbf{h}}{\partial \mathbf{x}} + \boldsymbol{\lambda}_{\mathrm{g}}^{\mathrm{T}} \frac{\partial \mathbf{g}}{\partial \mathbf{x}} = \mathbf{0} \\
& \mathbf{h}(\mathbf{x},\mathbf{s},\mathbf{d}) = \mathbf{0} \\
& \boldsymbol{\lambda}_{\mathrm{g}}^{\mathrm{T}} \mathbf{g}(\mathbf{x},\mathbf{s},\mathbf{d}) = \mathbf{0} \\
& \mathbf{g}(\mathbf{x},\mathbf{s},\mathbf{d}) \le \mathbf{0} \\
& \boldsymbol{\lambda}_{\mathrm{g}}^{\mathrm{T}} \ge \mathbf{0}
\end{aligned}
\tag{4.3}
$$

Recasting the problem in this manner is natural but suffers from a couple drawbacks. From a purely practical viewpoint, it results in an optimization problem which is very different from the standard OPF. This would prevent the rapid application of these ideas to present software platforms. From a theoretical viewpoint, it results in a subset of constraints which are complementary: $\boldsymbol{\lambda}_{\mathrm{g}}^{\mathrm{T}}\mathbf{g}(\mathbf{x},\mathbf{s},\mathbf{d}) = \mathbf{0}$, $\mathbf{g}(\mathbf{x},\mathbf{s},\mathbf{d}) \le \mathbf{0}$, and $\boldsymbol{\lambda}_{\mathrm{g}}^{\mathrm{T}} \ge \mathbf{0}$. As shown in [49], complementary constraints are difficult to enforce for an optimization routine because they require two complementary variables to be nonnegative and nonpositive, respectively, yet at the same time require their product to be zero. Because of this difficulty, it is of interest to consider an alternative solution technique as is developed next.

4.3 Solution of Individual Welfare Maximization through Iterative Means

As discussed in the previous section, recasting the nested optimization problem as a standard optimization problem results in complementary conditions which are very difficult to enforce. In this section, an alternative technique is presented that makes minimal modifications to an existing OPF to solve Equation (4.2).

Consider solving the OPF problem for a given set of bids. Then from the information available at this OPF solution, the individual's profit sensitivity to variations in its bid can be used to determine a Newton-step that improves profits. This Newton-step is defined the customary way as

$$\mathbf{k}_{new} = \mathbf{k}_{old} - \left[\frac{\partial^2 f}{\partial \mathbf{k}^2}\right]^{-1}\Bigg|_{\mathbf{k}_{old}} \frac{\partial f}{\partial \mathbf{k}}\Bigg|_{\mathbf{k}_{old}} \tag{4.4}$$

Evaluation of Equation (4.4) requires determination of $\frac{\partial^2 f}{\partial \mathbf{k}^2}$ and $\frac{\partial f}{\partial \mathbf{k}}$.

$$\begin{aligned}\frac{\partial f}{\partial \mathbf{k}} &= \left(-2\mathbf{d}^T\mathbf{C}_\mathbf{d} + \mathbf{B}_\mathbf{d}^T - \boldsymbol{\lambda}^T\right)\frac{\partial \mathbf{d}}{\partial \mathbf{k}} \\ &\quad + \left(-2\mathbf{s}^T\mathbf{C}_\mathbf{s} - \mathbf{B}_\mathbf{s}^T + \boldsymbol{\lambda}^T\right)\frac{\partial \mathbf{s}}{\partial \mathbf{k}} + \left[\frac{\partial \boldsymbol{\lambda}}{\partial \mathbf{k}}\right]^T(\mathbf{s}-\mathbf{d})\end{aligned} \tag{4.5}$$

$$\begin{aligned}\frac{\partial^2 f}{\partial \mathbf{k}^2} &= -2\left(\left[\frac{\partial \mathbf{d}}{\partial \mathbf{k}}\right]^T\mathbf{C}_\mathbf{d} + \left[\frac{\partial \boldsymbol{\lambda}}{\partial \mathbf{k}}\right]^T\right)\frac{\partial \mathbf{d}}{\partial \mathbf{k}} \\ &\quad + 2\left(-\left[\frac{\partial \mathbf{s}}{\partial \mathbf{k}}\right]^T\mathbf{C}_\mathbf{s} + \left[\frac{\partial \boldsymbol{\lambda}}{\partial \mathbf{k}}\right]^T\right)\frac{\partial \mathbf{s}}{\partial \mathbf{k}} \\ &\quad + \left(-2\mathbf{d}^T\mathbf{C}_\mathbf{d} + \mathbf{B}_\mathbf{d}^T - \boldsymbol{\lambda}^T\right)\frac{\partial^2 \mathbf{d}}{\partial \mathbf{k}^2} \\ &\quad + \left(-2\mathbf{s}^T\mathbf{C}_\mathbf{s} - \mathbf{B}_\mathbf{s}^T + \boldsymbol{\lambda}^T\right)\frac{\partial^2 \mathbf{s}}{\partial \mathbf{k}^2} + \left[\frac{\partial^2 \boldsymbol{\lambda}}{\partial \mathbf{k}^2}\right]^T(\mathbf{s}-\mathbf{d})\end{aligned} \tag{4.6}$$

Evaluation of Equations (4.5) and (4.6) requires determination of $\frac{\partial \mathbf{d}}{\partial \mathbf{k}}, \frac{\partial \mathbf{s}}{\partial \mathbf{k}}, \frac{\partial \boldsymbol{\lambda}}{\partial \mathbf{k}}, \frac{\partial^2 \mathbf{d}}{\partial \mathbf{k}^2}, \frac{\partial^2 \mathbf{s}}{\partial \mathbf{k}^2}$, and $\frac{\partial^2 \boldsymbol{\lambda}}{\partial \mathbf{k}^2}$. Because **s**, **d**, and λ are variables of the OPF solution, these derivatives can be determined directly from values available from the OPF solution. In a Newton-based OPF, an iteration of the mismatch equation $\Delta\mathbf{z} = -\mathbf{H}^{-1}(\nabla\mathbf{L})$ is done until $\Delta\mathbf{z} = 0$,

where $\mathbf{z} = \begin{bmatrix} \mathbf{s}^T & \mathbf{d}^T & \mathbf{x}^T & \lambda^T \end{bmatrix}^T$. Therefore, the derivatives of **s**, **d**, and λ can be found by taking derivatives of this mismatch equation. These can be found to be

$$\frac{\partial \mathbf{z}}{\partial \mathbf{k}} = -\mathbf{H}^{-1}\frac{\partial \mathbf{H}}{\partial \mathbf{k}}\Delta\mathbf{z} - \mathbf{H}^{-1}\frac{\partial \nabla \mathbf{L}}{\partial \mathbf{k}} \tag{4.7}$$

$$\begin{aligned}\frac{\partial^2 \mathbf{z}}{\partial \mathbf{k}^2} = &-\mathbf{H}^{-1}\frac{\partial^2 \mathbf{H}}{\partial \mathbf{k}^2}\Delta\mathbf{z} - \mathbf{H}^{-1}\frac{\partial^2 \nabla \mathbf{L}}{\partial \mathbf{k}^2} \\ &+ 2\mathbf{H}^{-1}\frac{\partial \mathbf{H}}{\partial \mathbf{k}}\mathbf{H}^{-1}\Delta\mathbf{z} + 2\mathbf{H}^{-1}\frac{\partial \mathbf{H}}{\partial \mathbf{k}}\mathbf{H}^{-1}\frac{\partial \nabla \mathbf{L}}{\partial \mathbf{k}}\end{aligned} \tag{4.8}$$

These equations can be simplified by recalling that at an OPF solution $\Delta\mathbf{z} = 0$, and because of the structure of our problem, **k** only shows up as a linear term in both the gradient and the Hessian (see Appendix A), therefore $\frac{\partial^2 \mathbf{H}}{\partial \mathbf{k}^2} = 0$ and $\frac{\partial^2 \nabla \mathbf{L}}{\partial \mathbf{k}^2} = 0$. Thus, Equations (4.7) and (4.8) may be simplified to

$$\frac{\partial \mathbf{z}}{\partial \mathbf{k}} = -\mathbf{H}^{-1}\frac{\partial \nabla \mathbf{L}}{\partial \mathbf{k}} \tag{4.9}$$

$$\frac{\partial^2 \mathbf{z}}{\partial \mathbf{k}^2} = 2\mathbf{H}^{-1}\frac{\partial \mathbf{H}}{\partial \mathbf{k}}\mathbf{H}^{-1}\frac{\partial \nabla \mathbf{L}}{\partial \mathbf{k}} = -2\mathbf{H}^{-1}\frac{\partial \mathbf{H}}{\partial \mathbf{k}}\frac{\partial \mathbf{z}}{\partial \mathbf{k}} \tag{4.10}$$

The technique being developed improves computation because both $\frac{\partial \nabla \mathbf{L}}{\partial \mathbf{k}}$ and $\frac{\partial \mathbf{H}}{\partial \mathbf{k}}$ are extremely sparse. The partial derivative $\frac{\partial \nabla \mathbf{L}}{\partial \mathbf{k}}$ is a matrix which has exactly one entry in each column, while $\frac{\partial \mathbf{H}}{\partial \mathbf{k}}$ is a three-dimensional tensor that has exactly one diagonal element in each matrix as one moves in the dimension corresponding to **k** (see Appendix A). Because these are so sparse, the computation time for calculating these derivatives is extremely small.

Using Equations (4.9) and (4.10) to substitute into Equations (4.5) and (4.6), use Equation (4.4) to perform a Newton-step which improves an individual's welfare. The following algorithm is used to determine an individual's best bidding strategy.

Algorithm: *Preliminary Individual Welfare Maximization*

1. Choose an initial guess for vector **k**.
2. Solve the OPF maximization of social welfare given the individual's assumption of other individual's bids and the individual's guess at its own vector **k**.
3. Use Equation (4.4) to determine a step direction for vector **k**.
4. If $\|\mathbf{k}_{new} - \mathbf{k}_{old}\|$ is below some tolerance, then stop; else go back to step 2.

This algorithm will be effective as long as the binding inequalities of the OPF algorithm do not change. Changes in binding inequalities result in discontinuities of $\frac{\partial f}{\partial \mathbf{k}}$, which means that the function f becomes nondifferentiable. A change in binding inequality, however, can be detected from other available information. From one side of the nondifferentiable point, the value limited by the inequality approaches its limit. From the other side of the point, the Lagrange multiplier associated with the inequality approaches zero. This is shown in Figure 4.2.

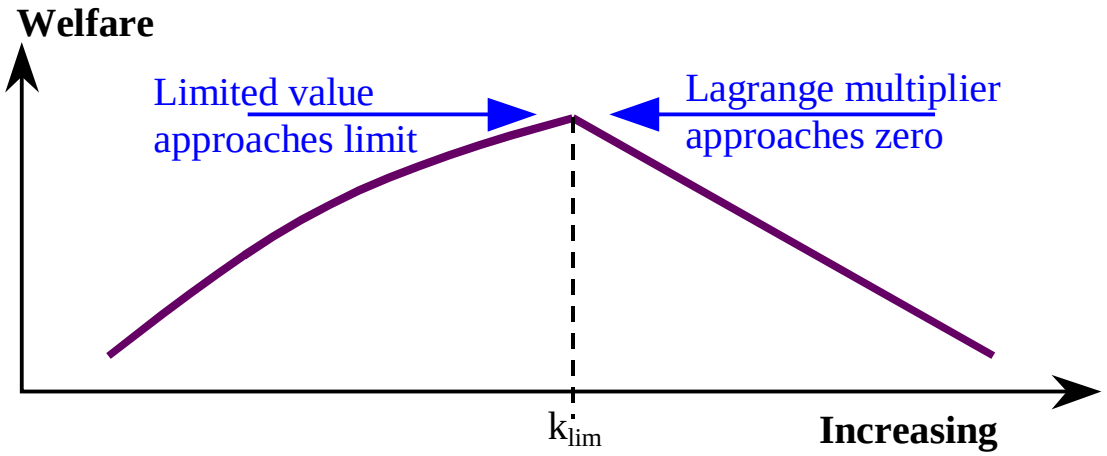

Figure 4.2 Binding Inequality Change in One Dimension

If only one bid parameter and one inequality constraint are being considered, the Preliminary Individual Welfare Maximization algorithm could be simply modified so a multiplier reduces the step direction determined by Equation (4.4) if this step direction will move across a non-differentiable point. The multiplier would then bring the answer directly to this non-differentiable point. In order to extend this simple idea to the more general case of multiple bid parameters and multiple inequality constraints, consider the origins of the Newton step described in Equation (4.4). Newton's method solves for the zero crossing of a function by approximating it as a linear function using its present value and derivative. In a maximization problem, the zero crossing of the *derivative* of the objective function is desired; therefore, when using Newton's method, the objective function is inherently modeled as a second-order Taylor series:

$$f(\mathbf{k}_{new}) = f(\mathbf{k}_{old} + \Delta\mathbf{k}) \approx f(\mathbf{k}_{old}) + (\Delta\mathbf{k})^T \left.\frac{\partial f}{\partial \mathbf{k}}\right|_{\mathbf{k}_{old}} + \frac{1}{2}(\Delta\mathbf{k})^T \left.\frac{\partial^2 f}{\partial \mathbf{k}^2}\right|_{\mathbf{k}_{old}} (\Delta\mathbf{k}) \tag{4.11}$$

Equation (4.4) is then derived by solving $\frac{\partial f(\mathbf{k}_{old} + \Delta\mathbf{k})}{\partial \Delta\mathbf{k}} = \mathbf{0}$.

In order to follow the analogy of Figure 4.2, the $\Delta\mathbf{k}$ that maximizes Equation (4.11) without crossing any constraint boundaries is desired. This is determined by solving Equation (4.12).

$$\begin{aligned} \max_{\mathbf{k}} \quad & f(\mathbf{k}_{old}) + (\Delta\mathbf{k})^T \left.\frac{\partial f}{\partial \mathbf{k}}\right|_{\mathbf{k}_{old}} + \frac{1}{2}(\Delta\mathbf{k})^T \frac{\partial^2 f}{\partial \mathbf{k}^2}(\Delta\mathbf{k}) \\ \text{s.t.} \quad & (\Delta\mathbf{k})^T \frac{\partial g_m}{\partial \mathbf{k}} + g_m \le 0 \quad \forall g_m \le 0 \quad \begin{pmatrix} \text{ensure nonbinding constraints} \\ \text{do not become binding} \end{pmatrix} \\ & -(\Delta\mathbf{k})^T \frac{\partial \lambda_{gm}}{\partial \mathbf{k}} - \lambda_{gm} \le 0 \quad \forall g_m = 0 \quad \begin{pmatrix} \text{ensure binding constraints} \\ \text{do not become nonbinding} \end{pmatrix} \end{aligned} \tag{4.12}$$

Please note that $\frac{\partial^2 f}{\partial \mathbf{k}^2}$ is negative definite. Also, the only derivative in Equation (4.12) that has not already been discussed is $\frac{\partial g_m}{\partial \mathbf{k}}$. This derivative can be readily calculated using the chain rule:

$$\frac{\partial g_m}{\partial \mathbf{k}} = \frac{\partial \mathbf{d}}{\partial \mathbf{k}} \frac{\partial g_m}{\partial \mathbf{d}} + \frac{\partial \mathbf{s}}{\partial \mathbf{k}} \frac{\partial g_m}{\partial \mathbf{s}} + \frac{\partial \mathbf{x}}{\partial \mathbf{k}} \frac{\partial g_m}{\partial \mathbf{x}} \tag{4.13}$$

While adding another maximization problem as an outer loop to the problem may seem difficult, it is not because Equation (4.12) is a very simple constrained maximization problem. It is a quadratic objective function with linear inequality constraints: a quadratic programming problem. Many very efficient methods for the solution of this problem exist [56] and can be used to quickly solve the problem described by Equation (4.12) in a time much faster than the solution of the OPF. Thus this outer Newton-like step will be done much faster than the solution of the OPF, so solution time will be largely dependent on the number of OPF iterations needed. With this further development, the *Individual Welfare Maximization* algorithm is modified.

Algorithm: *Individual Welfare Maximization*

1. Choose an initial guess for vector **k**.
2. Solve the OPF maximization of social welfare given the individual's assumption of other individuals' bids and the individual's guess at its own vector **k**.
3. Use Equation (4.12) to determine a step direction for vector **k**.
4. If $\left\| \mathbf{k}_{new} - \mathbf{k}_{old} \right\|$ is below some tolerance, then stop; else go back to step 2.

Examples demonstrating the use of the Individual Welfare Maximization algorithm are presented throughout Sections 4.4 and 4.6 in conjunction with the use of this algorithm in finding economic equilibrium points. Issues addressed include the existence of local maxima, the computational requirements of the algorithm, as well as algorithm convergence. The existence of local maxima is discussed throughout the remainder of this chapter. The computational requirements of the algorithm are covered in Section 4.7, while algorithm convergence is discussed in Section 4.8.

4.4 Finding a Nash Equilibrium Using Individual Welfare Maximization

While the Individual Welfare Maximization algorithm is of use to market participants in general, using the algorithm as a model of individual behavior enables the study of other interesting market behavior. For example, the determination of economic equilibrium points such as *Nash equilibria* [57] is of interest.

Definition: *Nash Equilibrium*

- An individual looks at its opponents' behaviors.
- The individual determines that its best response to its opponents' behaviors is to continue its present behavior.
- This is true FOR ALL individuals in the market.

To determine a Nash equilibrium the individual welfare maximization can be iteratively solved by all individuals until a point is reached where each individual's best response is to continue with the same vector of bids. A similar iterative technique for finding Nash equilibria was used in [50], although a very different individual maximization algorithm was used. The following algorithm describes this process.

Algorithm: *Find Nash Equilibrium*

- Start all individuals with a bid vector $\mathbf{k} = \mathbf{1}$.
- Run the Individual Welfare Maximization algorithm for each individual. Update all bids.
- Continue running this until all individuals stop changing their bids.

Three issues must be addressed regarding the *Find Nash Equilibrium* algorithm: existence and uniqueness of the equilibria, computational requirements, and algorithm convergence. Existence and uniqueness of the equilibria are highlighted throughout this section. Section 4.7

discusses the computation requirements of this algorithm, while Section 4.9 discusses the convergence of the algorithm.

4.4.1 Example market with no constraints – two supplier competition

To demonstrate the *Find Nash Equilibrium* algorithm, consider the two-bus example with two suppliers and one consumer shown in Figure 4.3.

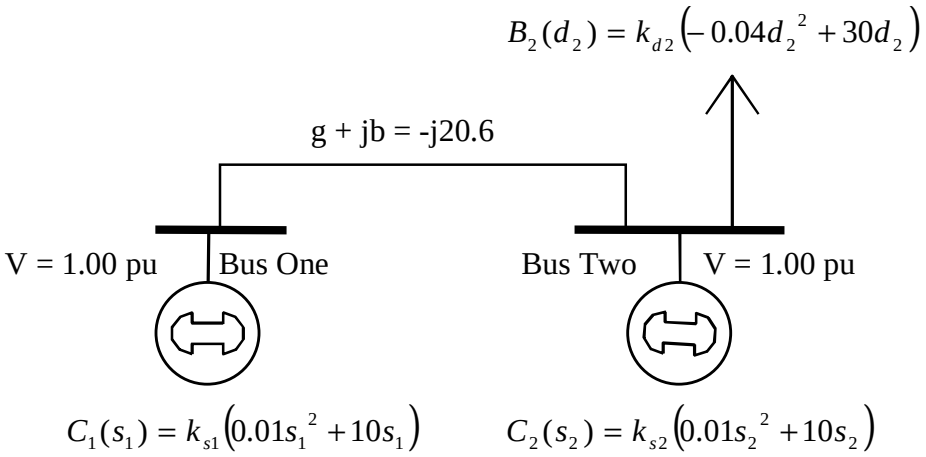

Figure 4.3 Two-Bus System: Two Suppliers and a Consumer

For this example only consider the supplier bidding behavior; therefore, assume the consumer in this market always bids according to its true benefit function, i.e., k_{d2} = 1.00. It is important to maintain the price-dependent demand. Otherwise, when a transmission line limit is added to the system, which will be done shortly, supplier 2 could have part of the constant load to serve with no competition. The solution for supplier 2 would be to bid k_{s2} equal to infinity resulting in an infinite price at bus 2 and an infinite profit. This would be the same unreasonable result found in Figure 2.8 for the six-bus system investigated before.

The Find Nash Equilibrium algorithm results in both suppliers bidding k_{s1} = k_{s2} = 1.1502. This is called a pure strategy equilibrium [57] because the equilibrium is at a point where each bidder continues to bid its same vector **k**. Figure 4.4 shows the bid progression of the algorithm toward the equilibrium point. Figure 4.5 shows a complete solution to the problem with the

optimal response of each supplier to any possible bid by the other supplier. The point where the two curves in Figure 4.5 meet is the Nash equilibrium point.

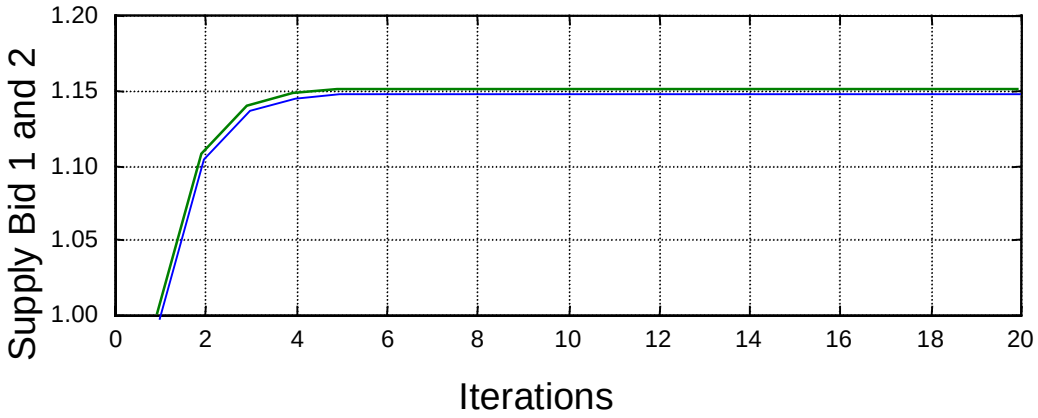

Figure 4.4 Two Suppliers' Bid Progression with No Line Limit

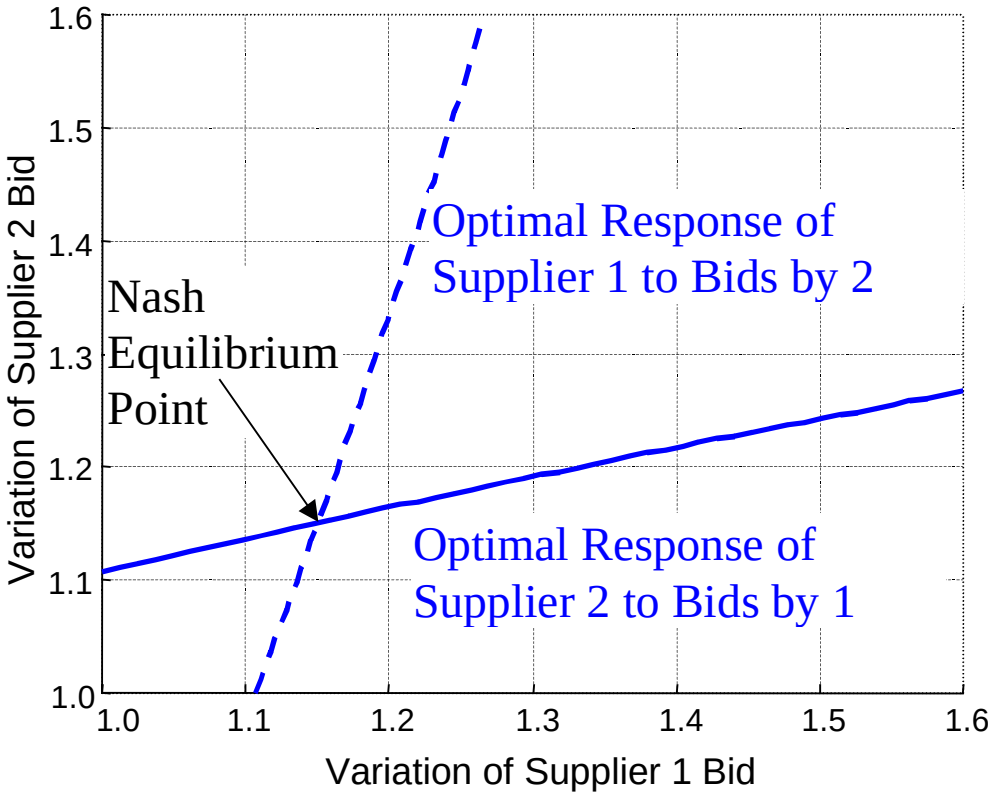

Figure 4.5 Two Suppliers' Optimal Responses with No Line Limits

4.4.2 Example market with constraints – two supplier competition

To further demonstrate the algorithm, consider the system of Figure 4.3 again, but now add a constraint to the system: limit the flow on the transmission line to 80 MVA. The bid progression that results from this system case is shown in Figure 4.6.

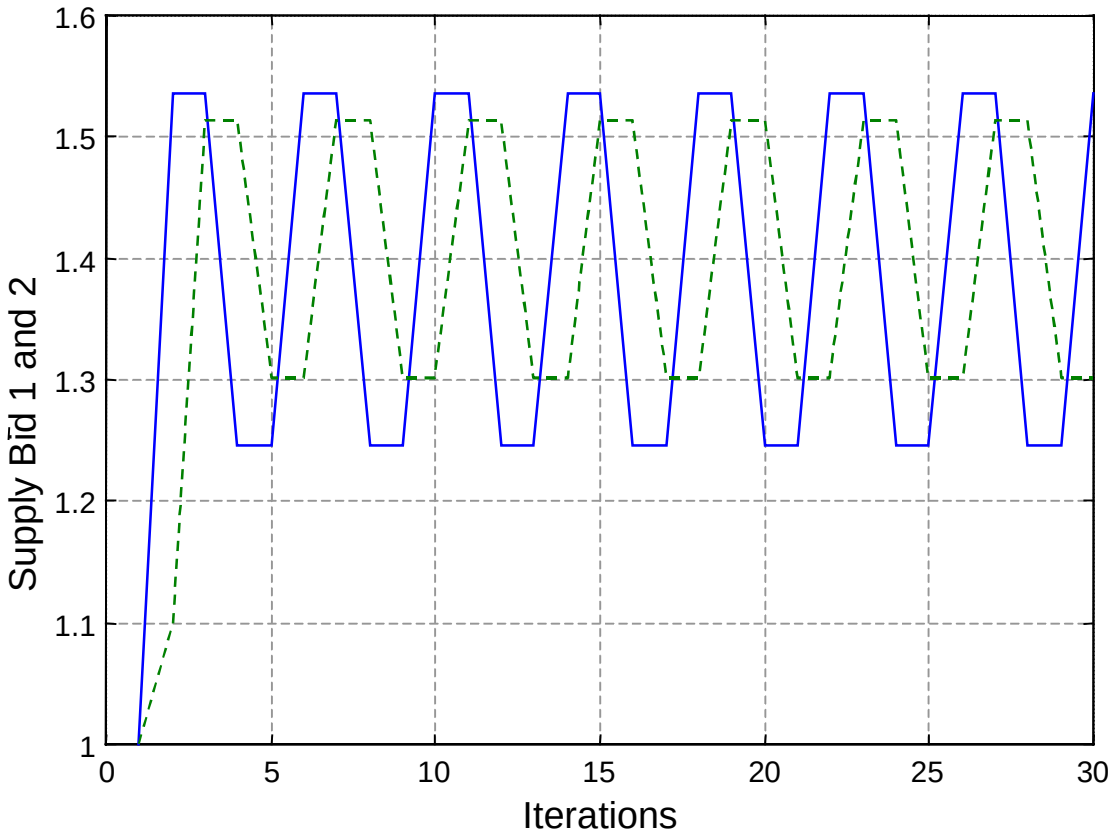

Figure 4.6 Two Suppliers' Bid Progression with 80-MVA Line Limit

This does not result in a Nash equilibrium point, but limit cycle-like behavior. To better show why no equilibrium point is reached, the optimal response curves over all possible bids by each individual are determined. These are shown in Figure 4.7.

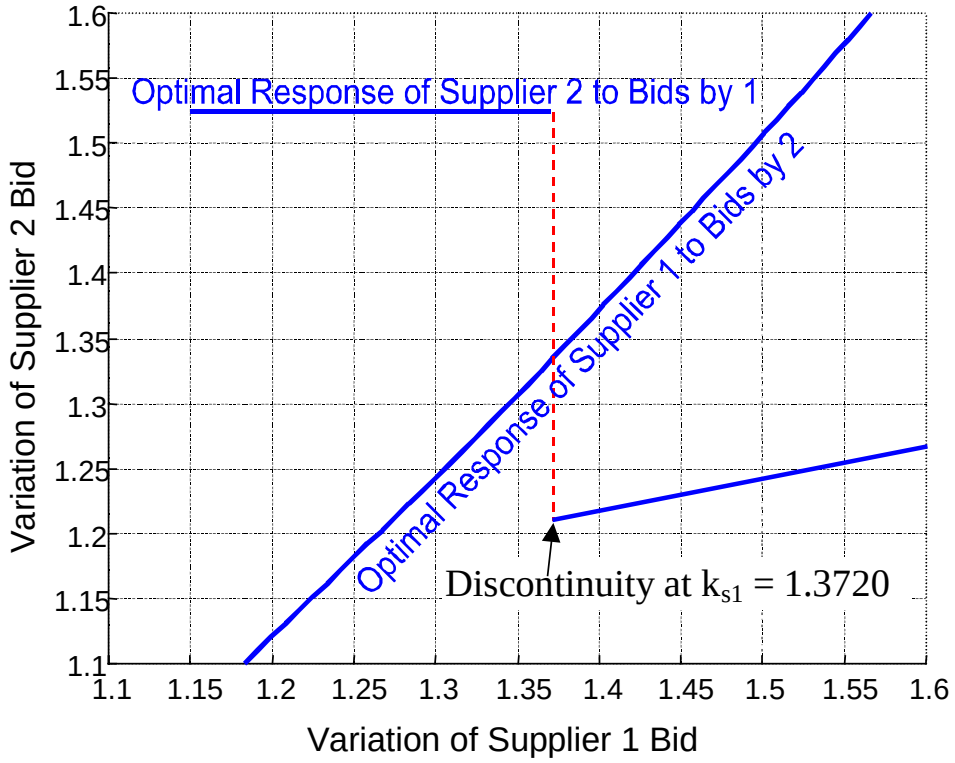

Figure 4.7 Two Suppliers' Optimal Responses with 80-MVA Line Limit

Figure 4.7 shows that the optimal response curves for the two suppliers never intersect because of a discontinuity in the supplier 2 best response curve. In order to determine what is causing this discontinuity, supplier 2 profit-versus-bid curves are created on either side of the discontinuity. These are shown in Figure 4.8.

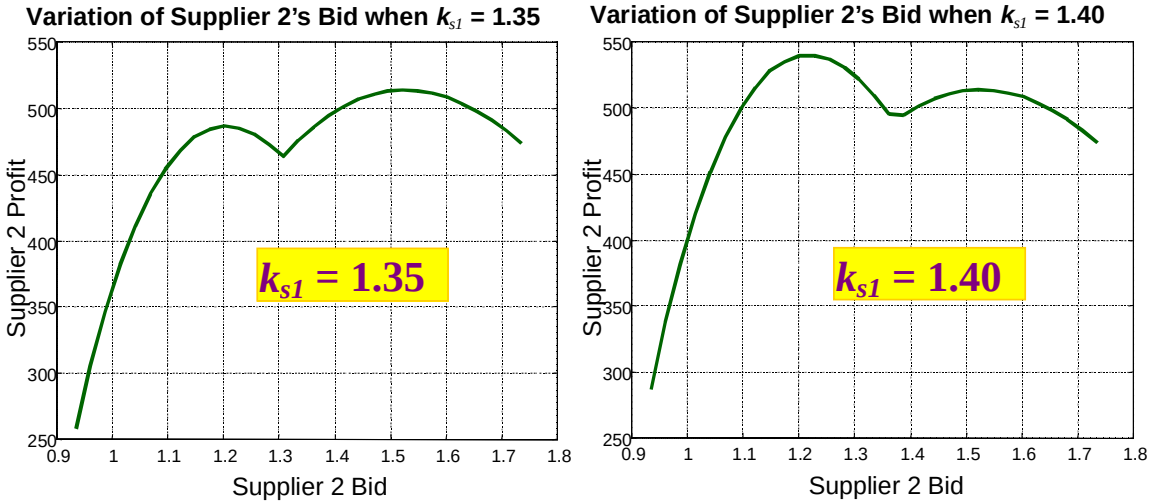

Figure 4.8 Supplier 2 Profit-versus-Bid on Either Side of the Discontinuous Point

Figure 4.8 shows that the profit function for supplier 2 is nonconcave, having two local maxima. When supplier 1 bids k_{s1} = 1.3720, these local maxima have exactly the same magnitude. At this point, supplier 2 has no preference between bidding either k_{s2} of 1.525 or 1.246. On either side of this point the optimal response "jumps" to the other local maximum. Ultimately, this is the reason that no pure Nash equilibrium exists. Thus, it has been shown that the introduction of a transmission line constraint, even in a trivial two-bus system, eliminates the pure strategy equilibrium point.

This does not mean that no Nash equilibria exist, however. Only pure strategies are considered by the algorithm introduced here. *Mixed strategies* [57] are also possible. A brief definition of a mixed strategy in our application follows.

Definition: *Mixed Strategy*

> An individual chooses several pure strategies and assigns a probability to each. The individual then submits these pure strategy bids according to their associated probabilities.

Allowing the possibility of mixed strategy equilibria in the previous example, a Nash equilibrium for the previous example can be produced from inspection of Figure 4.7. When supplier 1 bids k_{s1} = 1.372, supplier 2 has no preference between either bidding k_{s2} = 1.246 or k_{s2} = 1.525, thus bidding these two pure strategies with arbitrary probabilities is one optimal response. The probabilities are varied until the optimal bid of supplier 1 was indeed to bid k_{s1} = 1.372. A mixed strategy for this specific example is thus found.

Mixed Strategy Nash Equilibrium for Line Limited Case
Supplier 1: Bid k_{s1} = 1.372 with Probability 1.00
Supplier 2: Bid k_{s2} = 1.246 with Probability 0.56 and
k_{s2} = 1.525 with Probability 0.44

When supplier 2 bids these two strategies with the probabilities shown, the expected profit-versus-bid curve for supplier 1 is as shown in Figure 4.9. In Figure 4.9, the maximum is indeed at a bid of k_{s1} = 1.372. This shows that while pure strategy equilibria are eliminated by the inclusion of transmission limits, mixed strategy Nash equilibria may still exist.

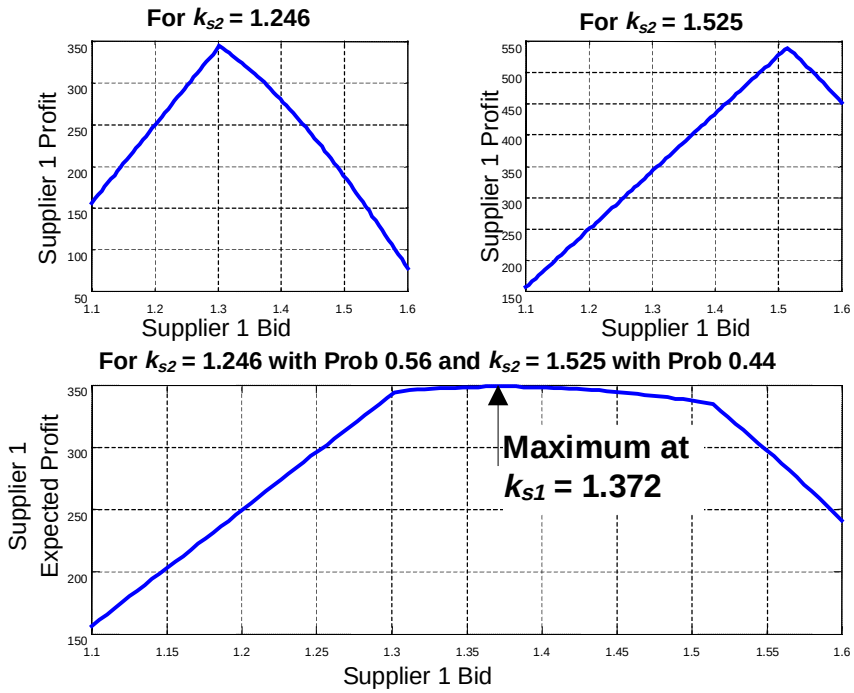

Figure 4.9 Optimal Bids for Supplier 1 in Response to a Mixed-Strategy by Supplier 2

Mixed strategies are not implemented in general in this dissertation, but are a natural extension of the work presented here.

4.4.3 Example market with no constraints – supplier and consumer competition

In the examples of Section 4.4.1 and 4.4.2, only supplier-versus-supplier competition was considered. Now consider the two-bus example shown in Figure 4.3 again, but assume supplier 2 does not participate in the market, and only supplier 1 and the consumer compete by varying their bids. The Find Nash Equilibrium algorithm results in bids of k_{s1} = 1.5714 and k_{d2} = 0.8571. As with two suppliers competing, without the transmission line constraint included the Nash

equilibrium is found to be a pure strategy. Figure 4.10 shows the progression of the algorithm toward the equilibrium. Figure 4.11 shows a complete solution to the problem with the optimal response of each participant to any possible bid by the other. The point where the two curves in Figure 4.11 meet is the Nash Equilibrium point.

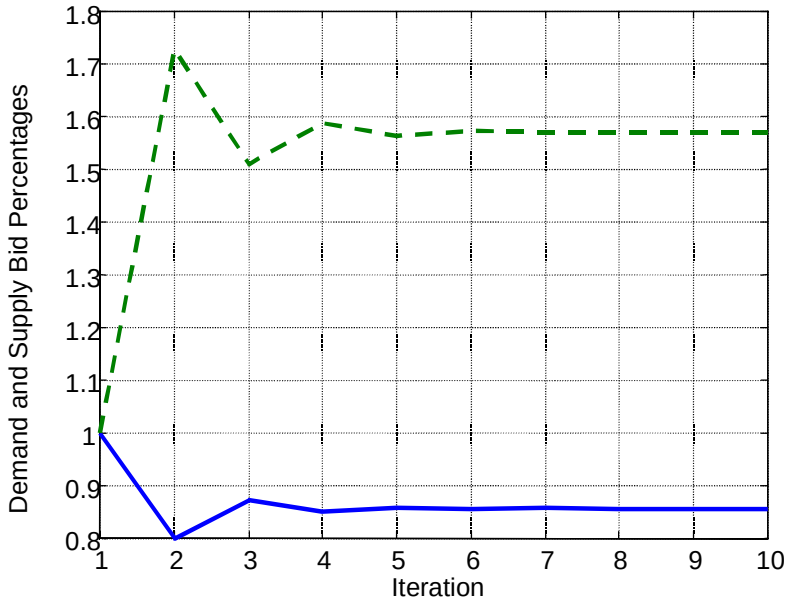

Figure 4.10 A Supplier's and a Consumer's Bid Progression with No Line Limits

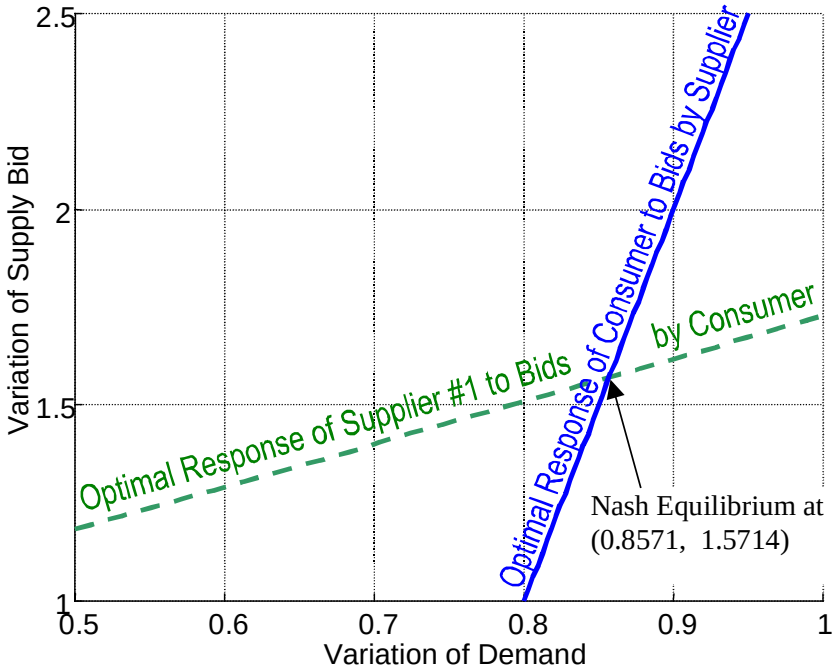

Figure 4.11 A Supplier's and Consumer's Optimal Responses with No Line Limits

4.4.4 Example market with constraints – supplier and consumer competition

Again, it is instructive to look at the same example, but with the addition of a transmission line constraint as was done in Section 4.4.2 with the two suppliers competing. Figure 4.12 shows the progression of the algorithm with the consumer and supplier 1 competing against one another while an 80-MVA transmission line limit is enforced.

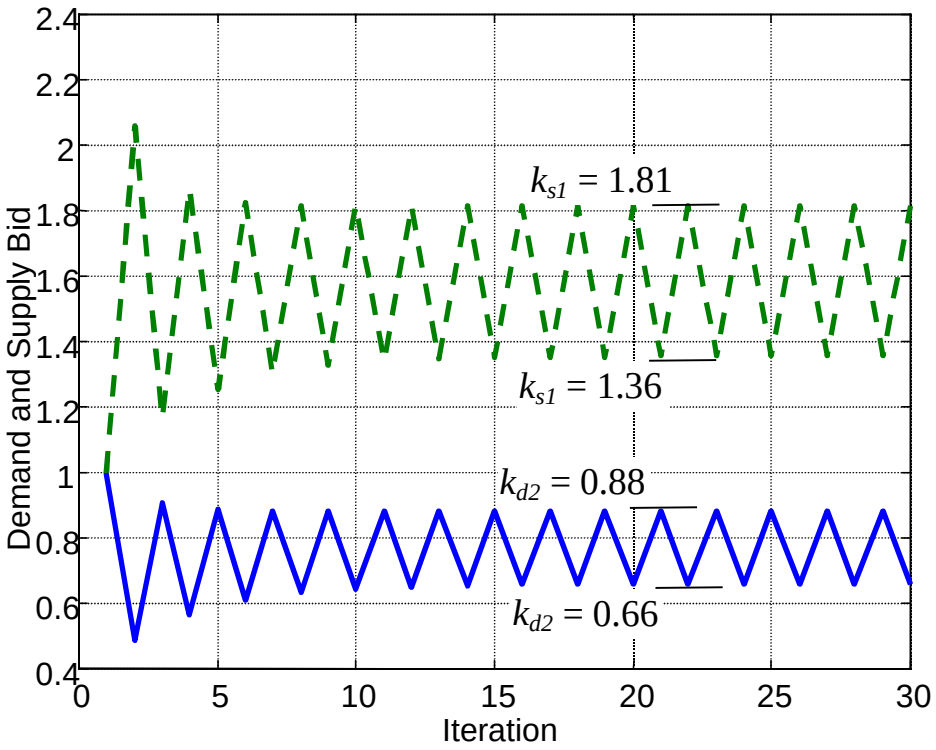

Figure 4.12 A Supplier's and a Consumer's Bid Progression with an 80-MVA Line Limit

As in Figure 4.6 with two suppliers competing, no equilibrium is reached using the Find Nash Equilibrium algorithm. Again, to better show why no equilibrium point is reached, the optimal response curves over all possible bids by each individual are determined. These are shown in Figure 4.13.

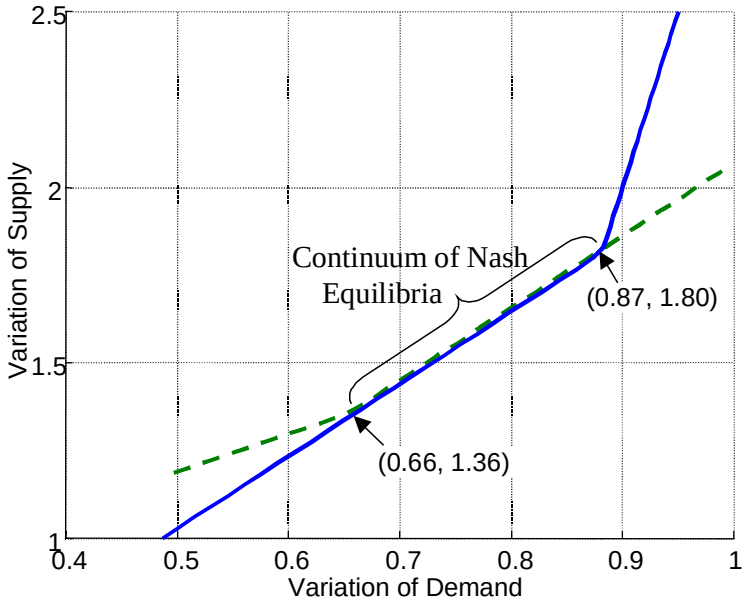

Figure 4.13 A Supplier's and Consumer's Optimal Responses with 80-MVA Line Limit

No equilibrium is reached by the Find Nash Equilibrium algorithm because the algorithm is bouncing back and forth across a continuum of Nash equilibria. As shown in Figure 4.13, a line of equilibrium points exists between k_{d2} = 0.66 / k_{s1} = 1.36 and k_{d2} = 0.87 / k_{s1} = 1.80. Table 4.1 shows the variation of the market solution along the Nash equilibrium continuum. Figure 4.14 graphs the supplier profit and consumer surplus along this continuum.

Table 4.1 Variation of the Market Solution along the Nash Equilibrium Continuum

k_{d2}	k_{s1}	Line Flow [MVA]	Price at Node 1 and 2 [$/MWh]	Supply and Demand [MW]	Consumer Surplus [$/h]	Supplier Profit [$/h]	Consumer Surplus + Supplier Profit [$/h]
1.36	0.66	80.0	15.69	77.79	382.3	870.9	1253.2
1.40	0.68	80.0	16.19	77.79	421.1	832.1	1253.2
1.44	0.70	80.0	16.69	77.79	460.0	793.3	1253.2
1.49	0.72	80.0	17.19	77.79	498.8	754.4	1253.2
1.53	0.74	80.0	17.69	77.79	537.6	715.6	1253.2
1.57	0.76	80.0	18.19	77.79	576.5	676.7	1253.2
1.62	0.79	80.0	18.69	77.79	615.3	637.9	1253.2
1.66	0.81	80.0	19.19	77.79	654.2	599.1	1253.2
1.70	0.83	80.0	19.69	77.79	693.0	560.2	1253.2
1.75	0.85	80.0	20.19	77.79	731.9	521.4	1253.2
1.79	0.87	80.0	20.69	77.79	770.7	482.5	1253.2

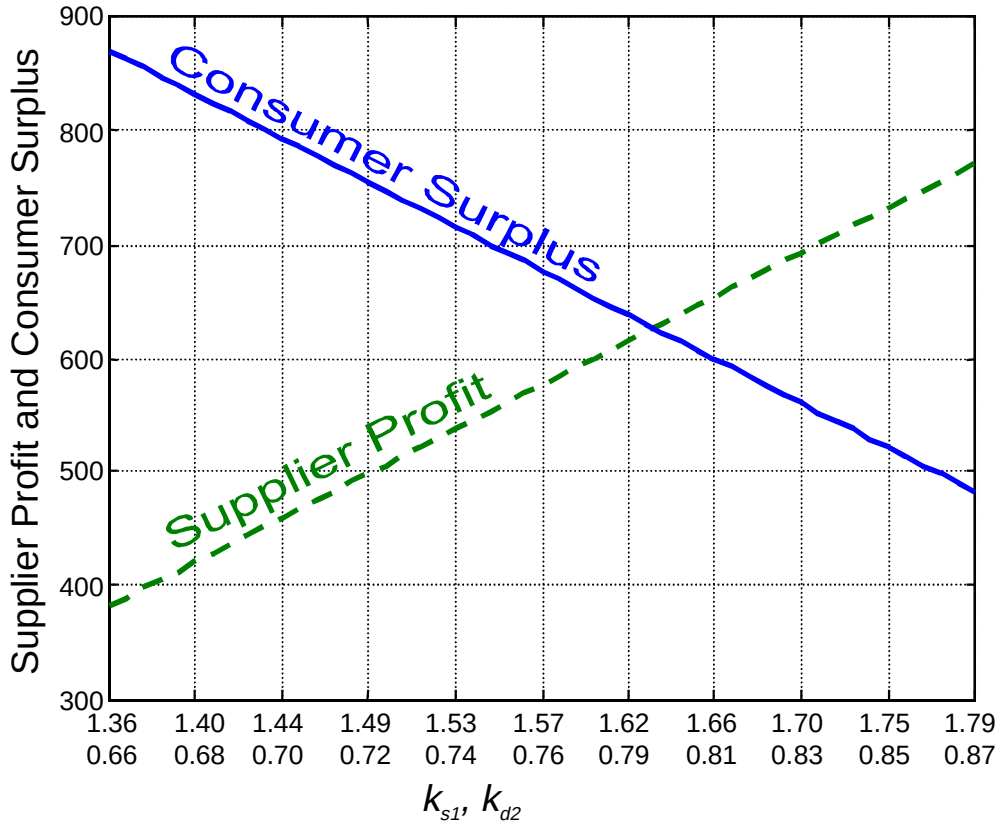

Figure 4.14 Supplier Profit and Consumer Surplus along the Nash Equilibrium Continuum

To understand what is occurring, consider the case when both the supplier and consumer submit bids according to their true benefit and cost functions, i.e., k_{s1} = 1.00 and k_{d2} = 1.00. The market solution for these bids is a supplier price at node 1 of 11.56 $/MWh and a consumer price at node 2 of 23.33 $/MWh, while 77.79 MW are exchanged between the supplier and the consumer. The difference in nodal prices results in a transmission rent collected by the pool operator of (77.79 MW)*(23.33 – 11.56 $/MWh) = 907.1 $/h. Thus a huge amount of money is being wasted as transmission rent due to the transmission line constraint. An intelligent supplier and consumer would find a way to mitigate this expense and come up with a manner in which this transmission rent could be split between the two parties instead of sending it to the pool operator. The profit, surplus, and transmission rent are summarized as follows:

- Consumer Surplus : 285.6 $/h
- Supplier Profit : 60.5 $/h
- Transmission Rent : 907.1 $/h
- Total : 1253.2 $/h

Note that the total of consumer surplus, supplier profit, and transmission rent is the same as the sum of supplier profit and consumer surplus along the Nash equilibrium (see Table 4.1). Thus, the continuum of Nash equilibrium shown in Figure 4.13 represents all the different ways the consumer and supplier can submit bids in a manner which results in a dispatch exactly at the transmission line limit, thus avoiding any transmission rent penalty due to a difference in nodal prices. The continuum of Nash equilibria represents all the different ways to split the transmission rent between the consumer and supplier. The continuum of Nash equilibria represents the ability of a competitive market to determine the best way to utilize scarce transmission resources.

4.5 Generalizing the Bid Curve

To this point, bidding in our electricity market has been limited to one dimension through changes in the multiplier k for each consumer and supplier. This does not allow the bidder to vary the slope and intercept of the bid curve independently. It can actually be shown that varying both slope and intercept will not result in increased personal welfare. To demonstrate this, the example with no line limits from Section 4.4.1 is considered. The optimal intercepts for several fixed slopes are determined, and the resulting optimal bid curves are shown in Figure 4.15.

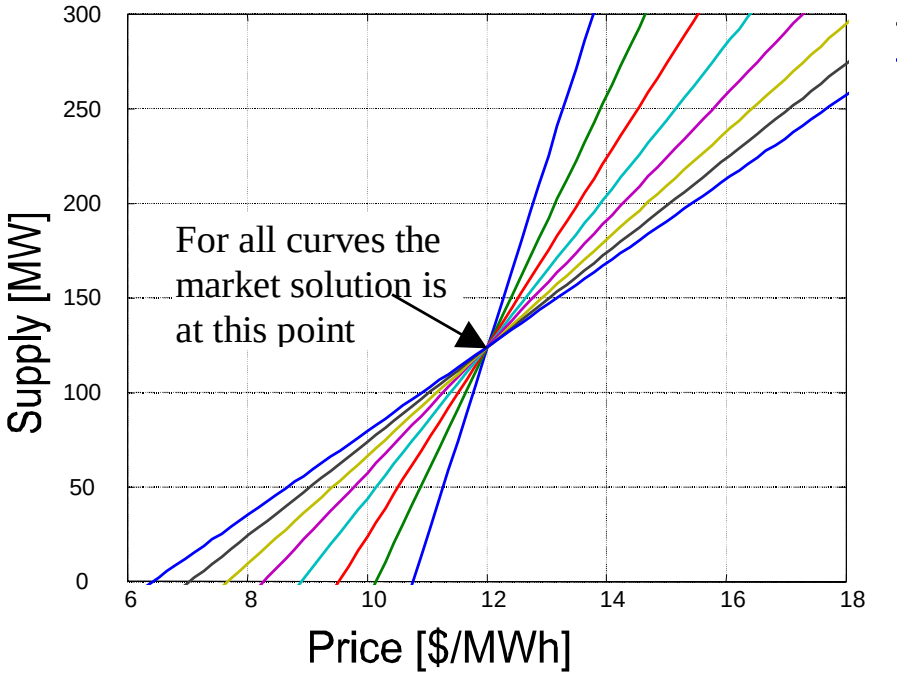

Figure 4.15 Optimal Curves for Several Fixed Slopes

These optimal bid curves all intersect at the same point in the supply-price space. Also, for all bids the market solution is at this intersection point. This means that independently varying both the slope and intercept will not result in a higher increase in personal welfare. An individual's supply and price are not independently controllable. Each is a function of the other because of the interaction with the market place.

From this it is also learned that when performing the individual maximization, the individual is really trying to find a point in the supply/demand–price space that maximizes its profit. The individual is merely looking for a bid curve that crosses this point. The multiplier **k** used throughout this dissertation is a very good variation parameter because varying **k** will cover the entire supply/demand-price space with positive values of slope and x-intercept, thus allowing the algorithm the potential to find any point in the space.

While the bidding algorithm is only looking for a single point in this development, a future extension of this work could study the effect that uncertainty in the estimates of other

individuals' bids plays in moving this optimal point around. It is likely that the shape of the bid curve could be chosen to maximize personal welfare for small perturbations around the optimal point found using this algorithm.

4.6 Example Nine-Bus System Illustrating Potential Horizontal Market Power

As mentioned in Section 1.4, the use of computer models for helping illustrate market power is of exceptional interest to the United States Department of Justice as well as state regulatory commissions throughout the United States. An example of the Find Nash Equilibrium algorithm used in the role is provided here.

Consider the nine-bus electricity system shown in Figure 4.16 with a supplier and a consumer at each bus. All transmission lines have the same characteristics (r + jx = 0 + j0.1; and C = 0), and the actual cost curves and benefit curves for the suppliers and consumers are of the form Consumer Benefit = $B_i(d_i) = b_i d_i + c_i d_i^2$ and Supplier Cost = $C_i(s_i) = b_i s_i + c_i s_i^2$ with the coefficients *b* and *c* defined as in Table 4.2.

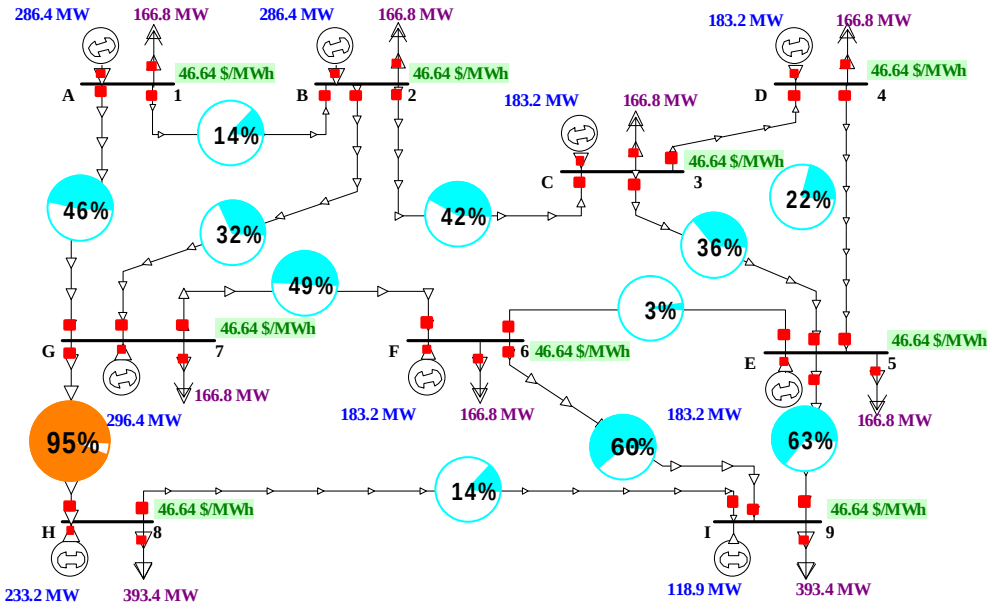

Figure 4.16 Nine-Bus Electricity Market

Table 4.2 Cost and Benefit Equation Coefficient for Illustrative Example

Bus	Supplier *b* Coefficient	Supplier *c* Coefficient	Consumer *b* Coefficient	Consumer *c* Coefficient
1 (A)	18	0.05	80	-0.10
2 (B)	18	0.05	80	-0.10
3 (C)	21	0.07	80	-0.10
4 (D)	21	0.07	80	-0.10
5 (E)	21	0.07	80	-0.10
6 (F)	21	0.07	80	-0.10
7 (G)	17	0.05	80	-0.10
8 (H)	0	0.10	440	-0.50
9 (I)	30	0.07	440	-0.50

As a reference point, the bids corresponding to true marginal benefit and welfare from all consumers and suppliers are assumed, and the OPF that maximizes social welfare is solved. The results are those shown in Figure 4.16 with a market price of $46.64/MWh throughout the system. A breakdown of the individual profit and welfare for each supplier and consumer is shown in Table 4.3.

Table 4.3 Economic Results When All Bids Correspond to True Marginal Cost

Bus	Price [$/MWh]	Supplier Output [MW]	Supplier Profit [$/h]	Consumer Demand [MW]	Consumer Welfare [$/h]
1	46.64	286.5	4,102.55	166.8	2,781.46
2	46.64	286.5	4,102.55	166.8	2,781.46
3	46.64	183.2	2,348.73	166.8	2,781.46
4	46.64	183.2	2,348.73	166.8	2,781.46
5	46.64	183.2	2,348.73	166.8	2,781.46
6	46.64	183.2	2,348.73	166.8	2,781.46
7	46.64	296.5	4,394.00	166.8	2,781.46
8	46.64	233.2	5,439.29	393.4	77,364.25
9	46.64	118.9	989.43	393.4	77,364.25
Totals		**1954.2**	**28,422.74**	**1954.2**	**174,198.74**

Note that the suppliers at buses 7 and 8 have a combined profit of $4,394.00/h + $5,439.29/h = $9,833.29/h. Also note that the flow on the transmission line from bus 7 to bus 8 is 189.5 MVA.

Now, assume that all the consumers in this market are fringe participants and exercise no strategic bidding behavior, i.e., they always submit offers representative of their true marginal benefit curve. Assume that all the suppliers, however, do exhibit strategic bidding behavior and will modify their bids in hopes of increasing their individual welfare.

Now suppose suppliers 7 and 8 collude with the hopes of increasing their combined profits. Both could raise their prices slightly hoping to increase profit. Looking at Figure 4.16, however, one notices that the line between buses 7 and 8 is loaded at 95% of its limit. As a result, suppliers 7 and 8 might also consider colluding to overload this line, thus increasing the price which supplier 8 will receive for its power. To do this, supplier 7 will have to lower its price and reduce its profit with the understanding that supplier 8 can increase its price and profit because of the overload. In order to force the individual welfare maximization algorithm into the region of parameter space which contains the other anticipated local maximum, the bid of supplier 8 is set to $k_8 = 2.0$. Then the algorithm is run again resulting in convergence into another local maximum.

Both of these scenarios are considered, and the individual welfare maximization algorithm is solved for each supplier (with suppliers 7 and 8 acting together) until Nash equilibria are reached. Different Nash equilibria are found for each scenario. Each supplier is unable to raise its profit by either lowering or raising its bid at the equilibrium points.

The results at the Nash equilibrium reached when suppliers 7 and 8 both try to raise prices while suppliers 1-6 and 9 individually try to maximize welfare are shown in Table 4.4.

Table 4.4 Nash Equilibrium Results When Suppliers 7 and 8 Both Raise Prices

Bus	Price [$/MWh]	Supplier Output [MW]	Supplier Profit [$/h]	Consumer Demand [MW]	Consumer Welfare [$/h]
1	48.51	275.8	4,612.36	157.4	2,478.55
2	48.51	275.8	4,612.36	157.4	2,478.55
3	48.51	183.0	2,690.69	157.4	2,478.55
4	48.51	183.0	2,690.69	157.4	2,478.55
5	48.51	183.0	2,690.69	157.4	2,478.55
6	48.51	183.0	2,690.69	157.4	2,478.55
7	48.51	262.1	4,824.89	157.4	2,478.55
8	48.51	216.1	5,813.56	391.5	76,630.97
9	48.51	123.1	1,218.26	391.5	76,630.97
Totals		**1885.0**	**31,844.19**	**1885.0**	**170,611.81**

Note that suppliers at buses 7 and 8 have a combined profit $4,824.89/h + $5,813.56/h = $10,638.45/h. Also note that the flow on the transmission line from bus 7 to bus 8 is 190.0 MVA. In this scenario the prices increase to $48.51/MWh. This is in increase of 4.0% above the $46.64/MWh seen when all supplier bid their exact marginal cost.

Results for the Nash equilibrium when suppliers 7 and 8 collude to try and overload the transmission line between buses 7 and 8 are shown in Table 4.5.

Table 4.5 Nash Equilibrium Results When Suppliers 7 and 8 Try to Overload a Line

Bus	Price [$/MWh]	Supplier Output [MW]	Supplier Profit [$/h]	Consumer Demand [MW]	Consumer Welfare [$/h]
1	47.08	241.9	4,108.89	164.6	2,709.01
2	47.80	257.5	4,357.63	161.0	2,592.32
3	49.95	192.4	2,978.58	150.3	2,257.62
4	50.67	196.1	3,125.79	146.7	2,151.16
5	51.38	198.3	3,272.70	143.1	2,047.09
6	50.67	196.1	3,126.40	146.7	2,150.68
7	46.36	295.9	4,310.76	168.2	2,828.57
8	60.73	183.3	7,771.83	379.3	71,921.82
9	54.29	84.0	1,546.03	385.7	74,387.47
Totals		**1845.4**	**34,598.62**	**1845.4**	**163,045.74**

Note that suppliers at buses 7 and 8 have a combined \$4,310.76/h + \$7,771.83/h = \$12,082.59/h. The flow on the transmission line from bus 7 to bus 8 is at its limit of 200 MVA. Comparing Table 4.4 and Table 4.5, suppliers 7 and 8 are able to increase their combined equilibrium profit from \$10,638/h to \$12083/h, an increase of 13.6%, when they choose a strategy of overloading the transmission line. In doing so they increase the equilibrium prices at buses 8 and 9 to \$60.73/MWh and \$54.29/MWh, which are 30.2% and 16.4% above the social welfare solution price. Thus there is definitely some concern regarding localized market power if suppliers 7 and 8 are to merge. If one ignores the transmission system, however, and only considers the problem of suppliers 7 and 8 acting to raise prices together, these market power concerns would not be readily apparent.

In order to get a better grasp of what the individual welfare maximization algorithm is facing, a complete solution to the problem is performed when all other suppliers bid $k = 1.0$. The bid for supplier 7 is then varied between 0.8 and 1.5 while varying the bid for supplier 8 between 1.0 and 1.8. Figure 4.17 and Figure 4.18 below show a contour plot and a three-dimensional plot of the combined welfare in this region. The plot on the right in Figure 4.17 shows a close-up of the local maximum.

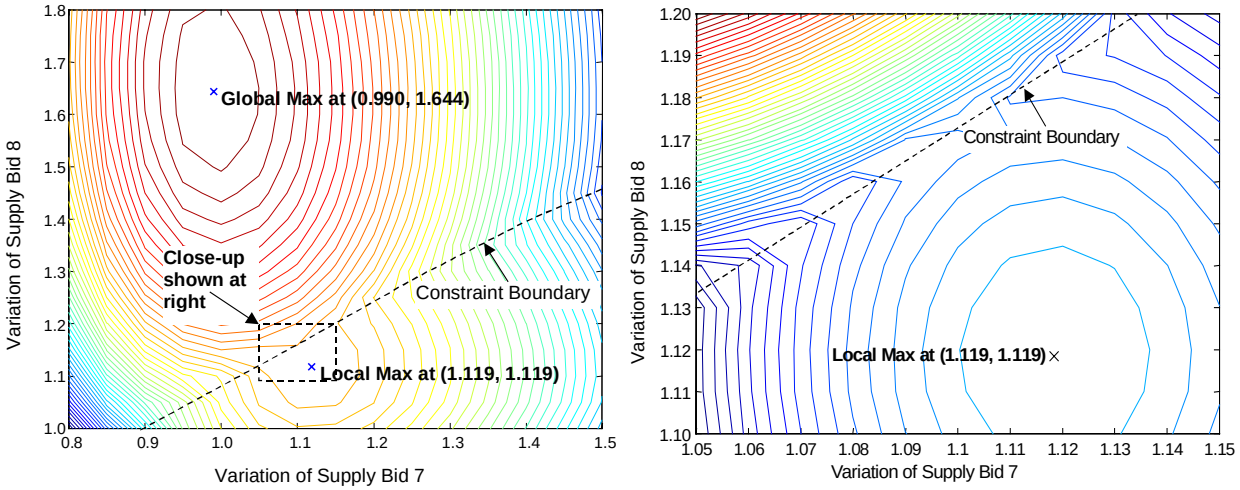

Figure 4.17 Contour Plots of Combined Profit of Supplier 7 and 8

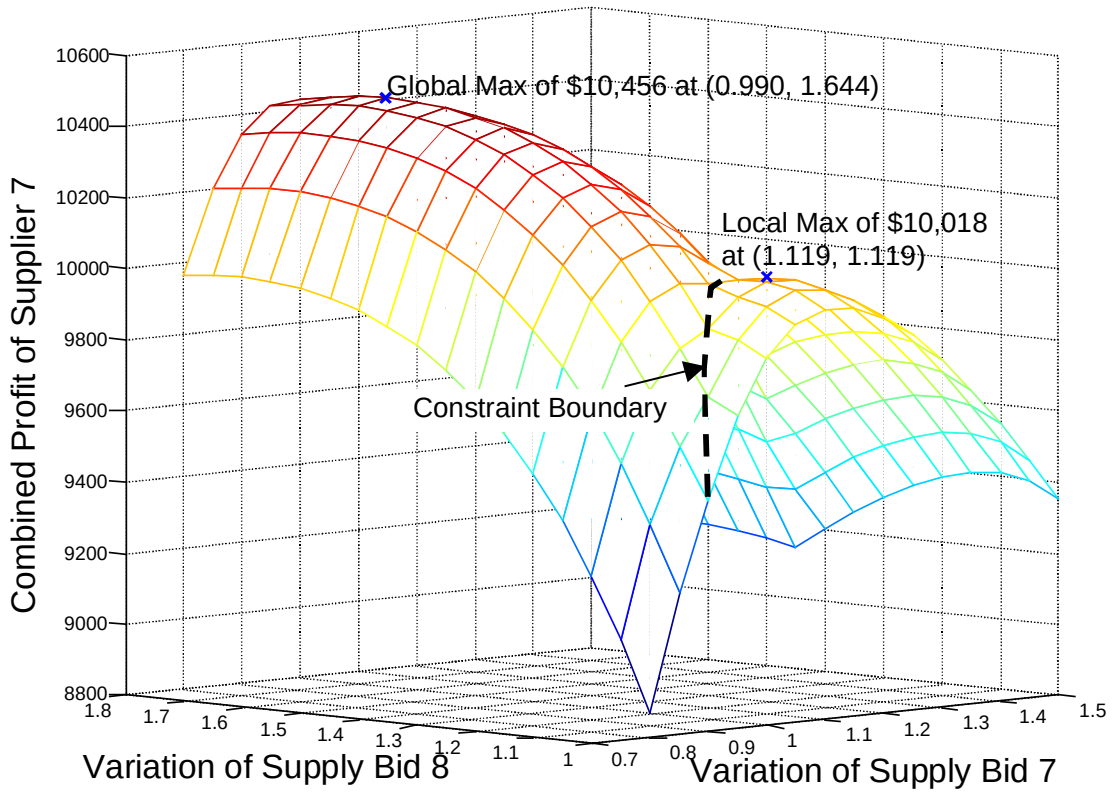

Figure 4.18 Three-Dimensional Plot of Combined Profit of Supplier 7 and 8

As can be seen from these figures, there are indeed two local maxima for the problem separated by a constraint boundary. This constraint boundary describes the region of the parameter space which results in the line between node 7 and 8 being exactly at its limit of 200 MVA. Again, as in the example from Section 4.4.2, this example shows that the individual welfare function even for very simple systems results in problems with many local optima. This continued reminder motivates the investigation of other more globally oriented optimization algorithms. While the calculus-based method developed thus far will be of invaluable use in finding a local maxima, it will invariably fail when trying to find other more interesting maxima. With this in mind, Chapter 5 will investigate the application of a genetic algorithm to this problem. Before continuing to Chapter 5, however, the computational requirements of this calculus-based method are considered.

4.7 Computational Requirements

The computational requirements for solving Equation (4.2) will scale linearly with the computation requirements of solving the OPF problem which represents the inner loop of the algorithm. The outer loop defined by Equation (4.12) is a very simple quadratic programming problem. As mentioned previously, very efficient methods for the solution of this problem exist [56] and can be used to quickly solve the problem described by Equation (4.12) in a time much faster than the solution of the OPF. As a result, the solution time for finding the local maxima will scale linearly with the OPF solution time.

The largest difficulty that is faced by the calculus-based method is the number of potential local maxima. A subset of the constraints in the system will exist which the individual has the ability to manipulate in an attempt to increase its welfare. If there are *n* constraints in this subset, there exists a potential for every combination of these constraints to result in a local maximum of the welfare function. This means that 2^n potential local maxima exist. While this looks to be a daunting task for any algorithm, the constraints in the system that the individual has the ability to manipulate will likely be known by the individual due to his experience with operating the system. Because of this, the user of the software algorithm could push the bids found for one local optimum into a region of the bidding space which would converge to another anticipated local optimum. Indeed, this is exactly what was done in Section 4.6 to find the second local maximum. Because of this, the calculus-based method will be of some use even without using a more globally oriented optimization routine. However, a global optimization technique, such as a genetic algorithm, will be useful in finding bidding strategies that an individual's experience does not point them toward.

4.8 Individual Welfare Maximization Algorithm Convergence

Convergence of the Individual Welfare Maximization algorithm for the systems studied thus far looks very promising. The primary reason for this is that a good initial guess is known: bid *k* = 1.0 for all suppliers and consumers. Unless a market is exceedingly noncompetitive, then market participants bid in the region of their true marginal costs and/or benefit curves, so this should be a reasonable initial guess. For all the systems studied thus far, convergence to the local maxima occurs within no more than four OPF iterations. The convergence characteristics of suppliers 7 and 8 of the nine-bus system studied in Section 4.6 are shown in Figure 4.19. This convergence is then superimposed on the contour plot of the combined profit for suppliers 7 and 8 in Figure 4.20.

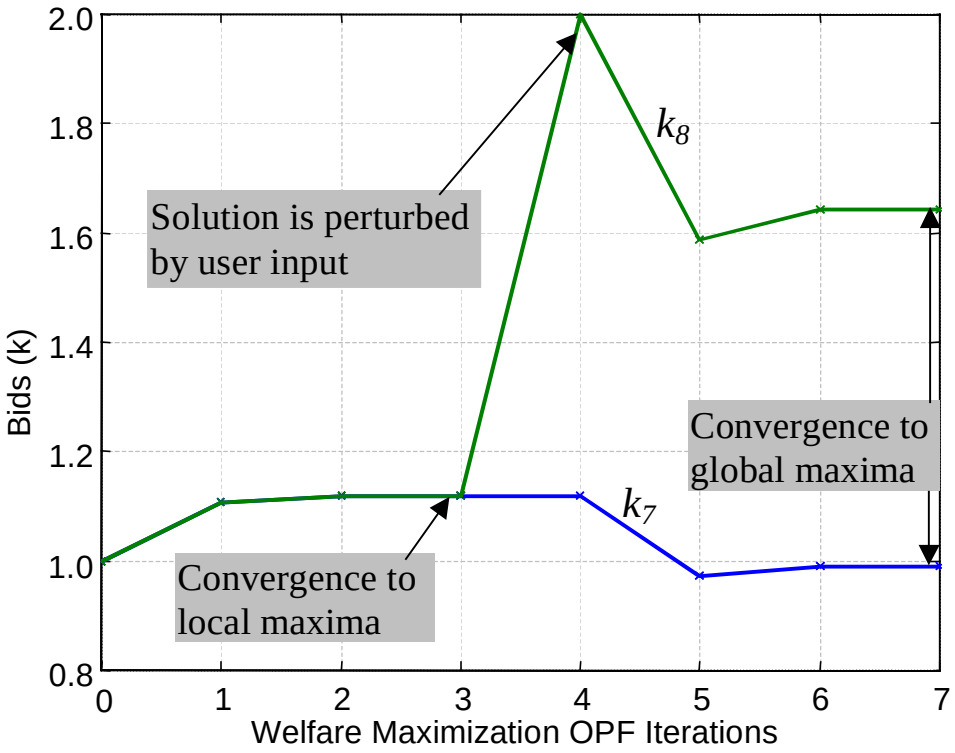

Figure 4.19 Bid Progression Using the Individual Welfare Maximization Algorithm for the Nine-Bus Example

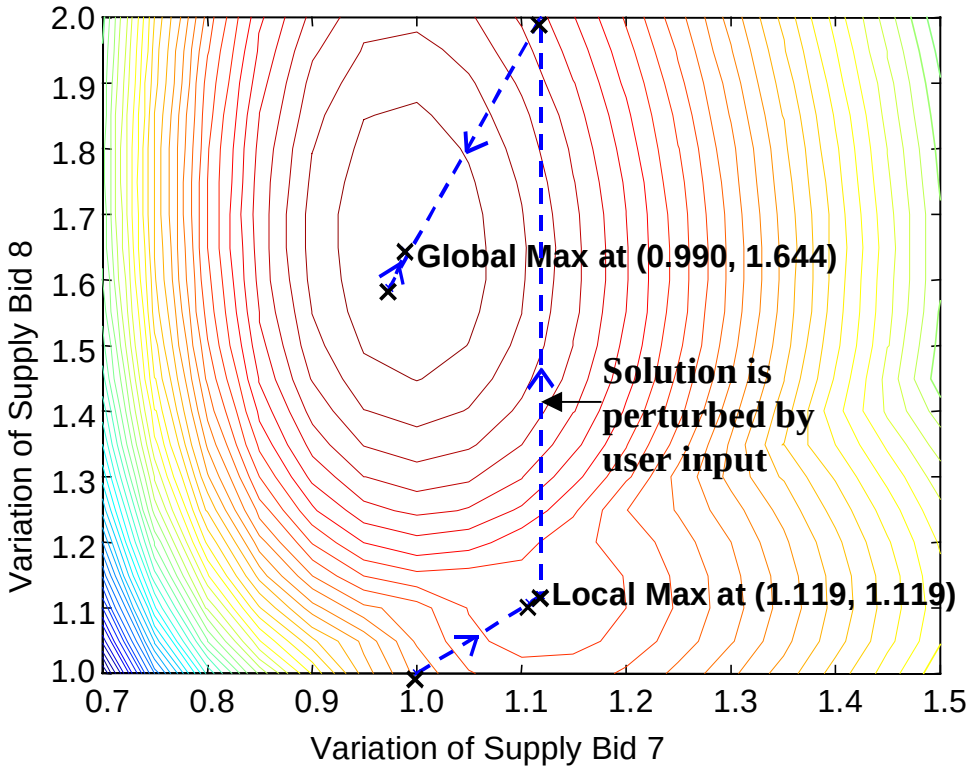

Figure 4.20 Bid Progression Superimposed on a Contour Plot of Combined Profit

4.9 Find Nash Equilibrium Algorithm Convergence

Convergence of the Find Nash Equilibrium algorithm for the systems studied thus far also looks very promising. Again, the primary reason is that good initial guesses are known. On all the systems studied thus far which had a Nash equilibrium to locate, convergence took no more than five generations of individuals solving their Individual Welfare Maximization algorithm. The convergence characteristics of the nine-bus system studied in Section 4.6 are shown in Figure 4.21.

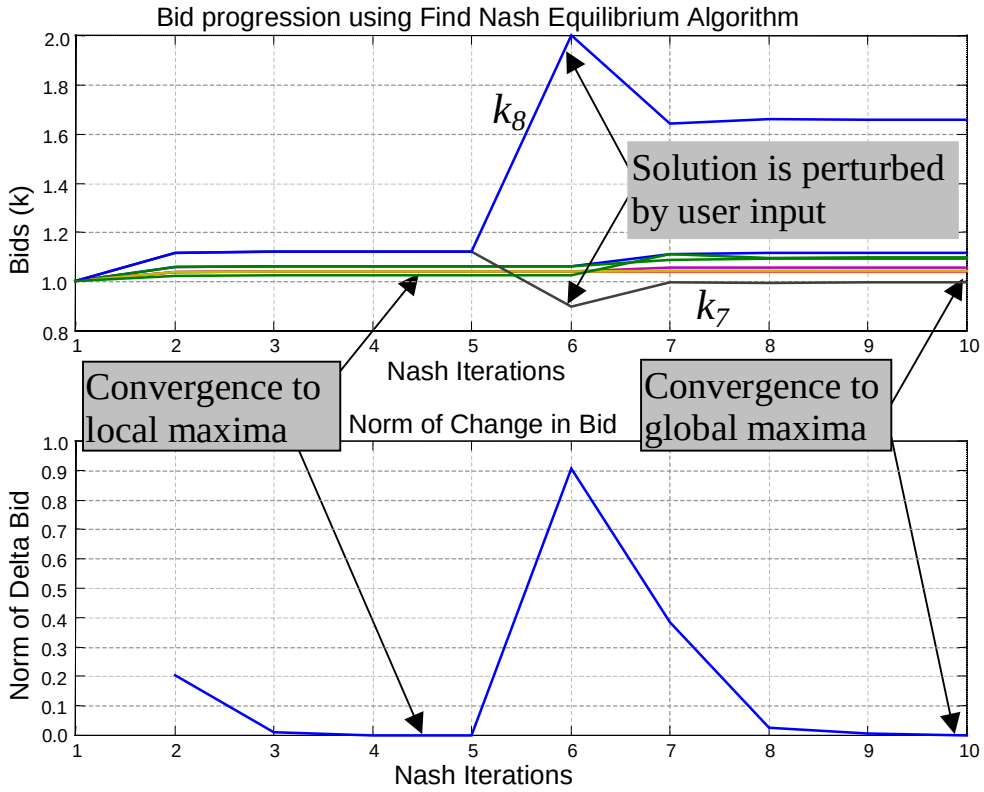

Figure 4.21 Convergence of the Find Nash Equilibrium Algorithm for the Nine-Bus Example

5. APPLICATION OF GENETIC ALGORITHMS TO INDIVIDUAL WELFARE MAXIMIZATION

Chapter 4 has shown that the individual welfare function can have multiple local maxima even in a simple two-bus, one-transmission-line system. The number of possible local maxima will be related to the number of consumers and demands controlled by an individual as well as the number of constraints which this set of consumers and demands can manipulate. No matter how effective the calculus-based method developed thus far becomes, it will only be able to aid in finding local maxima that the individual has some reason to expect might exist. As a result of this, for larger more realistic individual welfare maximization problems, other more global optimization techniques must be considered. Simulated annealing and genetic algorithms (GA) are two such techniques.

Simulated annealing is a search technique which draws inspiration from the formation of solids [58]. Annealing is the process of heating a solid (normally a metal) to a near liquid state and cooling it very slowly to form a solid. If the metal is cooled slowly enough, the potential energy of the resulting solid will be near the global minimum. A simulated annealing technique follows this analogy and uses a cooling (or annealing) schedule to help push a solution towards the global optimum.

Genetic algorithms (GA) are search techniques that draw inspiration from the natural selection found in nature [59]. A GA is initialized with a *population* of solutions and attempts to search the solution space by utilizing the ideals of nature: selection, mating (crossover), and mutation. Genetic algorithms are becoming more extensively used in power system research to help solve difficult problems [45], [60]-[66]. Genetic algorithms and simulated annealing have also been combined to make a hybrid algorithm with some success [67],[68].

This chapter will concentrate on applying genetic algorithms to the individual welfare maximization problem.

5.1 Brief Overview of Simple Genetic Algorithms

Before discussing the application of genetic algorithms to the problem of individual welfare optimization, a brief overview of genetic algorithms is provided. The first step in developing a genetic algorithm is defining a function, called the *fitness function*, that describes the fitness of an individual organism. In nature, an organism's fitness is determined by its ability to survive and reproduce while overcoming predators, disease, hunger, et cetera. In the artificial system of a GA, this complexity is removed and replaced with a single scalar fitness function. The fitness function in a GA typically represents a measure of profit, utility or performance. In a pure GA, this fitness function is the only problem-specific information used: no derivatives or other auxiliary information are used.

The next step in developing a genetic algorithm is representing the control parameters for the problem by a genetic coding or chromosome. The chromosome is represented by a binary string of ones and zeros. For example, if a problem has three real number control parameters, each parameter would be approximated by a binary string. Then these binary strings would be strung end-to-end to create a single binary string representing a coding for the entire problem.

With these defined, an initial population (set of chromosomes) is chosen at random and the genetic algorithm is applied to this population. The genetic algorithm uses three general processes to perform its search: selection, crossover, and mutation. These processes will be briefly described here.

5.1.1 Selection

The selection process performs a function analogous to competition in nature. In the artificial world of the GA, selection provides an organized way of determining which creatures in the population survive to move on to the new generation. Two very common general techniques used are stochastic sampling (also called roulette wheel) and tournament selection. In stochastic sampling, the probability that an individual survives and reproduces for the next generation is proportional to its fitness values. In this way, organisms with higher fitness are given more copies in the next generation. In tournament selection, two individuals are selected at random from the population and the more fit individual moves on to the next generation. This is done repeatedly to create the next generation.

5.1.2 Crossover

The crossover process performs a function analogous to sexual reproduction in nature. Pairs of organisms in the population are chosen at random. Then with a probability called the crossover probability, these pairs exchange parts of their chromosomes. This exchange is called crossover. Two simple examples of crossover are shown in Figure 5.1.

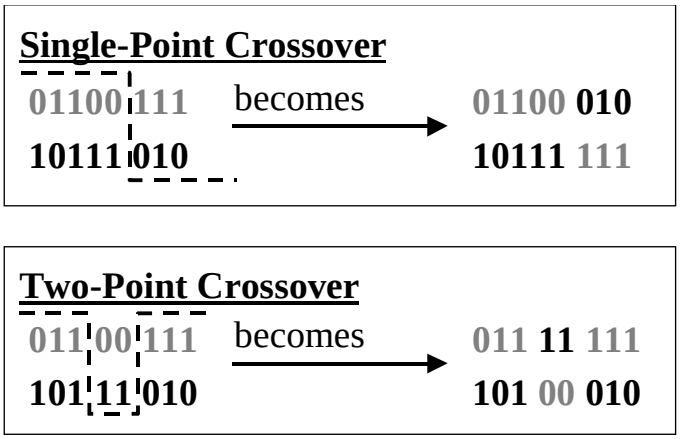

Figure 5.1 Examples of Simple Crossover

The exchange of genetic material serves as the searching process for the genetic algorithm. This is the primary manner in which the GA looks for better solutions throughout the parameter space.

5.1.3 Mutation

The final general process is mutation. It operates by randomly changing single bits during the solution process. Mutation is the most minor process done by the GA, serving only as a local search technique for the GA.

5.1.4 Genetic algorithm program flow

A genetic algorithm uses the following basic program flow:

GA Program Flow
1. Initialize population of generation 0
2. From generation k, create generation k+1 by performing three genetic operations:
   a. Selection
   b. Crossover
   c. Mutation
3. Increment k and redo step 2 until a predefined number of generations has past

5.1.5 What is a GA looking for?

At its heart, a genetic algorithm is looking for similarity templates of ones and zeros in the genetic code that tend to result in a good fitness. In GA theory, these similarity templates are called *schemata* [59]. Following the notation of [59], the * or *don't care* symbol is added to the existing alphabet of (0,1) to facilitate the representation of a schemata. For example, the schemata (*1*0**) represents a schemata of a 6-bit coding which has a 1 in the second bit and a 0 in the fourth bit. Also, the defining length of schemata H, denoted $\delta(H)$, is defined as the distance between the first and last string position specified in H. For example, δ (*1*0**) = 2 and δ (**0***) = 0.

Consider the simple 3-bit coding with the fitness function values shown in Table 5.1.

Table 5.1 Sample Fitness Function for a 3-bit Coding

Chromosome	Fitness
0 0 0	5
0 0 1	12
0 1 0	4
0 1 1	10

Chromosome	Fitness
1 0 0	8
1 0 1	20
1 1 0	7
1 1 1	18

From a cursory glance at this function, one can see that the schemata (**1) is a highly favorable one, as is the schemata (1*1).

Now consider how the genetic operations of selection, crossover, and mutation affect the ability of the GA to find these schemata. Selection operates only to determine which organisms survive and live on to mate. Therefore, selection acts to help determine which schemata are good. Selection does not directly impact the chromosome. Crossover acts directly on the chromosome itself, so it will act to look for new schemata, but will also act to split up good schemata that have already been found. A GA will have a much easier time finding schemata of lower defining length because crossover will be less likely to split apart these schemata.

5.2 Application of a Simple Genetic Algorithm to Individual Welfare Maximization

This section covers the application of a simple genetic algorithm to the maximization of individual welfare. The fitness function and coding for the problem are covered first. Then an example is shown.

5.2.1 Fitness and fitness scaling

Individual welfare maximization attempts to determine the vector of bids **k** which maximizes individual welfare. Thus, the fitness function is obvious: individual welfare. Individual welfare

will be called the raw fitness for a set of parameters **k**. Most GAs also introduce some form of fitness scaling. If no fitness scaling is done, a few highly fit individuals can take over the population in the first several generations, thus preventing a more full investigation of the parameter space. In this situation, objective functions must be scaled back to prevent this takeover. Also, when the population has mostly converged, the fitness values throughout the population will be very similar, making the selection process weaker. In this situation, objective function differences must be accentuated to encourage more competition. In this application developed to maximize individual welfare, linear scaling with sigma truncation is used [59].

5.2.2 Coding

The control parameters for individual welfare maximization are the elements of the vector **k**. A minimum and a maximum range is specified for consumer and supplier *k*, and a binary code is used to linearly map the values in the range specified as shown in Figure 5.2.

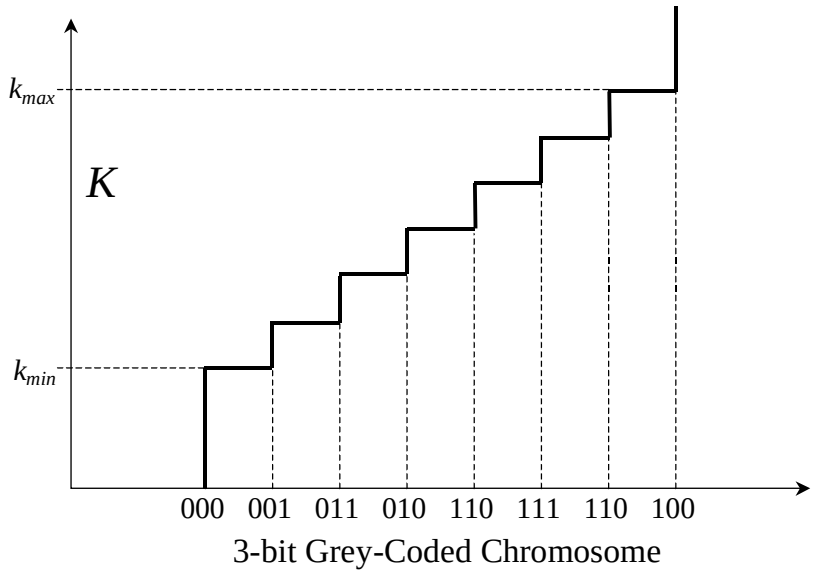

Figure 5.2 The Mapping of *k* Values to a Binary Grey Code

Note that the binary number scheme uses a grey code. A grey code is a binary number sequence for which consecutive numbers are only different by a single bit [69]. This is often done in genetic algorithms in order to avoid Hamming cliffs. A Hamming cliff occurs in a binary number sequence when every bit changes in consecutive numbers, e.g., three and four are represented in a normal binary sequence as 011 and 100, respectively. This sort of representation can make it difficult for a GA to find good schemata.

To form the complete chromosome for an organism represented by a set of parameters **k**, the binary representations of each element of **k** are strung together in a string. For example, define k_{max} = 1.7, k_{min} = 1.0, and use three bits to grey code the binary number. The chromosome representation for the three supplier bids k_1 = 1.2, k_2 = 1.6, and k_3 = 1.3 is then calculated. k_1 = 1.2 becomes 011; k_2 = 1.6 becomes 101; k_3 = 1.3 becomes 010. The chromosome is then 011 101 010.

5.2.3 Example of simple genetic algorithm used for individual welfare maximization

For illustrative purposes, the small two-bus example from Section 4.4.2 is used here. There are two generators competing against one another to serve one price-dependent consumer. A transmission line between the two buses has a limit of 80 MVA. Here, it assumed that supplier 1 submits a bid of k_1 = 1.35. Thus, it is known from Figure 4.8 that the individual welfare function for supplier 2 has two local maxima: 486 $/h at k_2 = 1.2 and 514 $/h at k_2 = 1.5. This part of Figure 4.8 is repeated here in Figure 5.3.

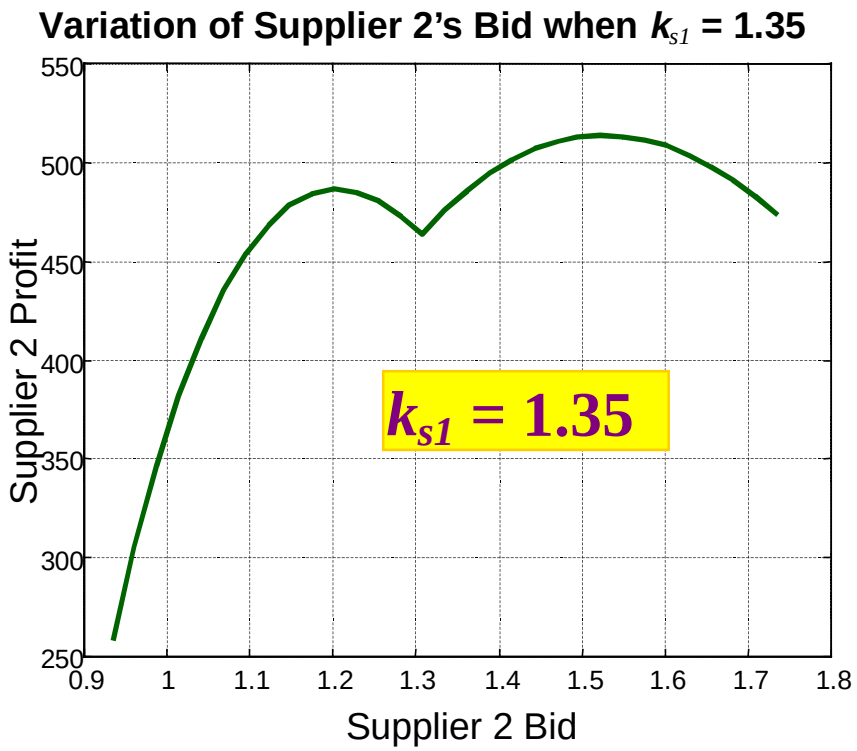

Figure 5.3 Supplier 2 Profit versus Bid

The bid for supplier 2 is coded as a 6-bit grey code with k_{max} = 2.0 and k_{min} = 0.9. The GA parameters are chosen:

- Population size = 20
- Crossover probability = 0.6
- Mutation probability = 0.0
- Roulette wheel selection is used.
- Linear scaling with sigma truncation is used.

The results for the first 10 generations of the GA are shown in Figure 5.4.

As can be seen from Figure 5.4, the action of the genetic algorithm does push the entire population to the global maximum fitness of 514 $/h at a bid of k_2 = 1.5. This example is obviously very simple, but is helpful for comparison to the method of species creation presented next.

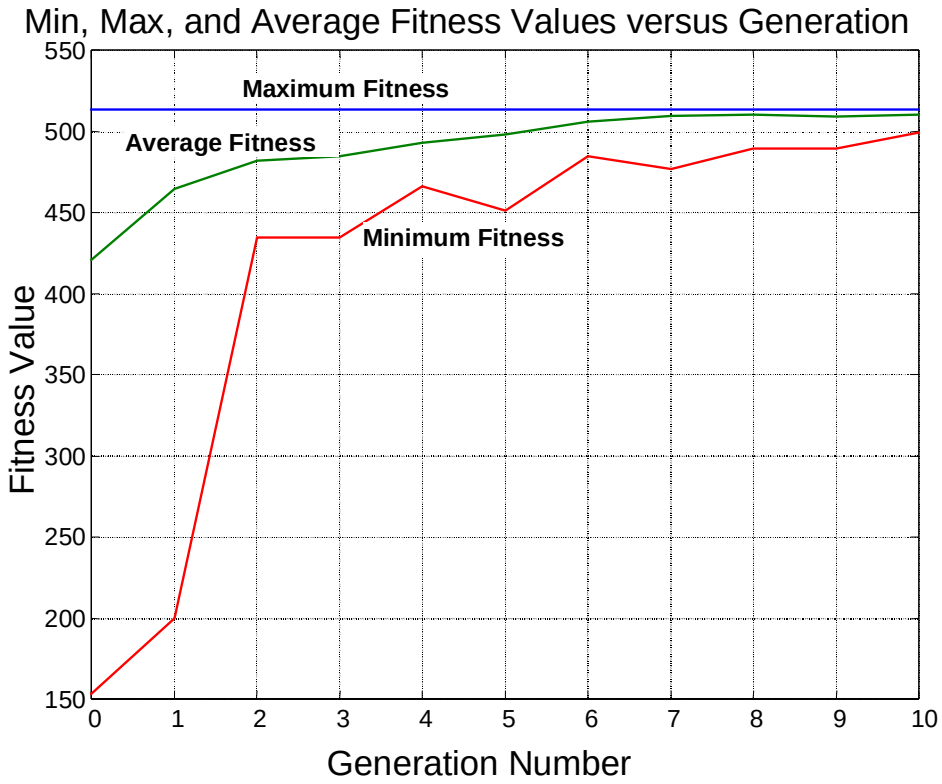

Figure 5.4 Fitness Progression of a Simple GA for the Two-Bus System

5.3 Species Creation through Fitness Sharing

As discussed thus far, a genetic algorithm can be an effective means of searching for a single global optimum in very complex function space. If a GA is run for enough generations, the population will converge to a single solution because of the selection pressure. Because a GA is searching a population of solutions, it might be hoped that the algorithm could converge to several local optima all at once. Drawing on the analogy to nature, these various local optima are referred to as species [68]. The different types of organisms in nature are called species, with each type filling a different niche in the environment. Several techniques exist in GA literature that make it possible to design a GA that will converge to several local optima [70],[71]. Here, following the development of [71], the technique of fitness sharing will be investigated for application to the individual welfare maximization problem.

5.3.1 Fitness sharing

In nature, a highly fit species takes over a niche, but not the entire population. Furthermore, the resources provided by the niche limits the number of organisms filling the niche. Essentially, all the organisms within the niche have to *share* the resources available in the niche. This analogy is used to develop a method of sharing.

In order to model a niche in a GA, a distance-metric, denoted d_{ij}, is defined to determine how close an organism is to another organism in the population. Organisms that are close to one another are then forced to share some of their fitness. This is modeled by defining a *sharing function*, $Sh(d_{ij})$, that is a function of d_{ij}:

$$Sh(d_{ij}) = \begin{cases} 1 - \left(\dfrac{d_{ij}}{\sigma_{share}} \right)^{\alpha} & ; \quad d_{ij} < \sigma_{share} \\ 0 & ; \quad d_{ij} \geq \sigma_{share} \end{cases} \tag{5.1}$$

The variable σ_{share} controls the distance at which sharing occurs. Finally, an organism's fitness is derated by dividing its fitness by the amount of sharing for the organism:

$$f_{shi} = \frac{f_i}{\sum_{j=1}^{n} Sh(d_{ij})} \tag{5.2}$$

When using this technique, having large numbers of highly fit organisms occupying the same area of the parameter space is discouraged. This is advantageous for the GA because once a highly fit niche is found, then it is only important to keep enough individuals in this space so that the niche does not die off. Using fitness sharing encourages some organisms in the population to search for other possibly even better niches, or at least other local optima.

The distance-metric d_{ij} has been introduced, but must still be defined. How the distance-metric is defined splits fitness sharing techniques into two categories: phenotypic sharing and

genotypic sharing. In natural systems, all the genetic material of an organism is called the *genotype*, while the organism formed by the interaction of the genotype with the environment is called the *phenotype*. In a GA, this analogy means the genotype is the coded binary string, while the phenotype is the actual control parameters of the problem. The distance-metric d_{ij} for genotypic sharing in a GA is typically defined as the total number of bits which are different when comparing chromosome i and chromosome j (called the Hamming distance). For phenotypic sharing, the distance-metric is often defined as the Euclidean distance in parameter space. For example, in the welfare maximization problem, the control parameters are the elements of vector $\mathbf{k}$: therefore, the distance-metric between parameter sets $\mathbf{k}_1$ and $\mathbf{k}_2$ is found using

$$d(\mathbf{k}_i, \mathbf{k}_j) = \left\| \mathbf{k}_i - \mathbf{k}_j \right\|_2 = \sqrt{\sum_{m=1}^{p} \left(k_{m,j} - k_{m,i} \right)^2} \tag{5.3}$$

In this dissertation, an investigation of only phenotypic sharing will be undertaken, as guidance from [71] suggests this is the best method of fitness sharing. Finally, some guidance for an estimate of the variable σ_{share} is also provided from [71]. Assuming that the local maxima are spaced equally throughout the parameter space, an estimate is determined by

$$\sigma_{share} = \frac{\sqrt{\sum_{m=1}^{p} \left(k_{m,\max} - k_{m,\min} \right)^2}}{2\sqrt[p]{q}} \tag{5.4}$$

where q is the number of local maxima expected, $k_{m,max}$ and $k_{m,min}$ are the maximum and minimum k_m allowed, and p is the number of parameters being determined.

Other more complex dynamic definitions of σ_{share} which change as the GA progresses are also possible [72], but are not investigated in this dissertation.

5.3.2 Mating restrictions

Fitness sharing can be very successful in encouraging a GA to find several local optima at once. However, once the GA converges to a point where most of the organisms are in niches, the mating between organisms in different niches can degrade the algorithm's performance. Consider Figure 5.5. The algorithm has converged to a point where Niche #1 and Niche #2 seem to be local optima for the problem. Crossover between organisms in the different niches would likely cause the algorithm to converge away from these highly fit areas, an undesirable result.

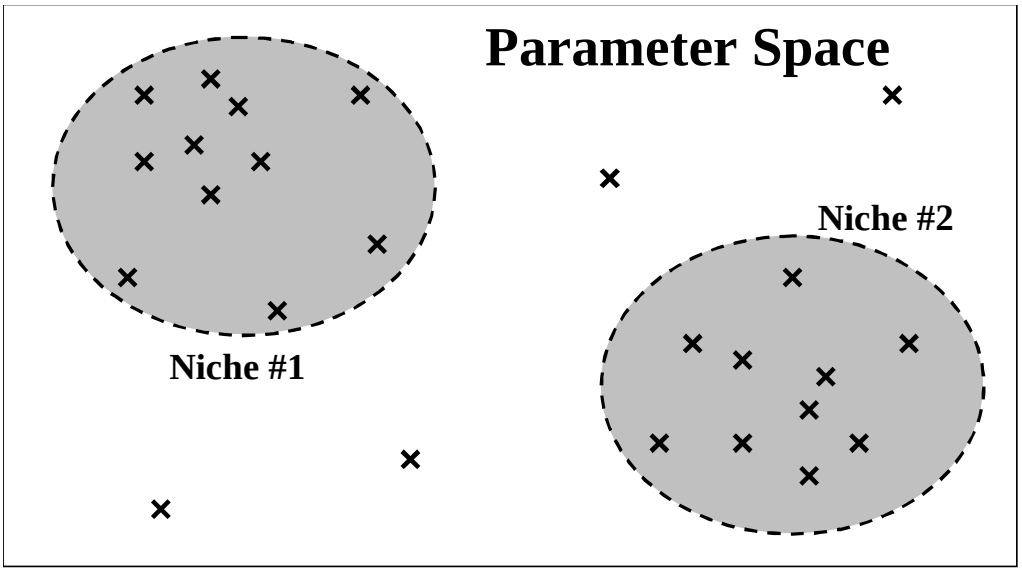

Figure 5.5 Illustration of Niche Formation in Parameter Space

In nature this problem is avoided by making mating between different species impossible. The same thing can be done in a genetic algorithm by restricting crossover to occur only between organisms that are within a specified distance of one another. This distance is called σ_{mating}. In this development, a simple restriction is placed on crossover so that only chromosomes within a distance $\sigma_{mating} = \sigma_{sharing}$ are allowed to mate. Other more complex arrangements are also possible, and future investigations into these may be fruitful [72].

5.4 Application of a GA with Fitness Sharing to Individual Welfare Maximization

This section provides two examples of the ability of GA to find more than one local maxima simultaneously.

5.4.1 Example with two local maxima

In order to demonstrate the effectiveness of adding fitness sharing to the GA, the same simple two-bus example of Section 5.2.3 is used again. The GA is run as done in Section 5.2.3, except that now fitness sharing is included in the GA. The results for the first 12 generations of the GA are shown in Figure 5.6.

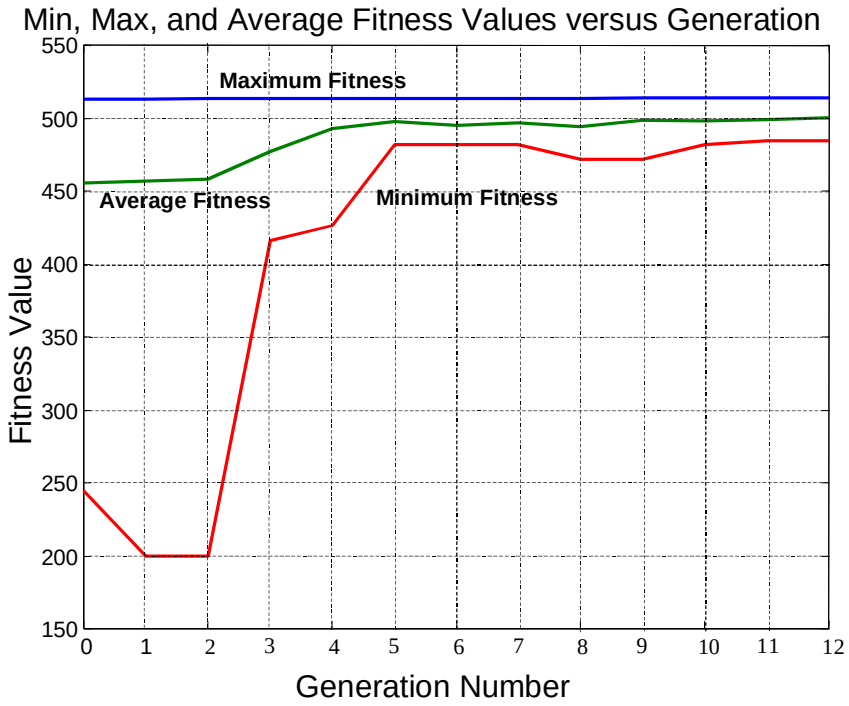

Figure 5.6 Fitness Progression of a GA with Fitness Sharing for the Two-Bus System

From looking at the minimum and maximum values in Figure 5.6, it is seen that the GA is not converging to a single solution as was occurring in Figure 5.4. In order to show that different species are indeed being developed, a plot of the final population's decoded parameters and their fitness values are superimposed on the actual individual welfare function from Figure 5.3.

Figure 5.7 shows this. The organisms in the final population are denoted by an X on the welfare curve. The number of copies of each organism at each X is denoted by the number next to the X.

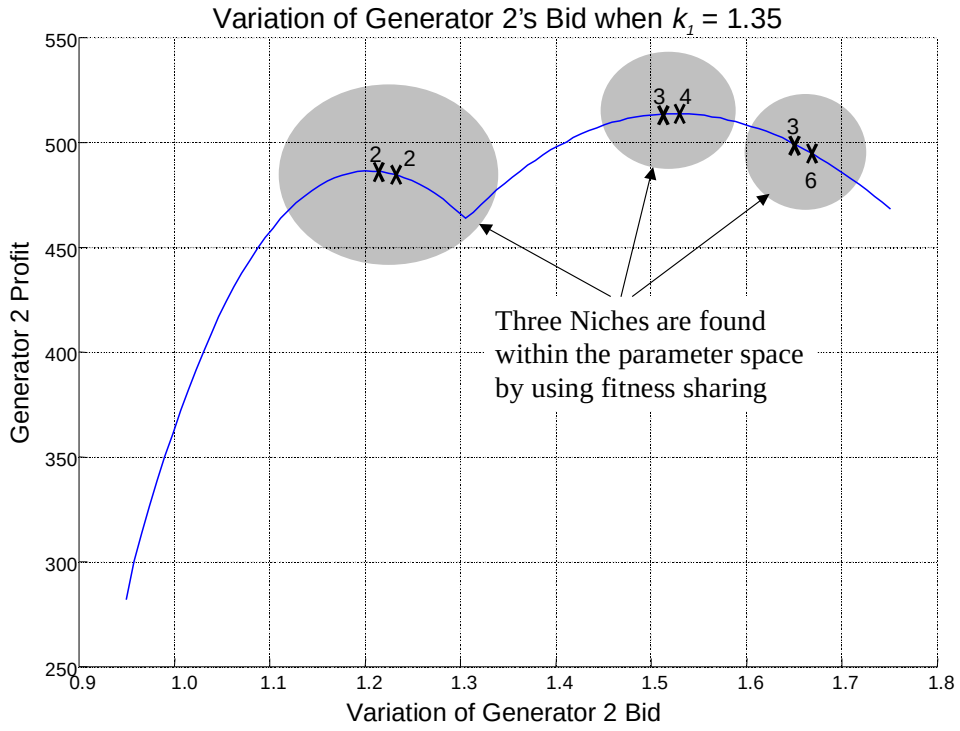

Figure 5.7 Final Population Superimposed on the Welfare Function

Figure 5.7 shows that fitness sharing has indeed helped the GA find the two local maxima of the individual welfare function. The third niche of organisms seen on the far right in Figure 5.7 occurs due to the properties of the distance-metric described in Equation (5.3). Chromosomes that are to the extremes of the defined bid range will inherently have larger distance-metric values because they are at the extremes of the bidding range. This will result in smaller sharing function values, meaning that chromosomes at the extremes will be unduly favored by the fitness sharing algorithm. This results in a tendency for niches to form at the extremes of the bidding range. This does not occur of the left in Figure 5.7 because the raw fitness value is low enough to offset the tendency. While this is a curiosity, it does not affect the utility of the GA. By simply making use of our calculus-based method at the end of the GA, the local maxima will all be found and the niche and the far right will converge into the local maximum.

5.4.2 Example with three local maxima

In order to further demonstrate the ability of the genetic algorithm in finding local maxima, consider the nine-bus system from Section 4.6 with new cost and benefit functions as described in Table 5.2.

Table 5.2 Cost and Benefit Equation Coefficient for New Illustrative Example

Bus	Supplier *b* Coefficient	Supplier *c* Coefficient	Consumer *b* Coefficient	Consumer *c* Coefficient
1 (A)	21	0.07	80	-0.10
2 (B)	21	0.07	80	-0.10
3 (C)	21	0.07	80	-0.10
4 (D)	21	0.07	80	-0.10
5 (E)	21	0.07	80	-0.10
6 (F)	21	0.07	80	-0.10
7 (G)	17	0.05	80	-0.10
8 (H)	0	0.10	440	-0.50
9 (I)	17	0.05	80	-0.10

The solution of the social welfare maximum when all consumers and suppliers submit their true marginal cost bids is shown in Figure 5.8 and summarized in Table 5.3.

Table 5.3 Economic Results When All Bids Correspond to True Marginal Cost

Bus	Price [$/MWh]	Supplier Output [MW]	Supplier Profit [$/h]	Consumer Demand [MW]	Consumer Welfare [$/h]
1	44.83	170.21	2,028.00	175.85	3,092.43
2	44.83	170.21	2,028.00	175.85	3,092.43
3	44.83	170.21	2,028.00	175.85	3,092.43
4	44.83	170.21	2,028.00	175.85	3,092.43
5	44.83	170.21	2,028.00	175.85	3,092.43
6	44.83	170.21	2,028.00	175.85	3,092.43
7	44.83	278.29	**3,872.38**	175.85	3,092.43
8	44.83	224.15	**5,024.19**	395.17	78,079.90
9	44.83	278.29	**3,872.38**	175.85	3,092.43
Totals		**1801.99**	**24,936.94**	**1801.99**	**102,819.33**

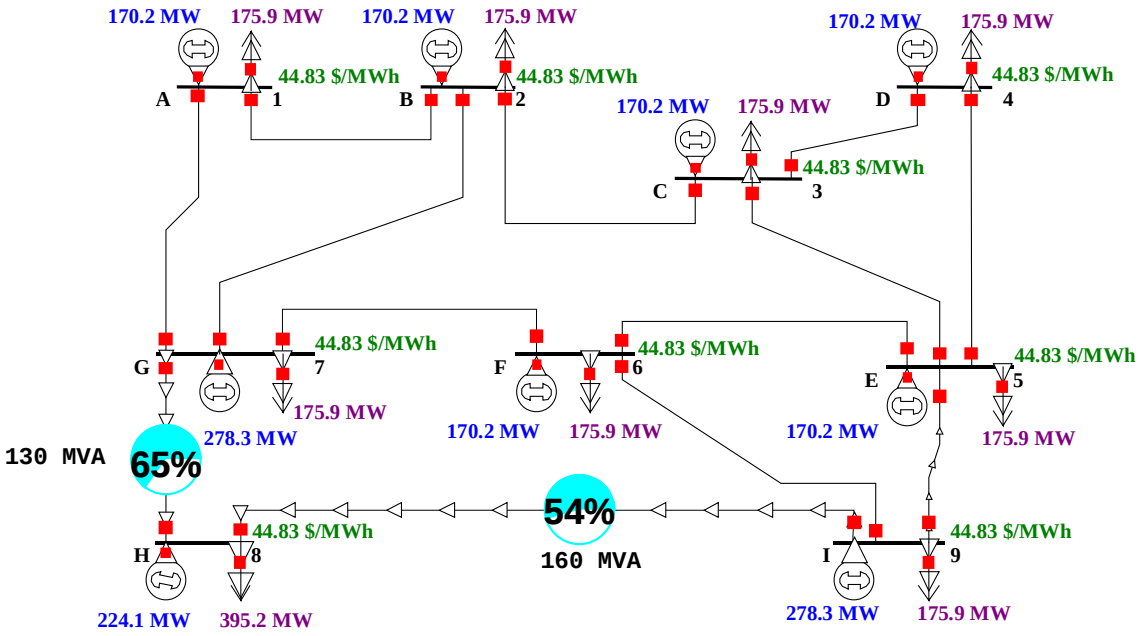

Figure 5.8 Social Welfare Maximum When All Consumer and Suppliers Bid Marginal

Two transmission line limits are defined for the system in hopes of inducing more than two local welfare maxima for the system. The transmission line between buses 7 and 8 is limited to 130 MVA, and the transmission line between buses 9 and 8 is limited to 160 MVA. Thus, four possible local maxima scenarios exist for this system:

1. Bid to induce no overloads.
2. Bid to induce an overload on the transmission line between buses 7 and 8.
3. Bid to induce an overload on the transmission line between buses 9 and 8.
4. Bid to induce an overload on both transmission lines.

In order to investigate the possibility of the local maxima, it is assumed that the suppliers at buses 1-6 and all of the consumers bid $k = 1$. The GA investigates the maximum welfare for an individual who controls the bid of suppliers 7, 8, and 9. The GA parameters are as follows.

- Population size = 50
- Crossover Probability = 0.7; Mutation Probability = 0.0001
- Roulette wheel selection is used.
- Linear Scaling with sigma truncation is used.
- Fitness sharing is used.

The progression of the maximum and average fitness from 40 generations of the GA is shown in Figure 5.9. The computation time for the GA was 1 h 18 min for these 40 generations, or about 2 min per generation of the GA.

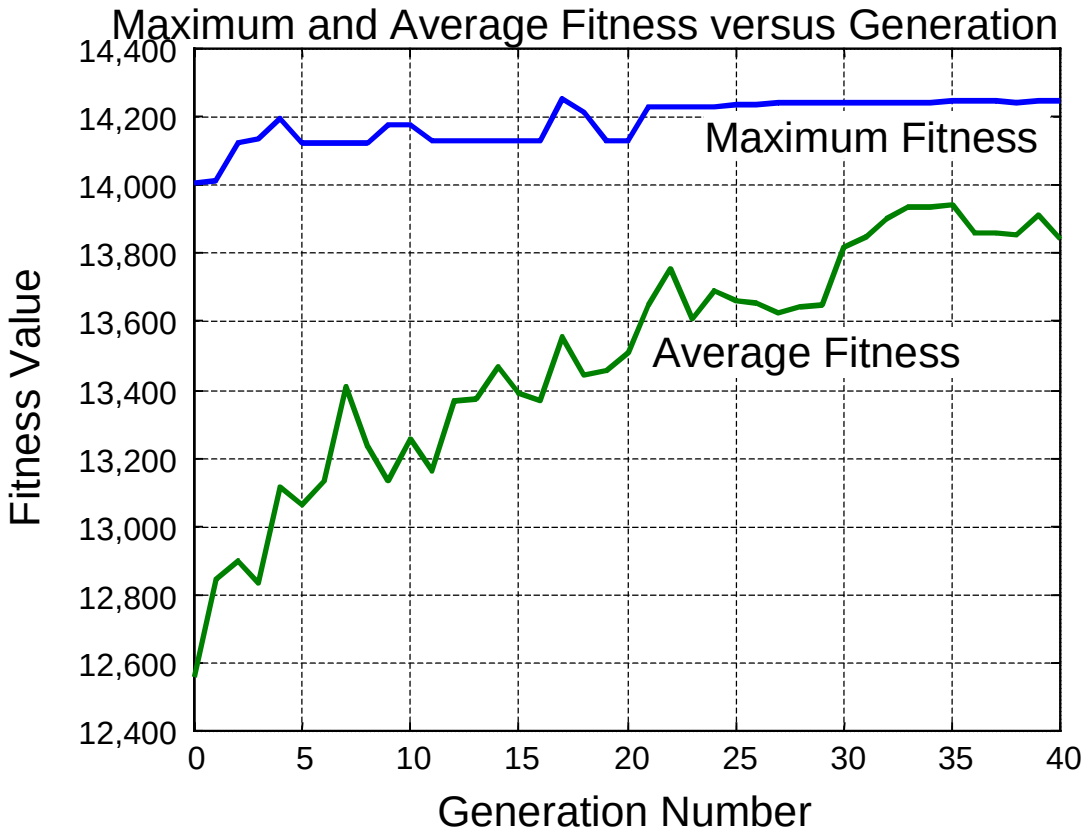

Figure 5.9 Fitness Progression of a GA with Fitness Sharing for the Nine-Bus System

The final population of the GA is described in Table 5.4, which shows bids determined for suppliers 7 - 9 as well as the total welfare for these three suppliers. From glancing at the bids shown in the table, one can roughly group them into four separate niches. The niches are signified in Table 5.4 by the thick black lines that surround parts of the table.

In order to see if these niches correspond to any local maxima, each of the 50 organisms is used as a starting point for the calculus-based method discussed in Chapter 4. All of the organisms converge into one of three solutions corresponding to three local maxima. The GA has indeed found three local maxima simultaneously. The local maximum that each organism

converges to is denoted in the "Conv. To" column of Table 5.4 by a number 0, 1, or 2. These numbers correspond to how many transmission lines are at their limit at the maximum which the organism converges to.

Table 5.4 Final Population of GA

Raw Fitness	k_7	k_8	k_9	Conv. to
13,190	1.040	1.329	1.302	0
13,190	1.040	1.329	1.302	0
12,839	0.900	1.238	1.302	1
12,860	0.900	1.238	1.721	1
13,188	1.040	1.329	1.721	1
13,188	1.040	1.329	1.721	1
13,258	1.040	1.329	1.598	1
13,258	1.040	1.329	1.598	1
13,907	0.900	2.796	1.302	1
13,907	0.900	2.796	1.302	1
13,939	0.900	2.521	1.302	1
14,017	1.040	2.521	1.721	1
14,017	1.040	2.521	1.721	1
14,017	1.040	2.521	1.721	1
14,062	0.900	2.521	1.721	1
13,904	1.040	2.796	1.302	1
13,962	1.040	2.796	1.721	1
14,009	0.900	2.796	1.721	1
13,887	1.040	2.888	1.302	1
13,887	1.040	2.888	1.302	1
13,887	1.040	2.888	1.302	1
13,887	1.040	2.888	1.302	1
13,887	1.040	2.888	1.302	1
13,887	1.040	2.888	1.302	1
13,887	1.040	2.888	1.302	1

Raw Fitness	k_7	k_8	k_9	Conv. To
13,363	1.040	4.538	1.721	2
13,363	1.040	4.538	1.721	2
13,839	0.900	4.538	1.162	2
14,089	1.040	4.538	1.162	2
14,089	1.040	4.538	1.162	2
14,089	1.040	4.538	1.162	2
14,089	1.040	4.538	1.162	2
14,089	1.040	4.538	1.162	2
14,122	1.040	4.538	1.302	2
14,122	1.040	4.538	1.302	2
14,122	1.040	4.538	1.302	2
14,122	1.040	4.538	1.302	2
14,122	1.040	4.538	1.302	2
13,484	1.040	6.028	1.721	2
13,484	1.040	6.028	1.721	2
14,243	1.040	6.028	1.302	2
14,243	1.040	6.028	1.302	2
14,243	1.040	6.028	1.302	2
14,243	1.040	6.028	1.302	2
14,243	1.040	6.028	1.302	2
14,243	1.040	6.028	1.302	2
14,245	1.075	6.028	1.302	2
13,478	1.040	6.400	1.721	2
14,237	1.040	6.400	1.302	2
14,237	1.040	6.400	1.302	2

The local maximum which has no transmission lines at their limits occurs for a bid k_7 = 1.194, k_8 = 1.194, and k_9 = 1.194. The market dispatch for this local maximum is summarized in Table 5.5 and Figure 5.10.

Table 5.5 Local Optimum With No Lines at a Limit

Bus	Price [$/MWh]	Supplier Output [MW]	Supplier Profit [$/h]	Consumer Demand [MW]	Consumer Welfare [$/h]
1	46.57	182.63	2,334.77	167.16	2,794.21
2	46.57	182.63	2,334.77	167.16	2,794.21
3	46.57	182.63	2,334.77	167.16	2,794.21
4	46.57	182.63	2,334.77	167.16	2,794.21
5	46.57	182.63	2,334.77	167.16	2,794.21
6	46.57	182.63	2,334.77	167.16	2,794.21
7	46.57	219.97	**4,084.75**	167.16	2,794.21
8	46.57	194.98	**5,278.19**	393.43	77,394.28
9	46.57	219.97	**4,084.75**	167.16	2,794.21
Totals		**1730.70**	**27,456.34**	**1730.70**	**99,747.93**

Note that the suppliers at buses 7 through 9 have a combined profit of $13,447.69/h. Also note that the flow on the transmission line from bus 7 to bus 8 is 102.6 MVA (79%), and on the transmission line from bus 9 to bus 8 is 96.1 MVA (60%).

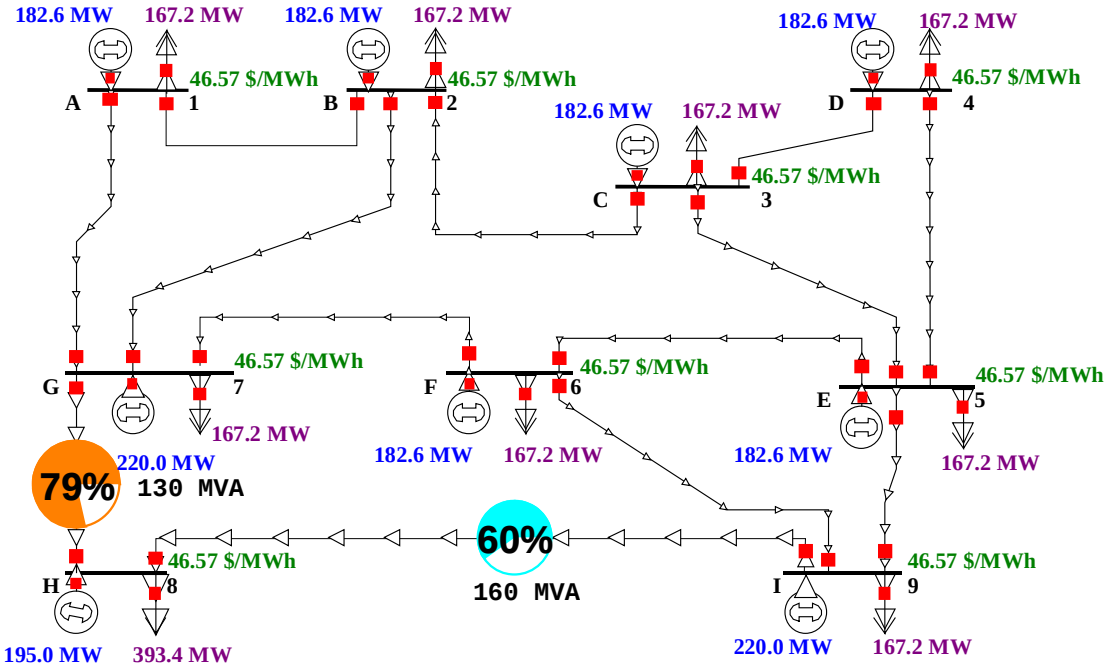

Figure 5.10 Local Optimum with No Lines at a Limit

The local maximum which has one transmission line at its limit occurs for a bid k_7 = 0.956, k_8 = 2.382, and k_9 = 1.636. The market dispatch for this local maximum is summarized Table 5.6 and Figure 5.11.

Table 5.6 Local Optimum With One Line at a Limit

Bus	Price [$/MWh]	Supplier Output [MW]	Supplier Profit [$/h]	Consumer Demand [MW]	Consumer Welfare [$/h]
1	43.83	163.08	1,861.52	180.85	3,270.61
2	44.72	169.43	2,009.57	176.40	3,111.55
3	47.39	188.53	2,487.95	163.03	2,657.93
4	48.28	194.89	2,658.70	158.58	2,514.70
5	49.17	201.24	2,835.02	154.13	2,375.52
6	48.28	194.89	2,658.70	158.58	2,514.70
7	42.94	279.34	**3,344.53**	185.30	3,433.62
8	60.81	127.64	**6,133.05**	379.19	71,890.77
9	52.74	173.31	**4,692.37**	136.30	1,857.73
Totals		**1692.35**	**28,681.40**	**1692.35**	**93,627.13**

Note that the suppliers at buses 7 through 9 have a combined profit of $14,169.95/h. Also note that the flow on the transmission line from bus 7 to bus 8 is 130.0 MVA (100%), and on the transmission line from bus 9 to bus 8 is 122.1 MVA (76%).

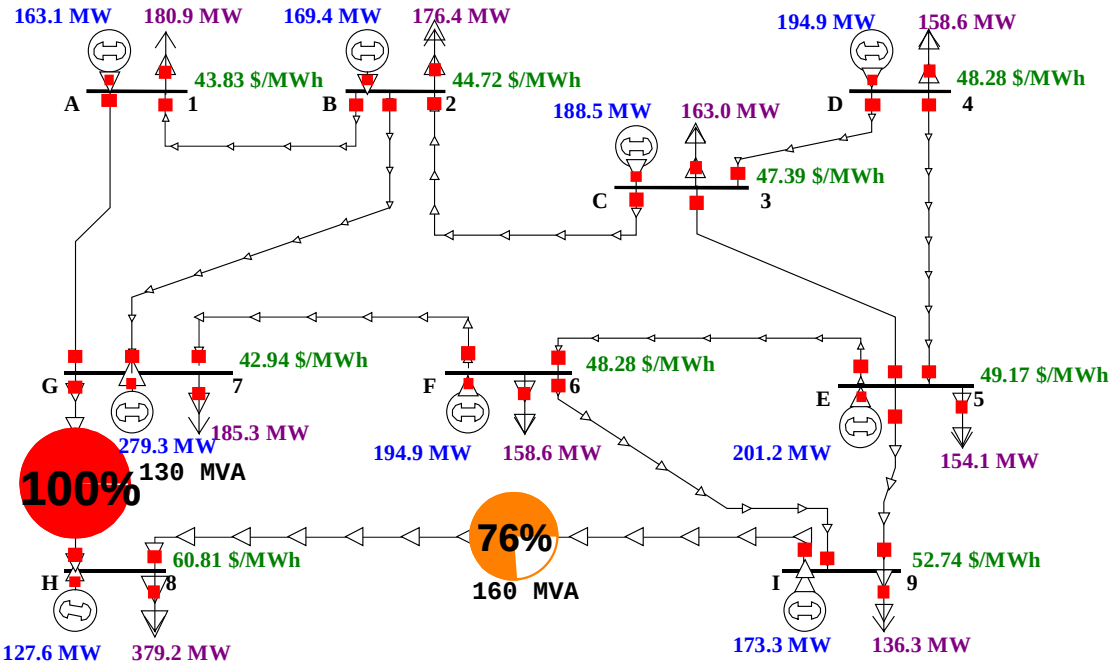

Figure 5.11 Local Optimum with One Line at a Limit

The local maximum which has both transmission lines at their limits occurs for a bid k_7 = 1.064, k_8 = 6.000, and k_9 = 1.249. The market dispatch for this local maximum is summarized in Table 5.7 and Figure 5.12.

Table 5.7 Local Optimum With Two Lines at a Limit

Bus	Price [$/MWh]	Supplier Output [MW]	Supplier Profit [$/h]	Consumer Demand [MW]	Consumer Welfare [$/h]
1	44.29	166.33	1,936.51	178.57	3,188.79
2	45.06	171.89	2,068.21	174.68	3,051.23
3	47.40	188.59	2,489.59	162.99	2,656.51
4	48.18	194.15	2,638.68	159.10	2,531.05
5	48.96	199.71	2,791.93	155.20	2,408.77
6	48.18	194.15	2,638.68	159.10	2,531.05
7	43.51	238.98	**3,479.07**	182.46	3,329.35
8	82.25	68.54	**5,167.49**	357.75	63,993.31
9	52.08	247.13	**5,614.38**	139.62	1,949.51
Totals		**1669.47**	**28,824.53**	**1669.47**	**85,639.57**

Note that the suppliers at buses 7 through 9 have a combined profit of $14,260.94/h. Also note that the flow on the transmission line from bus 7 to bus 8 is 130.0 MVA (100%), and on the transmission line from bus 9 to bus 8 is 160.0 MVA (100%).

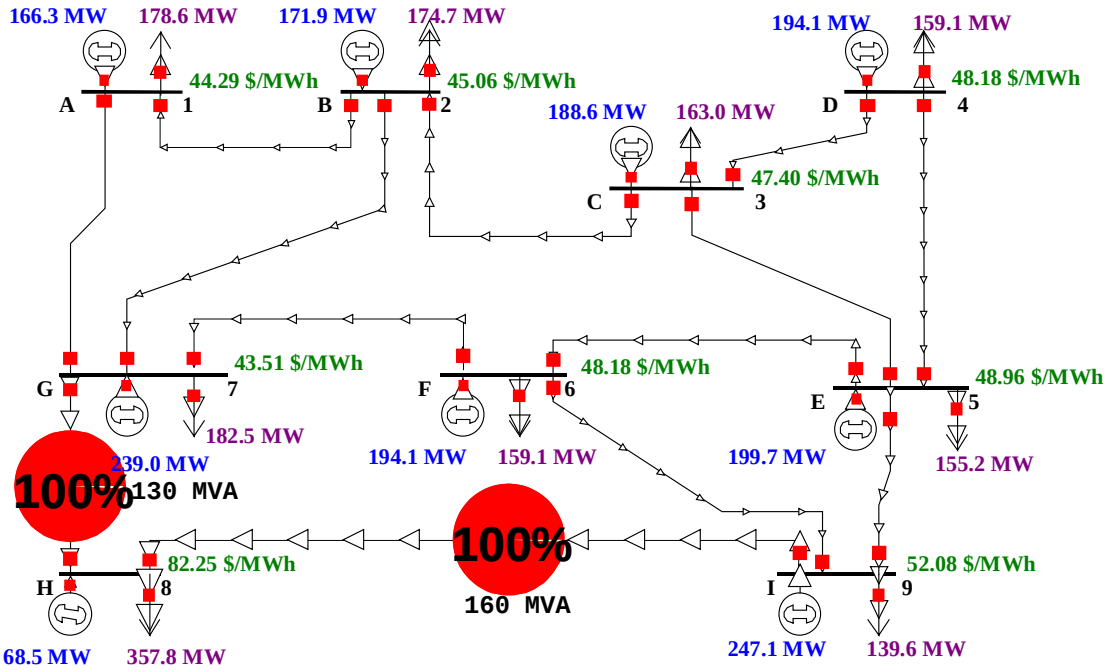

Figure 5.12 Local Optimum with Two Lines at a Limit

From this analysis, the welfare function of the individual controlling the bids for suppliers 7, 8, and 9 has three local optima, and the GA is able to find these local optima. Note, however, that the individual welfare values at the three local maxima are 13,447.69 $/h, 14,169.95 $/h, and 14,260.94 $/h, which are relatively close to one another allowing the GA a better chance of finding all three. Also note that 25 of the 50 organisms converge to the largest local max, and only two to the smallest local max, meaning the population of the GA will tend to contain local maxima in proportion to their fitness values. Because the GA only found two organisms in the smallest local maximum, it might be expected that if the relative magnitudes of these local maxima were different, then the GA could have difficulty finding all three.

In order to test this, the nine-bus system is further modified by changing the line limits from 130 and 160 MVA to 105 and 130 MVA, respectively. It can be shown using the calculus-based method that three local maxima still exist, but their welfare values are now 13,448 $/h, 15,627 $/h, and $16,856 $/h. The GA was again run on this example, and only the local maxima corresponding to the two higher fitness values were found. As the relative difference of local maxima fitness values increases, larger population sizes will be needed in order to find the less fit local maxima.

As parameters such as these line limits are varied, it is likely that the number of local maxima will change. In the example presented here, three local maxima existed, but one might ask why it was not four, two, or one. This topic is beyond the scope of this dissertation, but it is likely that bifurcations occur which cause the transition between different numbers of maxima [73]. The maxima experienced in the welfare function are related to the inequality constraints of the OPF problem. This might be similar to the mathematics describing immediate voltage instability caused by reactive power limits as addressed in [74].

6. USING CONTOURING VISUALIZATION FOR ANALYSIS AND MONITORING OF ELECTRICITY MARKETS [75]

While the bulk of this thesis concentrates on the optimization of electricity markets, this chapter takes a look at another computer tool which will be needed in restructuring electricity markets: computer visualization. Opening the electricity industry to competition inevitably involves introducing many new people to the vast amount of information available. To aid these people in making good decisions regarding the electrical system and the market, a new contouring visualization technique for power systems has been developed. This technique will have applications from the control center to the marketer. In the control center, system operators can use the visualization to help monitor the transmission system state, while the marketer can use the visualization to help analyze the vast amount of information regarding prospective energy trades. The remainder of this chapter explains the development of the contouring visualization technique. All visualization techniques presented here have been integrated into PowerWorld Simulator [52]-[53].

6.1 Motivation for the Development of New Visualization Techniques

As computing power continues to grow, engineers are both aided and burdened by the volumes of information these tools create. Within the electric utility industry, this is especially apparent as power engineers are confronted with analyzing and studying information regarding thousands of electrical nodes. Although extensive work has been done over the past decades in developing new ways to create greater and greater amounts of data, less work has been done in developing methods to aid understanding and interpretation of this data. However, with the advent of new hardware and software, this has begun to change. Specifically, much work has

been done recently in developing effective graphical user interfaces (GUIs) for energy management systems within present day control centers, with several examples described in [76]-[79].

When developing effective GUIs for any application, it is important to first consider the interaction between the computer and the user. These topics have been studied in detail in recent papers [80]-[82]. The investigations have found relatively good representations for power system information relating to branch data, such as line MVA flows, MW flows, line limits, etc., but have had less success in developing effective tools to visualize bus-related parameters such as voltage magnitudes and angles.

As a result, many power system engineers still rely heavily on text-based displays, such as tables or spreadsheets, for studying bus-related information. While this data is extremely accurate, the user can have a very difficult time perceiving patterns in large amounts of text. As an extension of this to a graphical environment, one-line displays have been created using digital numerical displays to provide bus-based information. While this is an improvement, it is still extremely difficult to quickly comprehend large amounts of data in this format.

6.2 Previous Voltage Visualization Work

An initial improvement on numerical displays has been to place an analog type display next to each bus. As an example, for bus voltage magnitudes, approaches based on placing a "thermometer" next to each bus have been used [83]-[86]. A simple thermometer is shown in Figure 6.1. In this example, more gray signifies a lower voltage.

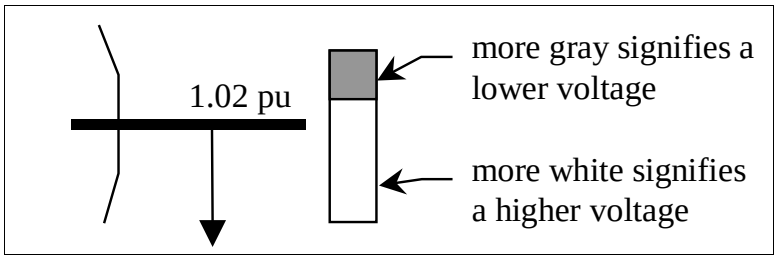

Figure 6.1 Basic Thermometer Graphic

The thermometer-based representation is definitely an improvement over the digital displays when looking at hundreds of buses, but it is still not easy find patterns in vast amounts of information this way.

As mentioned in [81], [83], and [84], possibly the first representation one thinks of for visualizing voltage information is the contour plot. However, before discussing contour plots in detail, it is useful to consider what constitutes a good graphical representation. Mahadev and Christie [81] lay out three guidelines which good graphical representations must follow:

1. Natural encoding of information
2. Task specific graphics
3. No gratuitous graphics

A contour plot meets all these requirements. First, it is a natural encoding of information. Anyone who has seen a temperature-forecast map on the evening news is familiar with this type of representation. For example, on the temperature map blue may signify low temperatures, while red signifies hot temperatures. Likewise, for power systems a contour can be developed where blue signifies low voltage magnitudes, while red signifies high voltage. Of course a gray scale can also be employed and is indeed preferable when presenting results in a dissertation printed in black and white.

Using customized one-line diagrams in which all the gratuitous graphics have been removed can satisfy the second and third guidelines. For example, graphics could be limited to the buses,

transmission lines, and the contour plot. Other graphics would make the display too busy and the user unable to distinguish between the different types of information being displayed.

While contour plots in general meet these guidelines, a key question must be addressed. Are contour plots an effective means for showing voltage information? Some potential objections include the following:

1. Voltages are defined at discrete points in a power system, not a continuum as assumed in a contour plot.
2. Tap-changing transformers may introduce sudden changes in voltage. Contour plots normally imply a slow variation in value.
3. Voltages that are near one another on a diagram may not be "near" one another electrically. This is especially true for different voltage levels.

While these objections certainly have merit, each can be adequately addressed [87]. The first is addressed by recognizing that the primary purpose of the contour is to aid in data interpretation. Contours let the user see the trends in voltages across a region. If desired, the contour can be augmented with traditional text-based information either from a printout or via numerical displays on the one-line diagram.

The second objection is a valid concern. Tap-changing transformers can introduce some problems in interpreting contour plots. When creating a contour, one assumes that a continuous change in the values occurs. This can be violated with the introduction of tap-changing transformers. Figure 6.2 shows this effect.

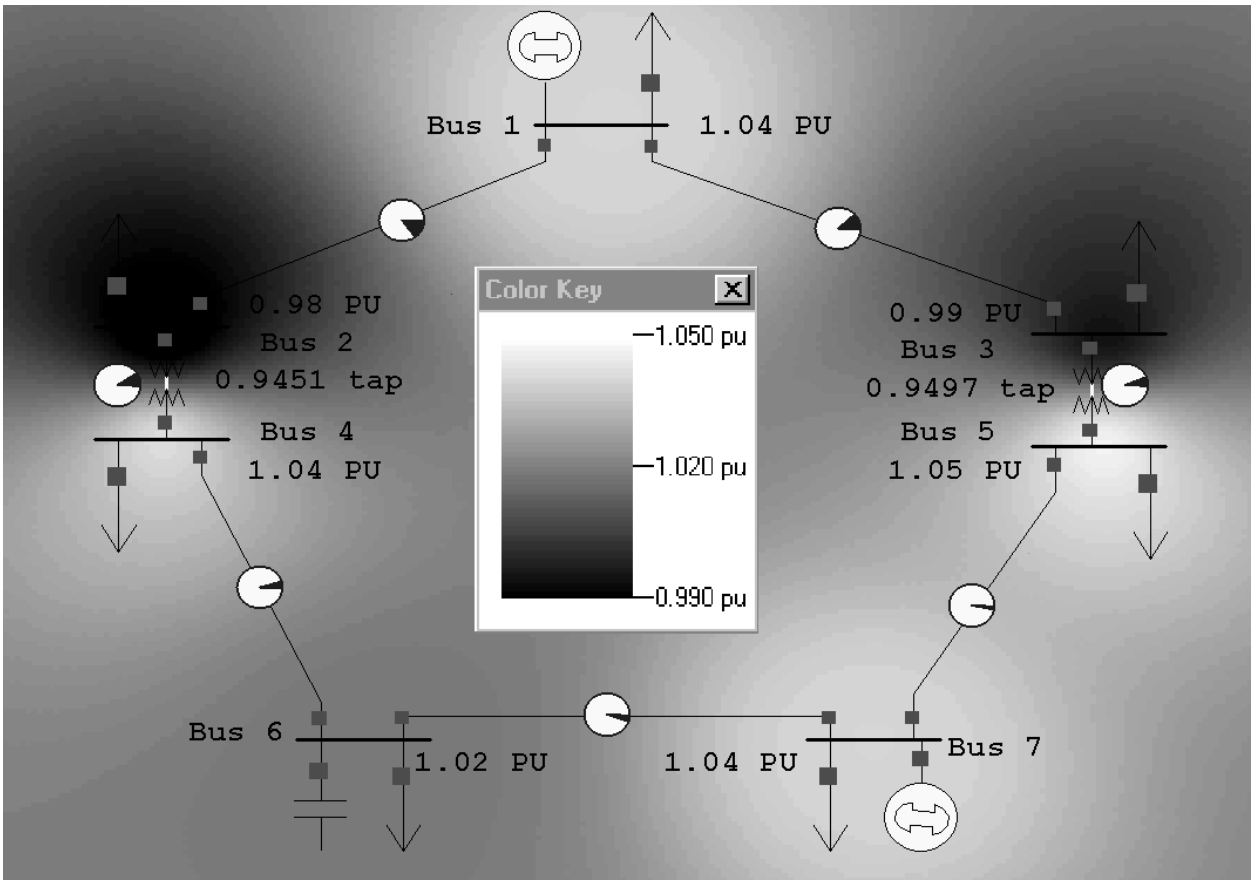

Figure 6.2 Tap-Changing Transformers Effects

In Figure 6.2, the buses at the upper-right and upper-left have tap-changing transformers connected to them. This results in having two buses next to one another with very different voltages. In the contour, having a dark and a light spot right next to one another depicts this. It is sometimes hard to see this effect, so caution must be used when looking at systems with a large number of tap-changing transformers. Avoid this problem by only contouring the buses at certain voltage levels.

The third objection is also overcome by only plotting one voltage level at a time and by judicious construction of the contouring diagram. For example, if a strictly geographical layout is used, normally buses of the same nominal voltage that are near each other geographically are

also near electrically. The example plots towards the end of this chapter help to show the effectiveness of the contouring approach.

6.3 Overview of Contouring Basics

Much of the data within a power system is referenced to the system buses. This includes information such as loads, generation, voltage magnitudes and angles, and bus spot prices. Buses, however, are only defined at discrete points within a power system. Therefore, a power system can be visualized as a two-dimensional region that has discrete values at points throughout the space. Thus the contour algorithm must map this discrete data into a continuous region. Essentially this can be thought of as low-pass filtering the data. Upon doing this filtering, a contour can be created which effectively displays the voltage profile of the system.

Of course for implementation on a computer this continuous space is represented by a grid of data points, in which the size of the grid is dependent upon the desired resolution on the computer screen. The job of the low-pass filter then is to calculate the *virtual values* of each point in this grid. These values can then be mapped to a color and the resulting contour plotted. In the calculation of these virtual values, buses that are closer to the virtual point should be weighted more than those that are farther away. Referring to Figure 6.3, the virtual value at the point (x_p, y_p) should weight the value at (x_5, y_5) more than the value at (x_6, y_6).

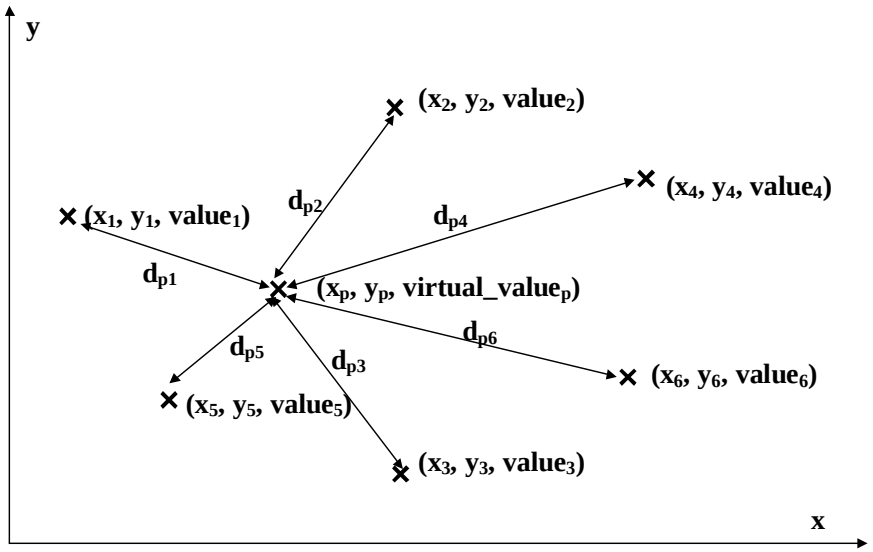

Figure 6.3 Calculation of the Virtual Value

The method presented in [87] for implementing this is to calculate a simple weighted-sum of the buses in the system for each virtual position as

$$v_p = \frac{\sum_{\text{i = all buses}} \left(v_i \frac{1}{d_{pi}^{\ \alpha}} \right)}{\sum_{\text{k = all buses}} \left(\frac{1}{d_{pk}^{\ \alpha}} \right)} \tag{6.1}$$

where v_p is the value for the virtual position p, v_i is the value for bus i, d_{pi} is the distance from p to the center of bus i, and α is a parameter controlling weighting.

By adjusting the parameter α, the user can control the relative weighting of close versus far buses. As α grows, buses that are closer receive higher weights, and as α grows toward infinity, only the bus that is closest to the virtual point is given any weight. For this thesis and for general purposes, using a value of $\alpha = 2$ is best as it provides the fastest computation time (computers calculate x^2 much faster than, say, $x^{1.5}$).

Calculating contours in this manner makes the basic assumption that buses near one another on the one-line diagram (i.e., near geographically) are "near" one another electrically. A sample

contour plot of the per unit voltage magnitudes for a six-bus system is shown in Figure 6.4. Here, white equates to higher and black to lower voltages. It is obvious at a glance what areas have high and low voltages.

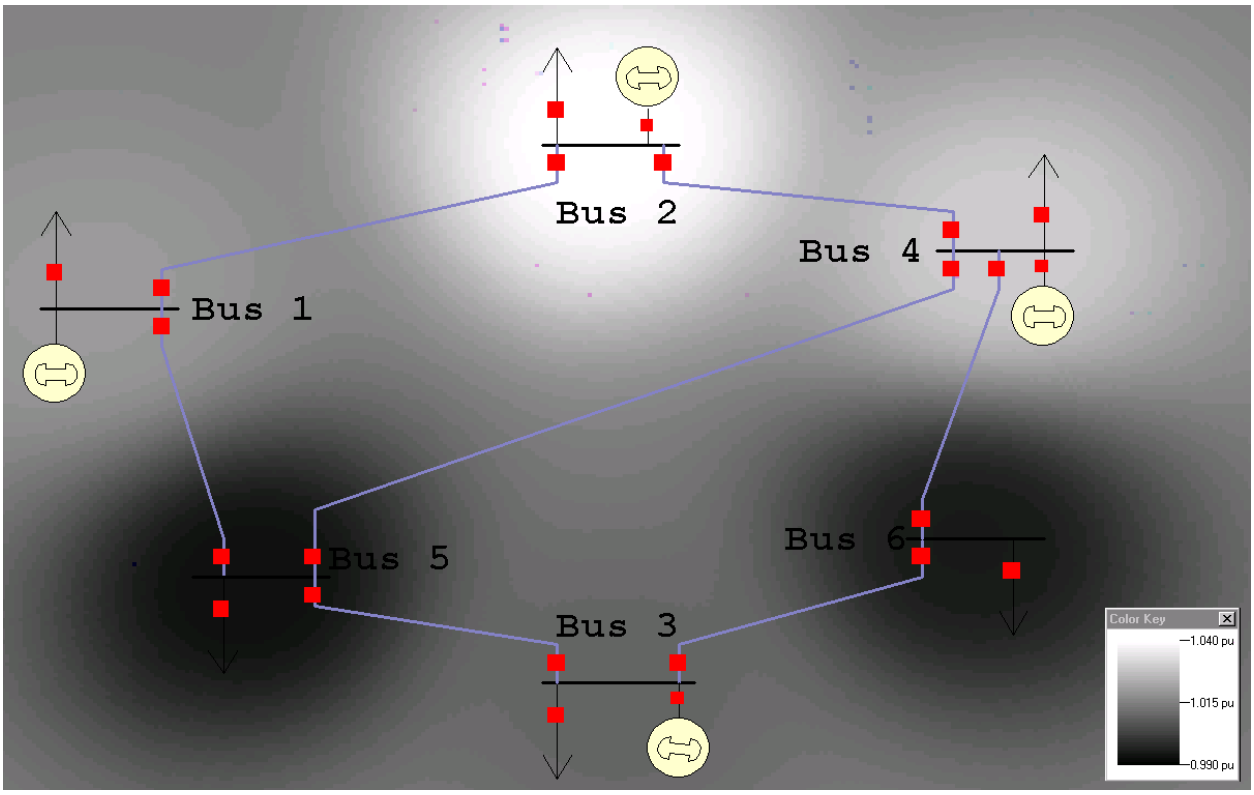

Figure 6.4 Sample Voltage Contour of Six-Bus System

Now that a method of calculating the virtual values across a two-dimensional area has been defined, it is important to consider how this value gets mapped to a color for display. To create the color-mapping, values were mapped to one of potentially 16.7 million different colors on a computer monitor. This corresponds to a value of between 0 and 255 for red, green, and blue. A common method for achieving this is shown in Figure 6.5. This is similar to the mapping used in Matlab's "Jet" color-map [88]. All values below some minimum value are mapped to dark blue and all values above some maximum value are mapped to dark red.

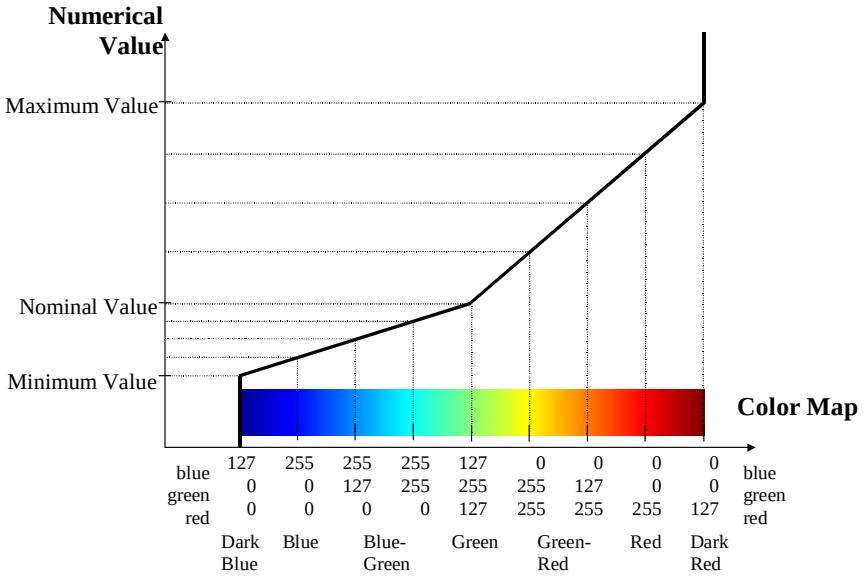

Figure 6.5 Color-Mapping for Red = High, Blue = Low

Within a power system, it is typical to maintain values within a specified limit. Thus when viewing system data it may be helpful to highlight any violations of these limits. This can be achieved by varying the color-mapping to include a discrete jump in color when the limit is crossed as shown in Figure 6.6.

Figure 6.7 shows the Figure 6.4 system with these discrete color changes implemented.

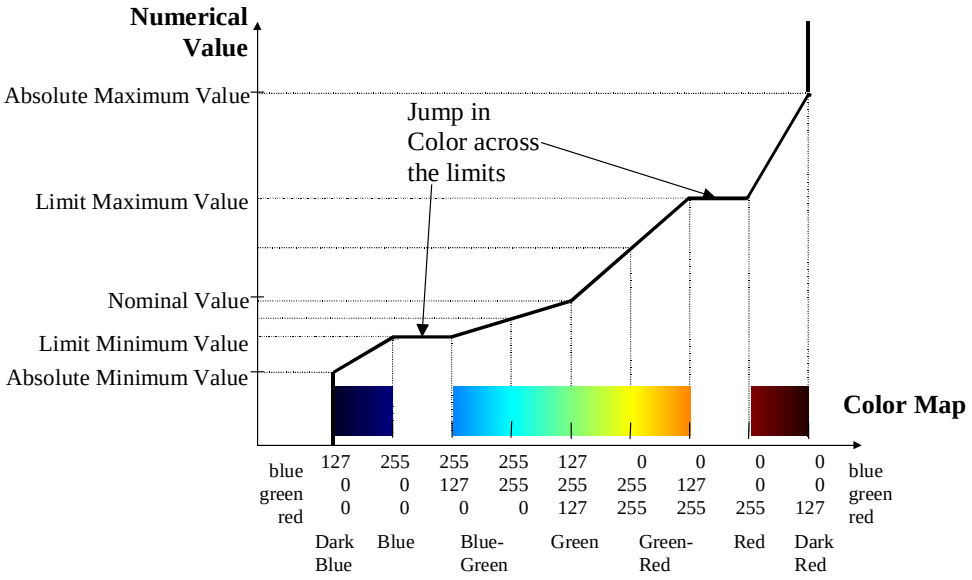

Figure 6.6 Color-Mapping with a Discrete Change at a Limit

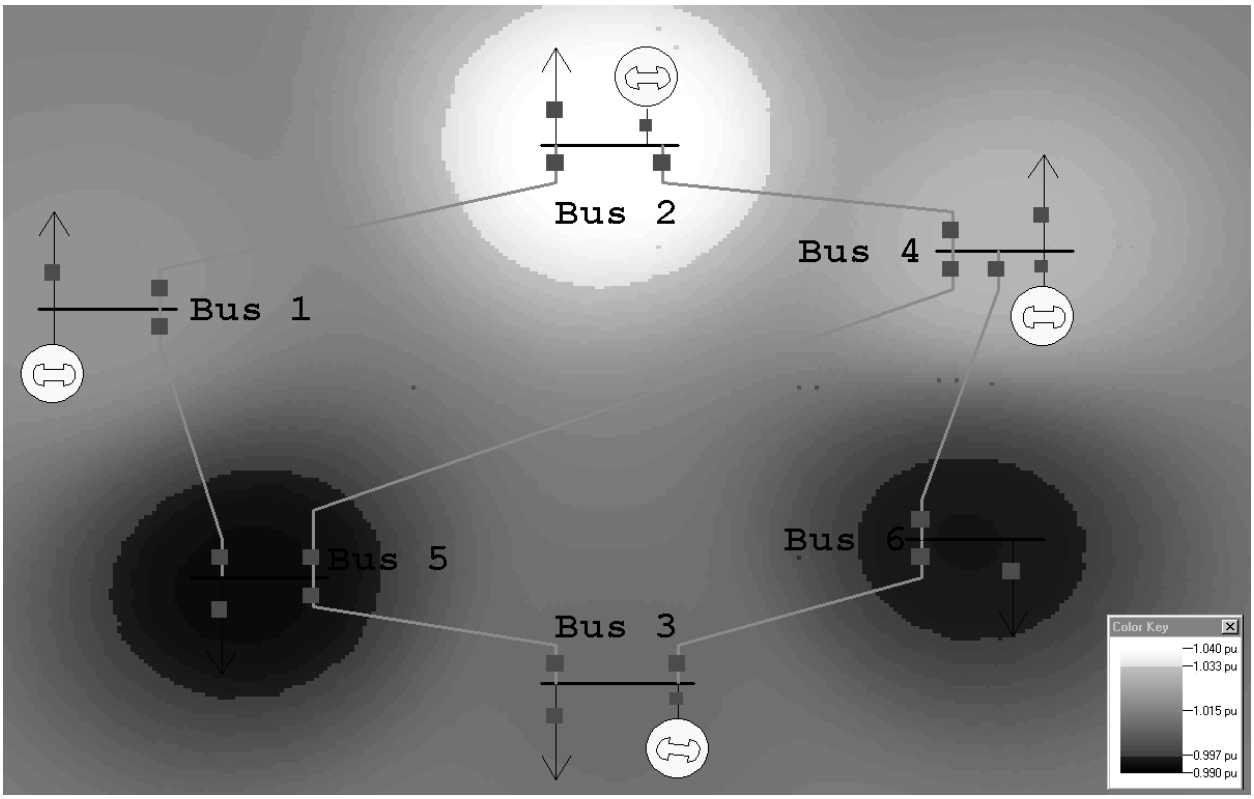

Figure 6.7 Voltage Magnitudes with Limits Highlighted

In Figure 6.7, the bus at the top of the figure and the two at the bottom left and right are outside their respective limits and are subsequently highlighted.

Of course any color-mapping is possible. For this dissertation, eight voltage magnitude color-mappings were implemented:

1. Blue = Low, Red = High : Best for visualizing values where high and low are both important.
2. Red = Low, Blue = High : The reverse of the previous color-mapping.
3. Black = Low, White = High : Only for use in creating black and white printouts.
4. White = Low, Black = High : The reverse of the previous color-mapping.
5. Red = High, Green = Normal : Useful for visualizing values where only the high limit is important. (Note: Radar Map High Limits is normally better.)
6. Green = Normal, Blue = Low : Useful for visualizing values where only the low limit is important. (Note: Radar Map Low Limits is normally better.)
7. Radar Map High Limits : Best for visualizing values where only the high limit is important. This mapping is based on the

colors typically used for radar maps of precipitation in the weather forecast.

8. Radar Map Low Limits : Best for visualizing values where only the low limit is important. This mapping is based on the colors typically used for radar maps of precipitation on the weather forecast.

Color-mappings 1-6 also have the option to highlight the limit violations as in Figure 6.7. Color-mappings 7-8 inherently highlight the limit violations all the time.

6.4 Fast Contouring Algorithm

The numerical algorithm used to calculate the contours initially reported in [87] was quite successful; however, calculation times to contour large systems took from 10-15 on a 200-MHz Pentium Pro-based PC. While this was adequate for creating snapshots of the voltage profile in a power system, it was far too slow for realistic implementation of real-time animation of the contours. As a result, a new technique was developed in [75] and is presented here again. In this technique each bus is processed in turn, with a conceptual circle drawn around the center of the bus to represent the influence region of the bus, as shown in Figure 6.8.

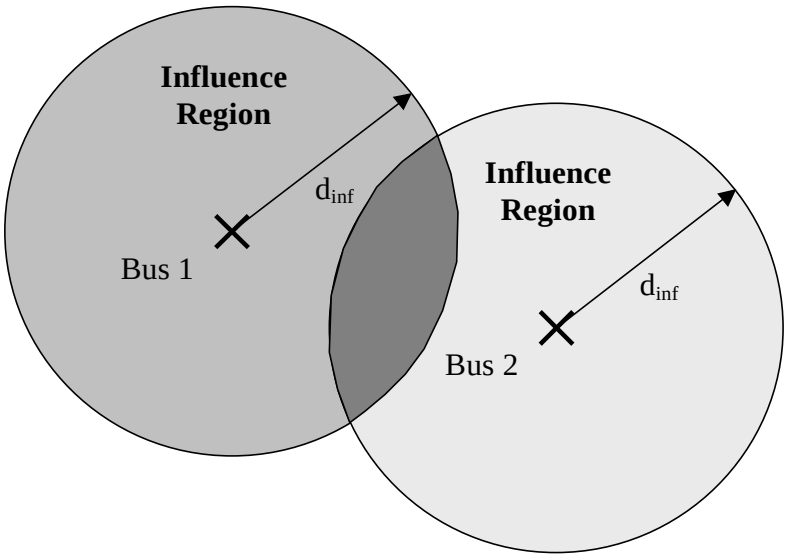

Figure 6.8 Bus Influence Regions

Only the virtual values that lie within this influence region for each bus need be updated. The update involves simply adding one additional term to the summations in Equation (6.1). Thus the inner loop for each bus j at location (x_1,y_2), assuming a voltage value of V_j, looks something like a double integral over a circular region as follows:

```
For x = (-d_inf+x_1) to (d_inf+x_1)
  For y = (-(d_inf^2–x^2)^0.5+y_1) to ((d_inf^2–x^2)^0.5+y_1)
    UpdateVirtualValue at (x,y) with value V_j
  Next y
Next x
```

An array with an entry for each point in the two-dimensional region of the contour is used to store these sums until all buses have been processed. Then the two sums are divided as shown in Equation (6.1) to calculate the virtual value.

While this technique improved the computation time greatly, a further speed up is still possible by recognizing that if the pixel regions within the influence region are square, then the computation can be further reduced by a factor of eight. This can be seen by considering only the shaded piece of the influence region seen in Figure 6.9. When calculating the influence of a bus on the virtual values, if the pixel regions are square, then the influence at the point (a,b) is the same as the influence at (b,a), (b,-a), (a,-b), (-a,-b), (-b,-a), (-b,a) and (-a,b). Therefore, instead of "integrating" over the entire circle, it is only necessary to integrate over a pie slice one-eighth the size of the circle. This reduces expected computations by a factor of eight.

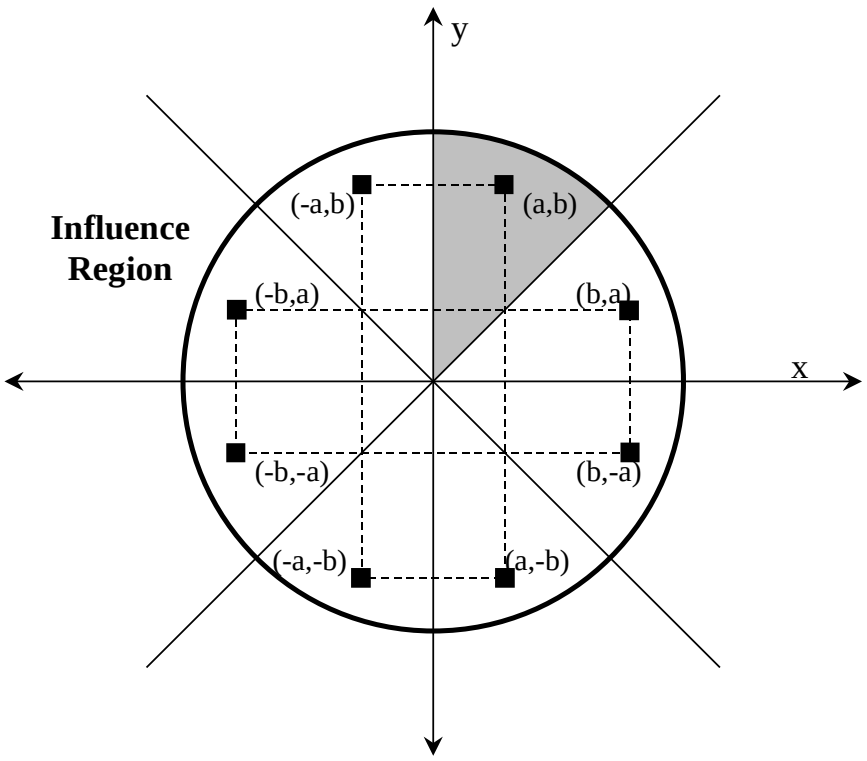

Figure 6.9 Reduction of Computation by a Factor of 8

6.5 Contouring in Animation

The use of the fast contouring algorithm decreases the time necessary to calculate a contour, even for large systems, to less than 1 s. With this order of magnitude decrease in computation time, it is now possible to implement the contouring as animation. This was done and the results are dramatically more interesting than those produced by a single snapshot contour. In a simulation, the contour can be updated dynamically, and the user is able to view the voltage profile as it changes, enabling the determination not only of the location of the voltage problems but also where voltage problems are developing.

While the animation itself cannot, of course, be presented in a dissertation format, the next several figures can be used to judge the effectiveness of contouring on several large systems, at

least from a static perspective. All these figures can be recontoured in less than 1 s to show either a changing system operating point, or results of a contingency.

Figure 6.10 shows the 345-kV buses for an 11,000-bus ECAR model. Figure 6.11 contours the voltage magnitudes of approximately 500 of the 115-kV, 138-kV, and 161-kV buses in a 4000-bus model of the Mid-American Interconnected Network (MAIN). Figure 6.12 shows a voltage angle contour for the same MAIN system. Figure 6.13 shows 440 of the 161-kV buses for a 23,500-bus model of the Tennessee Valley Authority (TVA). Figure 6.14 shows the MW marginal costs for the IEEE 118-Bus system with four areas defined. Notice how the different areas are highlighted by their marginal costs. For all figures a darker color indicates a lower voltage.

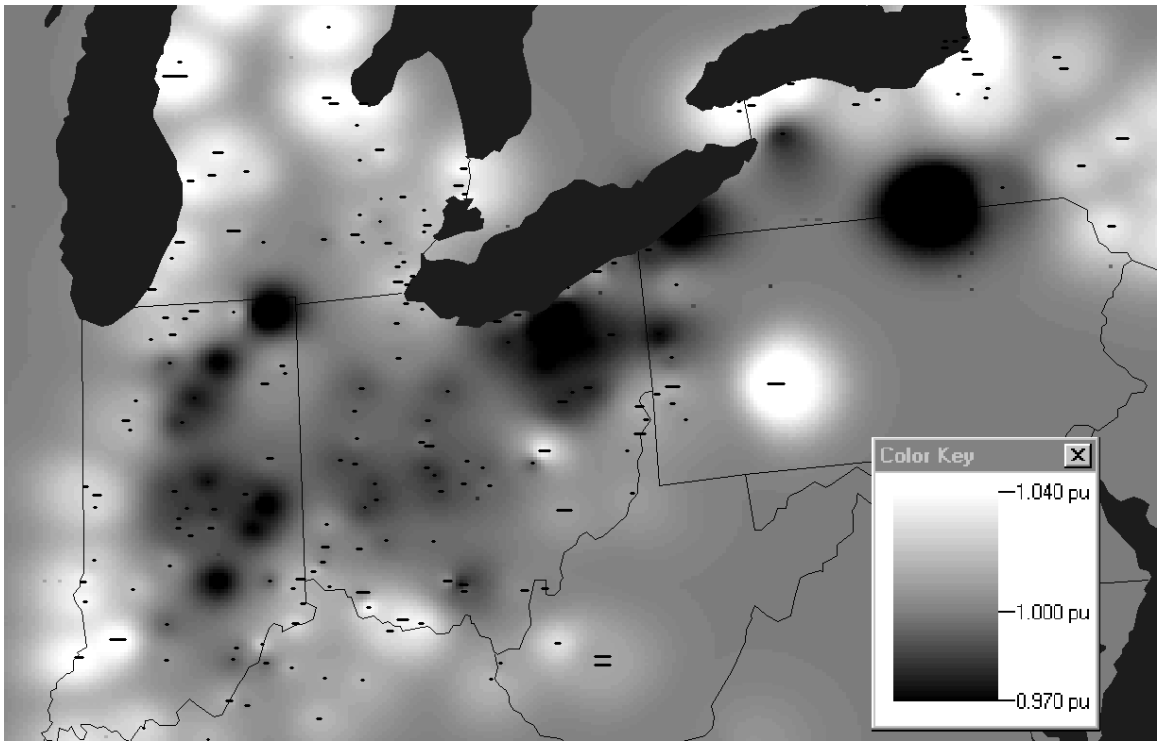

Figure 6.10 ECAR 345 kV-Bus Voltages

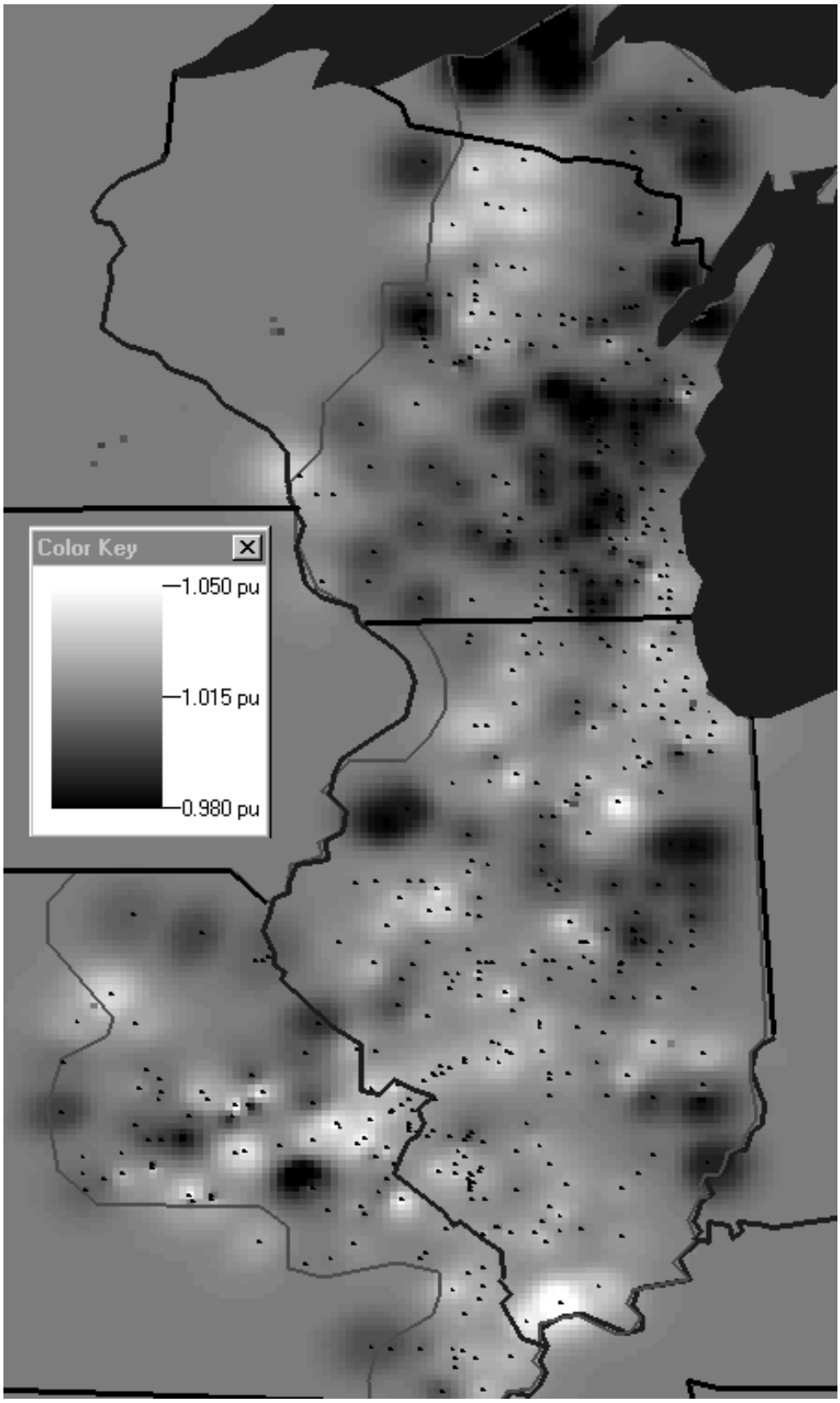

Figure 6.11 MAIN 115/138/161 kV-Bus Voltages

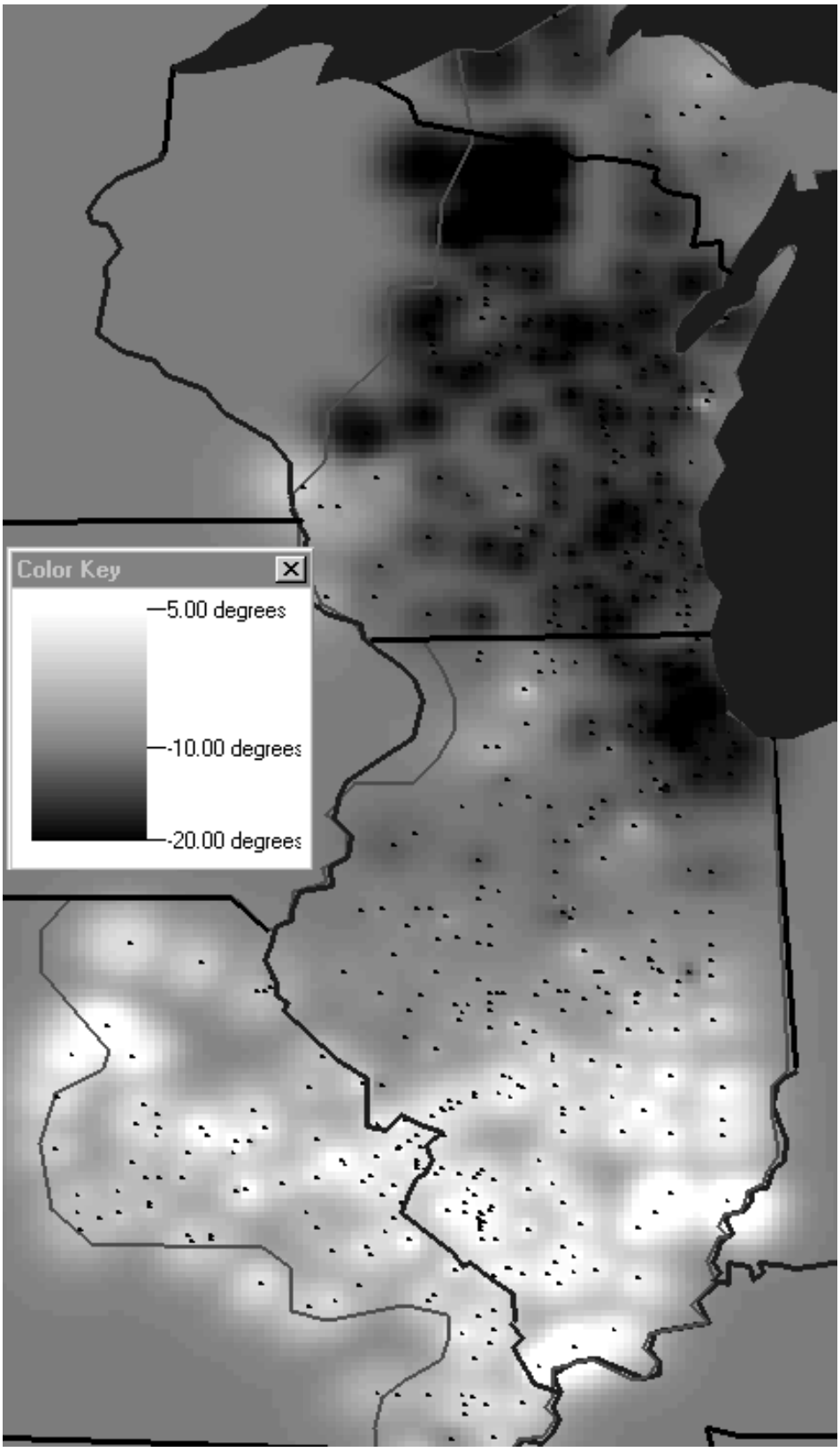

Figure 6.12 MAIN 115/138/161 kV-Bus Angles

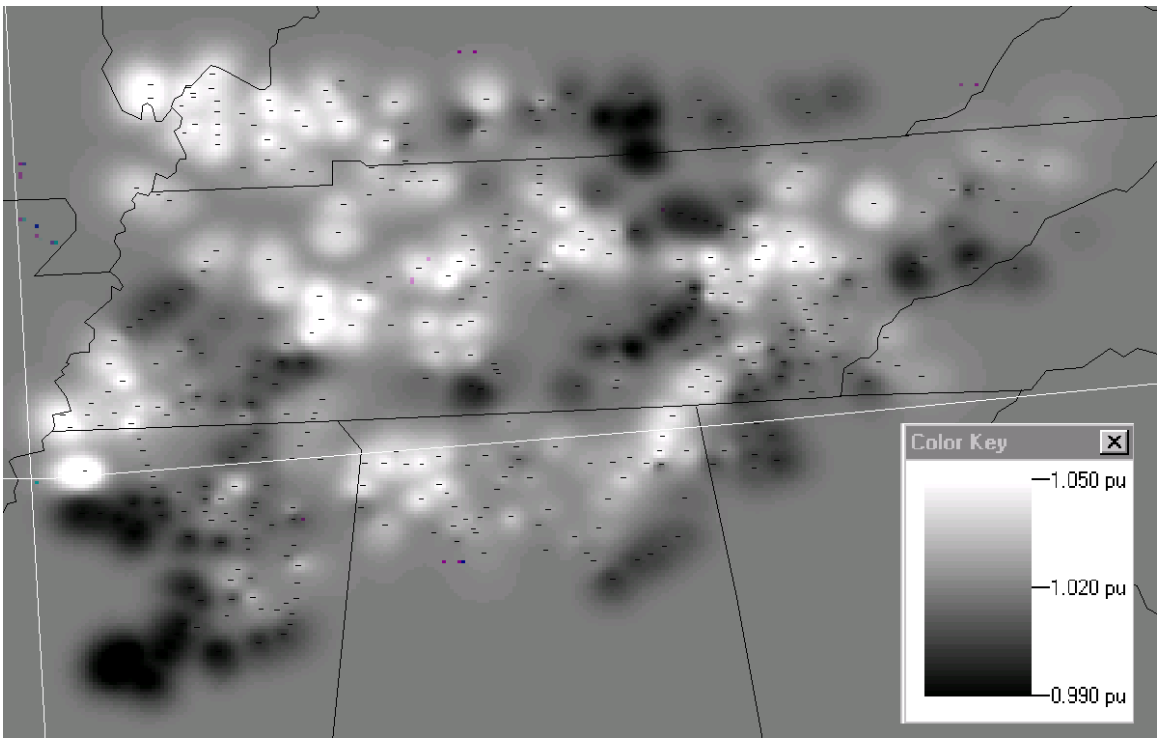

Figure 6.13 TVA 161 kV-Bus Voltages

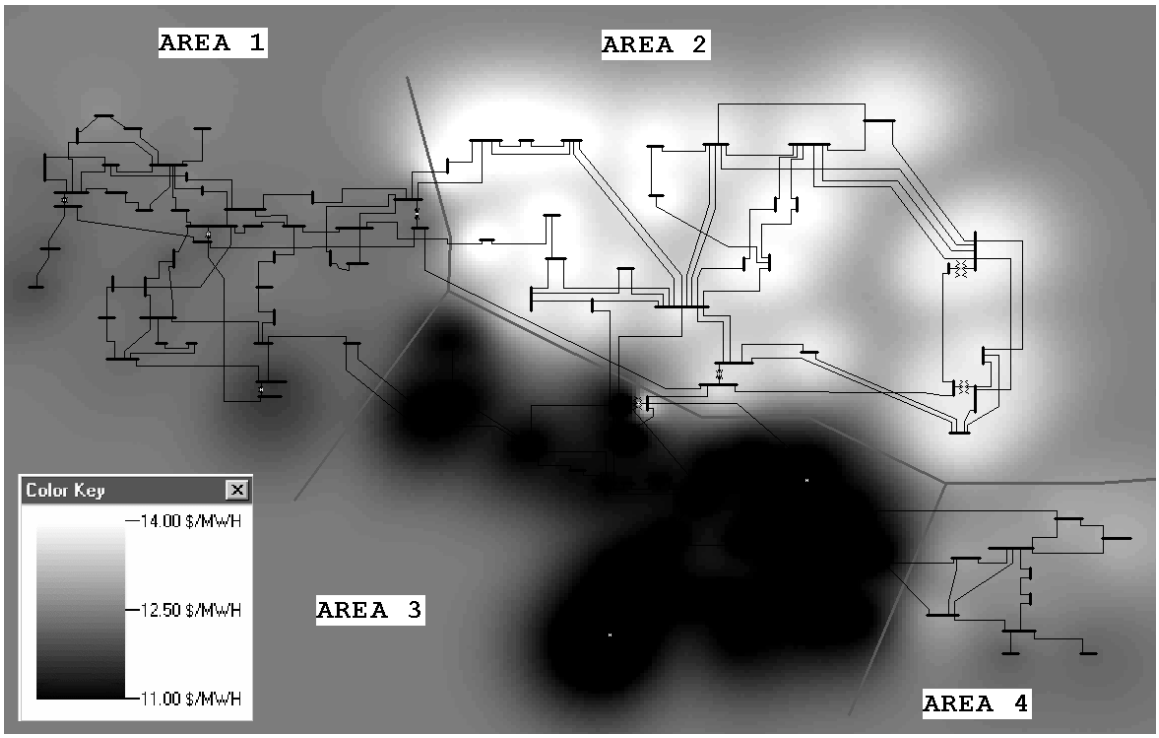

Figure 6.14 IEEE 118-Bus System Marginal Costs

6.6 Usability Test

Ultimately the usefulness of any visualization technique must be judged by its intended users. To aid in this assessment, as was done in [84], a simple test was developed and then presented to eight power system engineers and system operators from three different utilities. For this test, the IEEE 118-Bus system was used as a starting point. Then two different operating points were developed which had voltage problems in different regions. These two systems are shown in Figure 6.15 and Figure 6.16.

The discrete jump in color is seen in both figures, illustrating that voltages below 0.95 per unit exist in highlighted portions of the system. For both systems the voltage problems can be fixed by switching in a capacitor bank in the region which is experiencing low voltages.

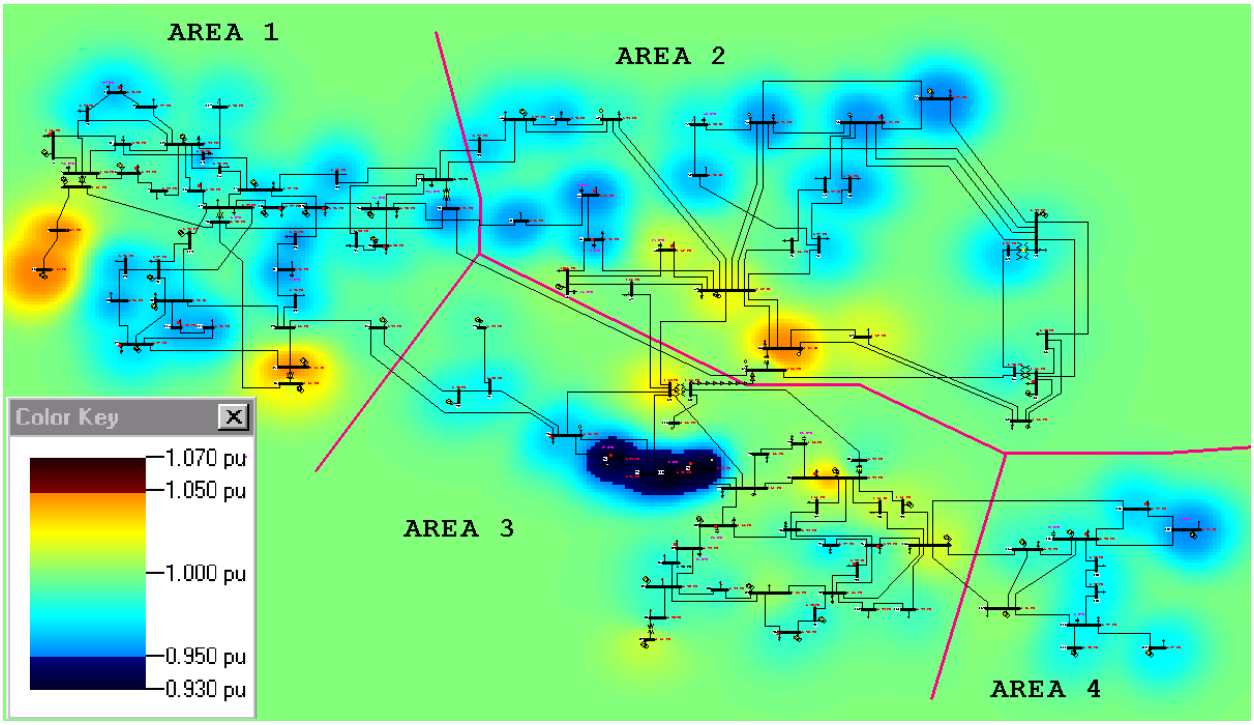

Figure 6.15 First Test Case with IEEE 118-Bus System

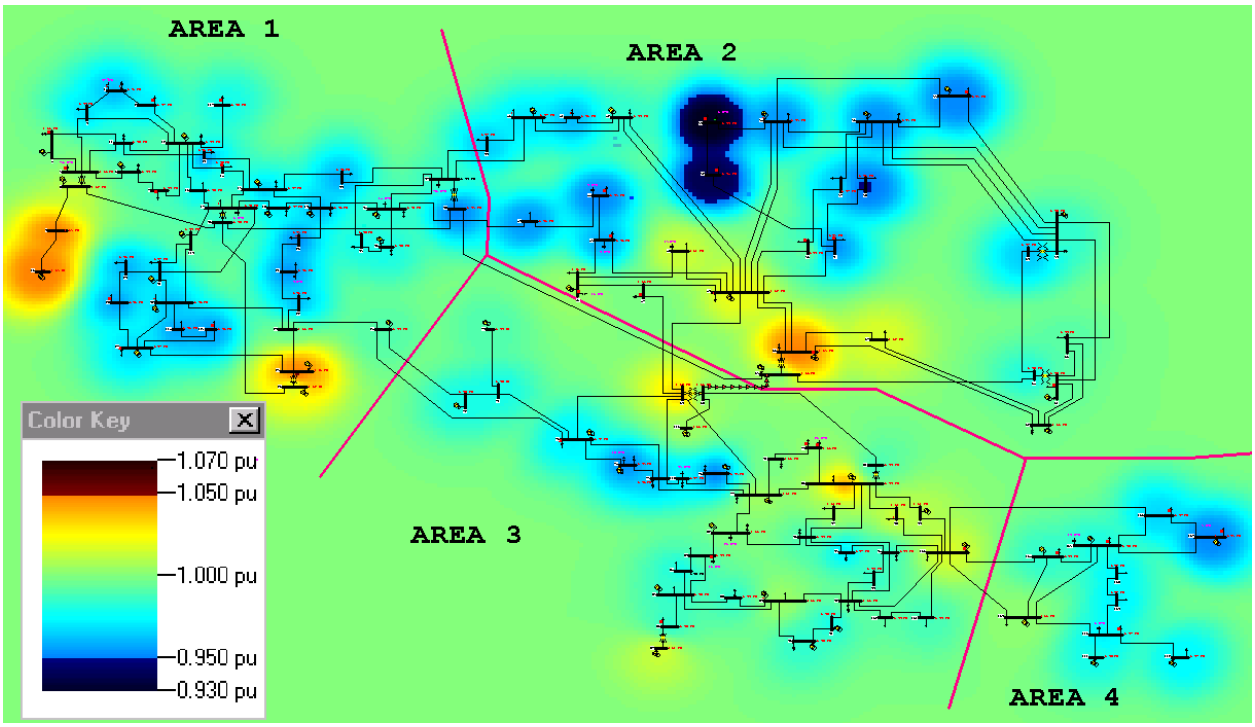

Figure 6.16 Second Test Case with IEEE 118-Bus System

In order to help measure whether the contour did indeed result in a faster response to voltage problems, the following test was given. For each system the individual was asked to identify the bus voltages which were being violated. After doing this they were asked to determine a corrective procedure that would remove the voltage violations.

The results of this test indicated that voltage contours were useful to all participants. Using the contours all participants were able to identify the violated buses within less than 5 s. Contours did indeed provide an "at a glance" overview of the voltage profile of the system. Once the violations were located, the user took from 20 to 30 s to fix the problem by switching in a capacitor bank located in the region. This varied due to the user's adeptness at using the pan/zoom capabilities of PowerWorld Simulator.

Without the contours, the participant was allowed to use a display that listed all the buses in a system above or below a specified limit. Essentially, this described an alarm-list in a present-day

EMS system. Using these instead of the contours, the time to find the voltage violations varied between 20 and 120 s with an average time of 65 s. While this may have largely been due to an unfamiliarity with the test system used, all participants felt that the use of the voltage contour would be useful even for a user with a great deal of experience with the system. Upon finding the violations in this test, the user had already pan/zoomed into the correct area of the one-line diagram and was able to quickly switch a capacitor bank in within 5-10 s of finding the voltage violations.

Before these tests were performed the participants, along with many other people at each utility, were presented with a brief background on how the contours were created. Following this background, they were asked whether the contours were useful and how they might be used. All respondents felt that the contours were definitely a useful tool. In addition to their use for general system monitoring, several other uses were suggested. These included the following

Good aid in distribution system operation. Contours could aid in determining capacitor-switching actions to correct voltage problems on a distribution system. (Note: This was only a good use if the utility presently monitored distribution system voltages on a large scale, which is not always done.)

Good for monitoring parts of a system that an operator is not familiar with. Contours could be helpful as OASIS information becomes more detailed. Engineers and operators will be faced with studying data for systems for which they have little experience. One utility interviewed was going through a merger that would make their transmission system 2-3 times larger.

Possibly a good tool for contingency analysis. Contours could be used to highlight contingencies with the most severe voltage deviations. This information could help to quickly determine the weakest spots in the transmission system.

System Planning Studies. Contours could be a good way to quickly determine which parts of a transmission system need more support. They could help determine which plans should be seriously considered and which could be ignored.

6.7 Contouring of Branch-Based Values

Thus far, this chapter has only discussed the contouring of bus-based values. After having developed bus-based contouring, one naturally wants to extend this technique to branch-based values such as line MVA loading percentages or power transfer distribution factors (PTDFs). Because the contouring technique developed involves creating an influence area around each bus as in Figure 6.8, the extension to lines is not immediate. Buses are easily represented as points on the computer screen, but lines are not. In order to extend this technique to lines, each line is represented by several points along the length of the line. Figure 6.17 shows a line represented by seven points along its length. By representing lines in this manner, the contouring algorithm is easily extended to allow for branches.

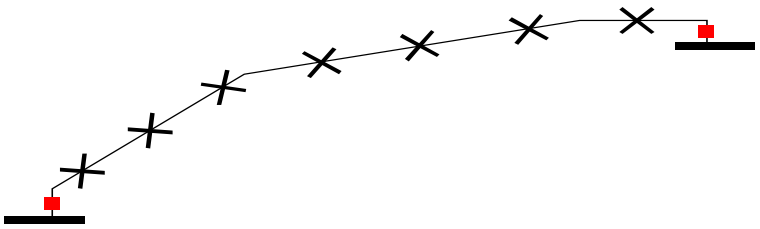

Figure 6.17 Seven Points (X) Representing a Transmission Line

In order to test this contouring technique on branches, a display was developed for a 30,400-bus ECAR model. This display included the 345-kV and above system for the entire eastern interconnection including 1023 buses and 1396 branches. Figure 6.18 shows the PTDFs for a transfer from Florida to Wisconsin, while Figure 6.19 shows the line MVA loading percentages for the same system. Both of these figures use the Radar Map High Limits color-mapping.

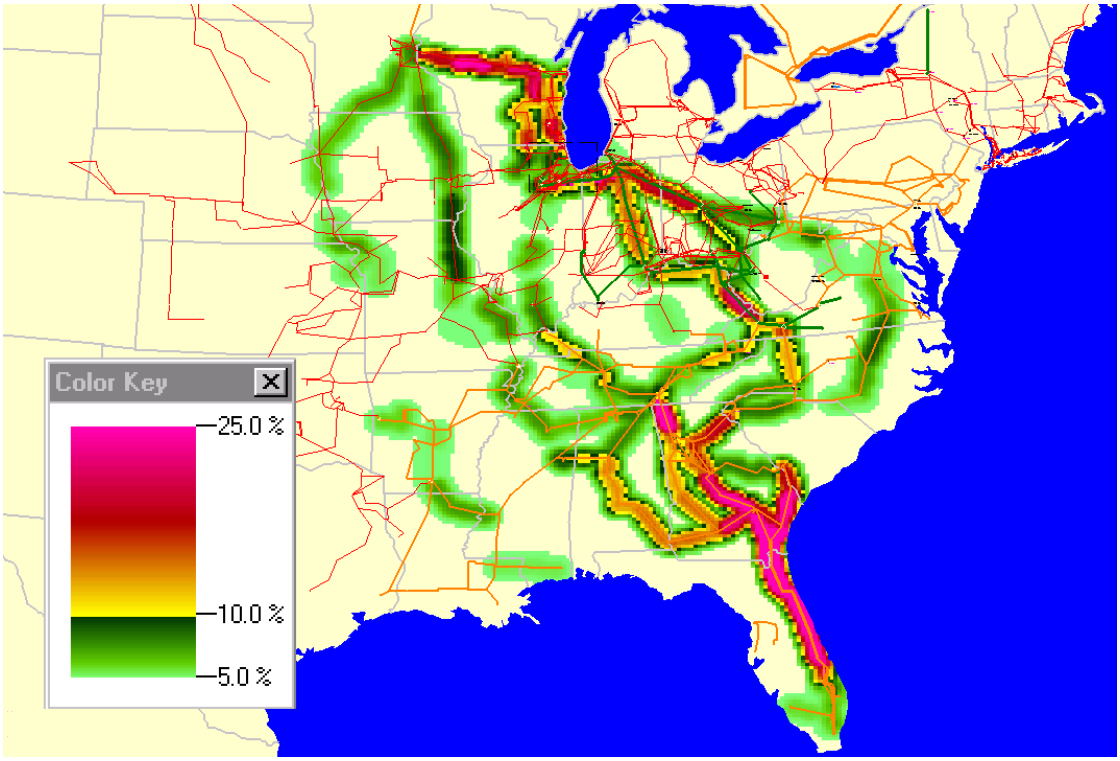

Figure 6.18 Eastern Interconnect PTDFs for a Transfer from Florida to Wisconsin

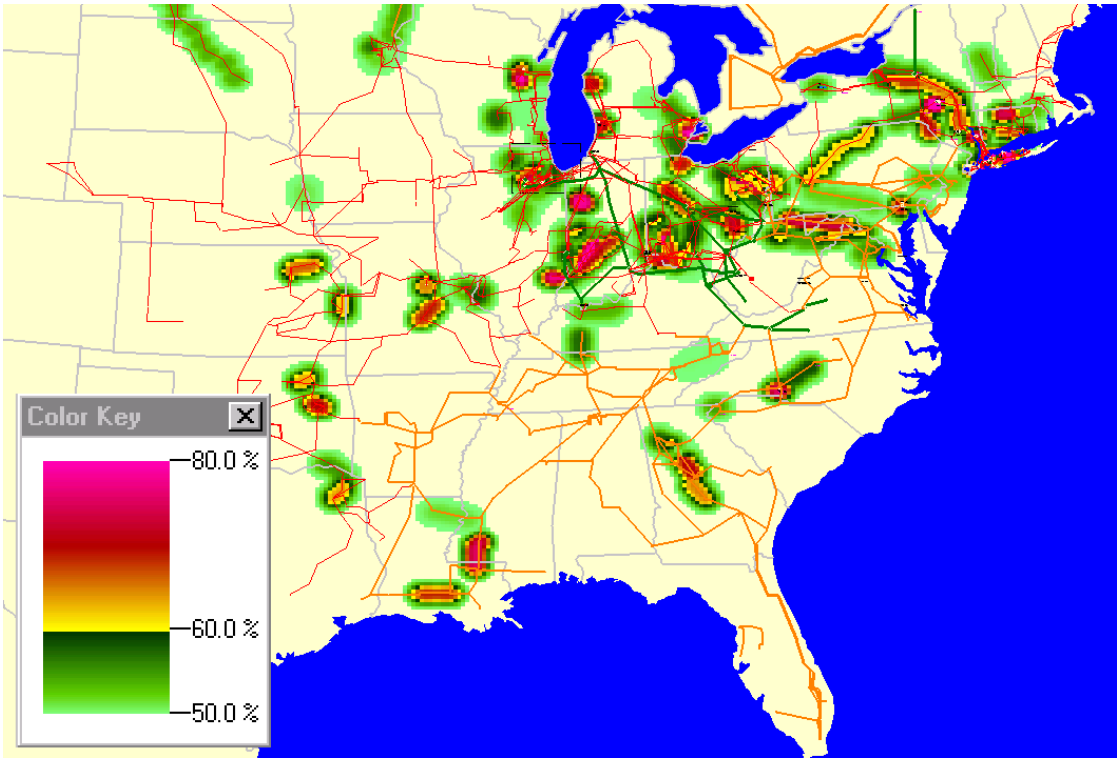

Figure 6.19 Line MVA Loading Percentages for the Eastern Interconnect

7. SUMMARY

This dissertation has presented a new algorithm that allows a market participant to maximize its individual welfare in the electricity spot market. The use of such an algorithm in determining market equilibrium points, called Nash equilibria, has also been demonstrated. Electricity markets throughout the world continue to be opened to competitive forces with the objective of making them more efficient. To achieve this objective, new algorithms such as those presented here are needed to help market participants behave in an efficient manner, helping them maximize their own welfare.

Chapter 2 introduced the use of the OPF as a model of the electricity spot market and verified the effectiveness of this model. The OPF will continue to serve as a platform for studying market behavior as well as individual market participant behavior. Any software that models the spot market will have the OPF at its core.

As the electricity industry continues to restructure, the incorporation of the consumer into the market structure will become more important. Because all suppliers and consumers have a stake in the electricity system, it is important that all receive the price feedback that allows them to make good energy use decisions. As consumers are presented with price variation, they will begin to modify their own energy consumption in a manner that reflects the benefits they receive from this consumption. This feedback between the suppliers and consumers will help the market make better long-term decisions such as where and when to invest in transmission system expansion. Chapter 3 showed that modeling the consumer is a natural extension to the OPF problem and provided a thorough mathematical justification for their inclusion. Chapter 3 also presented good models of the consumer demand for real and reactive power.

Regardless of whether suppliers and consumers are incorporated into a market structure, individuals participating in a spot market will need tools to help them determine good bidding strategies. Chapter 4 developed a novel Individual Welfare Maximization algorithm which was shown to be successful on several sample systems. Also, because of the structure of this approach, the computational requirements will scale linearly with the complexity of the OPF problem. Thus, the prospects of scaling the algorithm up to systems of realistic size appear very good.

The Individual Welfare Maximization algorithm presented in Chapter 4 will be of great use to individual market participants for market analysis. However, others, such as industry regulators, are interested in studying market equilibrium behavior. Using the Individual Welfare Maximization algorithm as a model of individual bidding behavior, the entire market can be simulated with individuals modifying their bids with the objective of maximizing welfare. This was done iteratively in Chapter 4 until equilibrium points, called Nash equilibria, were reached. This technique was shown to be very useful for finding Nash equilibria, as long as they existed. It also highlighted the fact that Nash equilibria do not always exist, and that when they do exist they may not be unique.

The new Individual Welfare Maximization technique developed in Chapter 4 is a calculus-based optimization routine. However, it was shown in Chapter 4 that the individual welfare, even for simple systems, can be a highly nonconcave function resulting in many local optima. The local optima correspond to the ability of the individual to manipulate its bidding strategy to take advantage of a system constraint, such as a transmission line constraint. Because these local optima will correspond to physically understandable phenomena, it is hoped that the user of the Individual Welfare Maximization algorithm will be able to nudge the initial guesses of the

algorithm into regions that will correspond to these local optima. This will make the algorithm of some use on its own; however, a more global optimization routine using a genetic algorithm (GA) was investigated in Chapter 5.

The genetic algorithm developed in Chapter 5 was shown to hold potential for helping to solve the individual welfare maximization problem. It was effective in finding local maxima, even in finding more than one local maxima simultaneously. As is often the case with a GA, however, solution time was a big problem. For example, for the nine-bus system from Section 5.4.2 it took approximately 2 h to simulate 50 generations of the GA. This compares to less than 10 s for using the calculus-based method to find on of the local optima. Regardless, the GA has some potential, and future work should concentrate on improving it, as well as on integrating the GA with the calculus-based routine.

Finally, Chapter 6 covers the development of a new computer visualization routine for power system analysis: contouring. The contouring algorithm was demonstrated to be useful in visualizing bus-based and transmission-line based quantities. The contouring algorithm was fully integrated into the commercially available software PowerWorld Simulator in the summer of 1997 and has indeed proved to be extremely useful to Simulator users.

APPENDIX A. SPARSITY STRUCTURE OF THE DERIVATIVES OF THE HESSIAN AND GRADIENT WITH RESPECT TO K

The bid vector **k** only appears in the OPF problem of Equation (4.2) as a linear multiplier on the cost and benefit functions of the supplier and consumer such as $C_i(s_i, k_{si}) = k_{si}(b_i s_i + c_i s_i^2)$ and $B_i(d_i, k_{di}) = k_{di}(\beta_i d_i - \gamma_i d_i^2)$. Essentially, *k* can be thought of as a linear multiplier on the coefficients *b* and *c*. These coefficients only show up in the gradient and Hessian matrices in a couple locations. From page 60 of [25], the only terms in the gradient which contain the *b* and *c* coefficients are $\frac{\partial L}{\partial s_i} = k_{si}(b_i + 2c_i s_i)$ and $\frac{\partial L}{\partial d_i} = k_{di}(\beta_i - 2\gamma_i d_i)$. From page 60 of [25], the only terms in the Hessian which contain the *b* and *c* coefficients are $\frac{\partial^2 L}{\partial s_i^2} = k_{si}(2c_i)$ and $\frac{\partial^2 L}{\partial d_i^2} = k_{di}(-2\gamma_i)$.

As a result, the derivative of the gradient with respect to **k** will have exactly one nonzero entry in each column:

$$\frac{\partial(\nabla \mathbf{L})}{\partial \mathbf{k}} = \begin{bmatrix} 0 & 0 & 0 \\ b_1 + 2c_1 s_1 & 0 & 0 \\ 0 & 0 & 0 \\ 0 & b_2 + 2c_2 s_2 & 0 \\ 0 & 0 & \beta_1 - 2\gamma_1 d_1 \\ 0 & 0 & 0 \end{bmatrix}$$

Similarly, the derivative of the Hessian matrix with respect to a single k_i will have exactly one nonzero element in the entire matrix. This nonzero will be on a diagonal:

$$\frac{\partial \mathbf{H}}{\partial k_{s1}} = \begin{bmatrix} 0 & 0 & 0 & 0 & 0 & 0 \\ 0 & 2c_1 & 0 & 0 & 0 & 0 \\ 0 & 0 & 0 & 0 & 0 & 0 \\ 0 & 0 & 0 & 0 & 0 & 0 \\ 0 & 0 & 0 & 0 & 0 & 0 \\ 0 & 0 & 0 & 0 & 0 & 0 \end{bmatrix}$$

Extending this insight to the derivate of the Hessian matrix with respect to the vector **k** results in a tensor with one nonzero element in each matrix as one moves along the **k** direction of the tensor. This is depicted in Figure A.1.

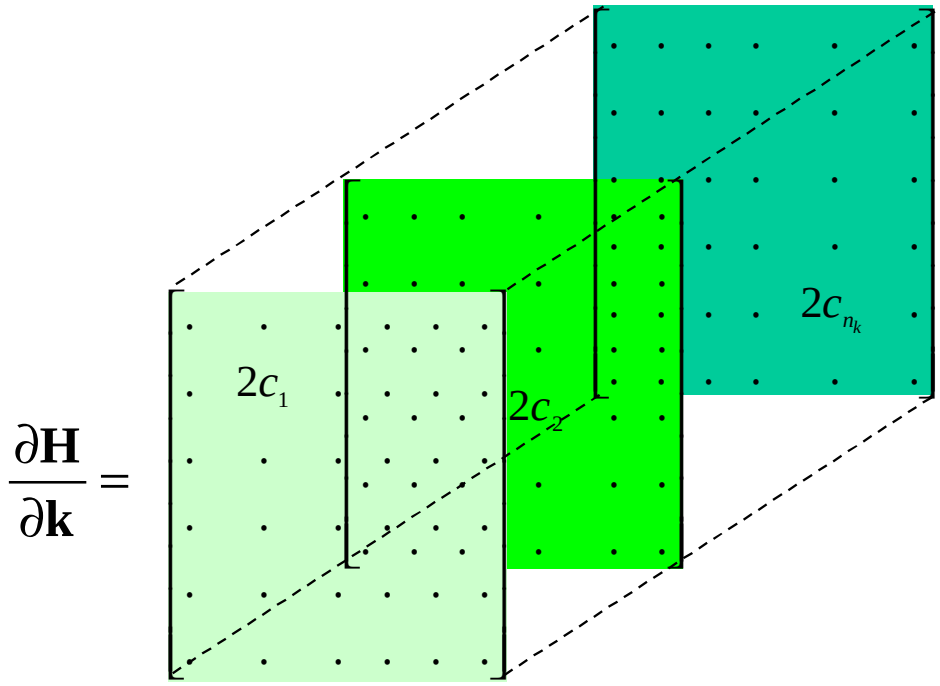

Figure A.1 Tensor for the Derivative of **H** with Respect to **k**

REFERENCES

[1] "Causes of Wholesale Electricity Pricing Abnormalities in the Midwest During June 1998," Staff Report to the Federal Energy Regulatory Commission, http://www.ferc.fed.us/news1/staffreports.htm, September 22, 1998.

[2] R. Gibbens and S. Turner, "Call routing in telephone networks," *Public Awareness and Schools Support for Mathematics*, Issue 2, May 1997, http://pass.maths.org.uk/issue2/dar.

[3] D. Shirmohammadi, X.V. Filho, B. Gorenstin, and M. Pereira, "Some fundamental technical concepts about cost based transmission pricing," *IEEE Transactions on Power Systems*, vol. 11, no. 2, May 1996.

[4] E. Hirst and B. Kirby, *Electric Power Ancillary Services*. Oak Ridge, TN: Oak Ridge National Laboratory, 1996.

[5] M.E. Northup and J.A. Rasmussen, "Electricity reform abroad and U.S. investment," Report from the United States Department of Energy – Energy Information Agency, October 1997, http://www.eia.doe.gov/emeu/pgem/electric.

[6] T. Alvey, D. Goodwin, X. Ma, D. Streiffert, and D. Sun, "A security-constrained bid-clearing system for the New Zealand wholesale electricity market," *IEEE Transactions on Power Apparatus and Systems*, vol. 13, no. 2, May 1998, pp. 340-346.

[7] The California Power Exchange Web site, http://www.calpx.com.

[8] F.C. Schweppe, M.C. Caramanis, R.D. Tabors and R.E. Bohn, *Spot Pricing of Electricity*, Boston: Kluwer Academic Publishers, 1988.

[9] The Pennsylvania-New Jersey Maryland (PJM) Interconnection Web site, http://www.pjm.com.

[10] The New England Independent System Operator Web site, http://www.iso-ne.com.

[11] Public Utility Regulatory Policy Act of 1978 (PURPA). (A good index is in the Web site http://www.ferc.fed.us/intro/acts/purpa.htm at FERC.)

[12] Energy Policy Act of 1992, Public Law 102-486, 106 Stat. 2776, 1992.

[13] Federal Energy Regulatory Commission (FERC), "Promoting wholesale competition through open access non-discriminatory transmission services by public utilities and recovery of stranded costs by public utilities and transmitting utilities," Docket Nos. RM95-8-000 and RM94-7-001, Order No. 888, Washington, DC, April 24, 1996.

[14] Federal Energy Regulatory Commission (FERC), "Open access same-time information system (formerly real-time information networks) and standards of conduct," Docket No. RM95-9-001, Order No. 889, Washington, DC, April 24, 1996.

[15] S. Hunt and G. Shuttleworth, "Unlocking the GRID," *IEEE Spectrum*, vol. 33, no. 7, July 1996, pp. 20-25.

[16] H. Rudnick, "Pioneering electricity reform in South America," *IEEE Spectrum*, vol. 33, no. 8, August 1996, p. 38-44.

[17] Transmission Transfer Capability Task Force, "Transmission transfer capability," North American Electric Reliability Council, Princeton, New Jersey, May 1995.

[18] Transmission Transfer Capability Task Force, "Available transfer capability definitions and determination," North American Electric Reliability Council, Princeton, New Jersey, June 1996.

[19] J.D. Weber, T.J. Overbye, and P.W. Sauer, "Simulation of electricity markets with player bidding," Bulk Power System Dynamics and Control IV – Restructuring, Santorini, Greece, August 24-28, 1998.

[20] T.J. Overbye, G. Gross, P.W. Sauer, and M.J. Laufenberg, "Market power evaluation in power systems with congestion," Game Theory Applications in Electric Power Markets, 99TP-136-0, IEEE PES Winter Meeting 1999, pp. 61-69.

[21] United States Federal Energy Regulatory Commission, Order No. 592, RM96-6-000, December 1996.

[22] United States Justice Department and Federal Trade Commission, "Horizontal merger guidelines," issued April 1992, revised April 1997, http://www.usdoj.gov/atr/public/guidelines/guidelin.htm.

[23] Federal Energy Regulatory Commission (FERC), "Revised filing requirements under Part 33 of the commission's regulations. Notice of proposed rulemaking," Docket No. RM98-4-000 (April 16, 1998), Washington, DC.

[24] J. Carpienter, "Contribution e l'étude do dispatching economique," *Bulletin Society Française Electriciens*, vol. 3, August 1962.

[25] J.D. Weber, "Implementation of a Newton-based optimal power flow into a power system simulation environment," M.S. thesis, University of Illinois at Urbana-Champaign, Department of Electrical and Computer Engineering, January 1997.

[26] A. J. Wood and B. F. Wollenberg, *Power Generation Operation and Control*. New York, NY: John Wiley & Sons, Inc., 1996.

[27] H. W. Dommel and W. F. Tinney, "Optimal power flow solutions," *IEEE Transactions on Power Apparatus and Systems*, vol. PAS-87, October 1968, pp. 1866-1876.

[28] D.I. Sun, B. Ashley, B. Brewer, A. Hughes, and W.F. Tinney, "Optimal power flow by Newton approach," *IEEE Transactions on Power Apparatus and Systems*, vol. PAS-103, October 1984, pp. 2864-2880.

[29] O. Alsac, J. Bright, M. Prais, and B. Stott, "Further developments in LP-based optimal power flow," *IEEE Transactions on Power Systems*, vol. 5, no. 3, August 1990, pp. 697-711.

[30] Y. Wu, A. S. Debs, and R. E. Marsten, "Direct nonlinear predictor-corrector primal-dual interior point algorithm for optimal power flows," *1993 IEEE Power Industry Computer Applications Conference*, pp. 138-145.

[31] J.A. Momoh, M.E. El-Hawary, and R. Adapa, "A review of selected optimal power flow literature to 1993," *IEEE Transactions on Power Systems*, vol. 14, no. 1, February 1999, pp. 96-111.

[32] J. A. Momoh, R. J. Koessler, M. S. Bond, B. Stott, D. Sun, A. D. Papalexopoulos, and P. Ristanovic, "Challenges to optimal power flow," *1996 IEEE/PES Winter Meeting*, 96 WM 312-9 PWRS, Baltimore, MD, January 21-25, 1996.

[33] H. Chao and S. Peck, "A market mechanism for electric power transmission," *Journal of Regulatory Economics*, July 1996, pp. 25-59.

[34] W.W. Hogan, "Markets in real electric networks require reactive prices," *The Energy Journal*, vol. 14, no. 3, September 1993, pp. 171-200.

[35] D. Chattopadhyay, K. Bhattacharya, and J. Parikh, "Optimal reactive power planning and its spot pricing: an integrated approach," *IEEE Transactions on Power Systems*, vol. 10, no. 4, November 1995, pp. 2014-2020.

[36] J.D. Weber, M.J. Laufenberg, T.J. Overbye, and P.W. Sauer, "Assessing the value of reactive power services in electric power systems," Conference on Unbundled Power Quality Services, Key West, Florida, November 17-19, 1996, pp. 160-167.

[37] S. Hao and A. Papalexopoulos, "Reactive power pricing and management," *IEEE Transactions on Power Systems*, vol. 12, no. 1, February 1997, pp. 95-104.

[38] R.S. Fang and A.K. David, "Optimal dispatch under transmission contracts," *IEEE Transactions on Power Systems*, vol. 14, no. 2, May 1999, pp. 732-737.

[39] H. Glavitsch and F. Alvarado, "Management of multiple congested conditions in unbundled operation of a power system," *IEEE Transactions on Power Systems*, vol. 13, no. 3, August 1998, pp. 1013-1019.

[40] H. Singh, S. Hao, and A. Papalexopoulos, "Transmission congestion management in competitive electricity markets," *IEEE Transactions on Power Systems*, vol. 13, no. 2, May 1998, pp. 672-680.

[41] M.L. Baughman and S.N. Siddiqi, "Real-time pricing of reactive power: Theory and case study results," *IEEE Transactions on Power Systems*, vol. 6, no. 1, February 1991, pp. 23-29.

[42] J.D. Weber, T.J. Overbye, and C. DeMarco, "Modeling the consumer benefit in the optimal power flow," *Decision Support Systems*, vol. 24, no. 3-4, March 1999, pp. 279-296.

[43] D.J. Finlay, "Optimal bidding strategies in competitive electric power pools," M.S. thesis, University of Illinois at Urbana-Champaign, Department of Electrical and Computer Engineering, May 1995.

[44] C. Li, A.J. Svoboda, X. Guan, and H. Singh, "Revenue adequate bidding strategies in competitive electricity markets," *IEEE Transactions on Power Systems*, vol. 14, no. 2, May 1999, pp. 492-504.

[45] C.W. Richter, Jr. and G. Sheblé, "Genetic algorithm evolution of utility bidding strategies for the competitive marketplace," *IEEE Transactions on Power Systems*, vol. 13, no. 1, February 1998, pp. 256-261.

[46] X. Bai, S.M. Shahidehpour, V.C. Ramesh, and E. Yu, "Transmission analysis by nash game method," *IEEE Transactions on Power Systems*, vol. 12, no. 3, August 1997, pp. 1046-1052.

[47] R.W. Ferrero, S.M. Shahidehpur, and V.C. Ramesh, "Transaction analysis in deregulated power systems using game theory," *IEEE Transactions on Power Systems*, vol. 12, no. 3, August 1997, pp. 1340-1347.

[48] R.W. Ferrero, J.F. Rivera, and S.M. Shahidehpour, "Application of games with incomplete information for pricing electricity in deregulated power pools," *IEEE Transactions on Power Systems*, vol. 13, no. 1, February 1998, pp. 184-189.

[49] J.B. Cardell, C.C. Hitt, and W.W. Hogan, "Market power and strategic interaction in electricity networks," *Resource and Energy Economics*, 1997, pp. 109-137.

[50] C.A. Berry, B.F. Hobbs, W.A. Meroney, R.P. O'Neill, and W.R. Steward, "Analyzing strategic bidding behavior in transmission networks," Game Theory Applications in Electric Power Markets, 99TP-136-0, IEEE PES Winter Meeting 1999, pp. 7-32.

[51] H.W. Kuhn and A.W. Tucker, "Nonlinear programming," *Proceedings of Second Berkeley Symposium on Mathematical Statistics and Probability*, University of California Press, 1961, pp. 481-492.

[52] T.J. Overbye, P.W. Sauer, G. Gross, M.J. Laufenberg, and J.D. Weber, "A simulation tool for analysis of alternative paradigms for the new electricity business," *Proceedings of 30th Hawaii International Conference on System Sciences*, Maui, HI, January 1997, pp. V634-V640.

[53] PowerWorld Corporation Web site, http://www.powerworld.com.

[54] P. Skantze and J. Chapman, "Price dynamics in the deregulated California energy market," *Proceedings of IEEE PES Society 1999 Winter Meeting*, New York, New York, Jan. 31 – Feb 4, 1999.

[55] Federal Energy Regulatory Commission (FERC), "Order establishing hearing procedures," Wisconsin Electric Power Co., Northern States Power Co., Docket No. EC95-16-000 (January), Washington, DC, 1996.

[56] D.P. Bertsekas, *Nonlinear Programming*. Belmont, MA: Athena Scientific, 1995.

[57] D.M Kreps, *A Course in Microeconomic Theory*. Princeton, N.J.: Princeton University Press, 1990, chapters 11 and 12.

[58] E. Aarts and J. Korst, *Simulated Annealing and Boltzmann Machines: A Stochastic Approach to Combinatorial Optimization and Neural Computing*. New York, NY: John Wiley & Sons, 1989.

[59] D.E. Goldberg, *Genetic Algorithms*. Reading, MA: Addison-Wesley,1989.

[60] J.R. Ferreira, J.A. Popes, and J.T. Saraiva, "Identification of preventative control procedures to avoid voltage collapse using genetic algorithms," *Proceedings of the 13th Power System Computation Conference*, Trondheim, Norway, June 28 – July 2, 1999.

[61] F. Li, "A comparison of genetic algorithms with conventional techniques on a spectrum of power economic dispatch problems," *Expert Systems with Applications*, vol. 15, issue 2, 1998, pp. 133-142.

[62] M.A. Abido and Y.L. Abdel-Magid, "A genetic-based fuzzy logic power system stabilizer for multimachine power systems," *1997 IEEE International Conference on Computational Cybernetics and Simulation*, vol. 1, pp. 329-334.

[63] C.J. Aldridge and J.R. McDonald, "Unit commitment for power systems using a heuristically augmented genetic algorithm," *Genetic Algorithms in Engineering Systems: Innovations and Applications*, 1997, pp. 433-438.

[64] Q.H. Wu and J.T. Ma, "Genetic search for optimal reactive power dispatch of power systems," *International Conference on Control*, 1994, vol. 1, pp. 717-722.

[65] C. Dai-Seub, K. Chang-Suk, and J. Hasegawa, "An application of genetic algorithms to the network reconfiguration in distribution for loss minimization and load balancing problem," *Proceedings of International Conference on Energy Management and Power Delivery*, 1995, vol. 1, pp. 376-381.

[66] P. Ju, E. Handschin, and F. Reyer, "Genetic algorithm aided controller design with application to SVC," *IEE Proceedings – Generation, Transmission and Distribution*, May 1996, vol. 143, no. 3, pp. 258-262.

[67] S.W. Mahfoud and D.E. Goldberg, "Parallel recombinative simulating annealing: A genetic algorithm," *Parallel Computing*, vol. 21, 1995, pp. 1-28.

[68] D.E. Goldberg, "A note on boltzmann tournament selection for genetic algorithms and population-oriented simulated annealing," *Complex Systems 4*, 1990, pp. 445-460.

[69] E.W. Weisstein, *CRC Concise Encyclopedia of Mathematics*. Boca Raton, FL: CRC Press, 1998, http://www.treasure-troves.com/math.

[70] S.W. Mahfoud, "Crowding and preselection revisited," in *Parallel Problem Solving from Nature 2*, R. Männer and B. Manderick Editors. New York, NY: Elsevier Science Publishers, 1992.

[71] K. Deb and D.E. Goldberg, "An investigation of niche and species formation in genetic function optimization," *Proceedings of the Third International Conference on Genetic Algorithms*, 1989, San Mateo, CA, pp. 42-50.

[72] M. Jelasity and J. Dombi, "GAS, a concept on modeling species in genetic algorithms," *Artificial Intelligence*, vol. 99, issue 1, February 1998, pp. 1-19.

[73] R. Seydel, *Practical Bifurcation and Stability Analysis*. New York, NY: Springer-Verlag, 2nd Edition, 1994.

[74] I. Dobson and L. Lu, "Voltage collapse precipitated by the immediate change in stability when generator reactive power limits are encountered," *IEEE Transactions on Circuits and Systems*, vol. 39, no. 9, September 1992, pp. 762-766.

[75] J.D. Weber and T.J. Overbye, "Voltage contours for power system visualization," *IEEE Transactions on Power Systems*, notified of acceptance in January 1999 for publication in an upcoming issue.

[76] P.M. Mahadev and R.D. Christie, "Minimizing user interaction in energy management systems: task adaptive visualization," *IEEE Transactions on Power Systems*, vol. 11, no. 3, August 1996, pp. 1607-1612.

[77] R.D. Christie, "Toward a higher level of user interaction in the energy management task," *Proceedings of the IEEE International Conference on Systems, Man and Cybernetics*, San Antonio, TX, October 2-5, 1994, pp. 1086-1091.

[78] P.R. D'Amour and W.R. Block, "Modern user interface revolutionizes supervisory systems," *IEEE Computer Applications in Power*, January 1994, pp. 34-39.

[79] K. Ghoshal and L.D. Douglas, "GUI display guidelines driving winning SCADA projects," *IEEE Computer Applications in Power*, April 1994, pp. 39-42.

[80] G.P. de Azevedo, C.S. de Souza, and B. Feijo, "Enhancing the human-computer interface of power system applications," *IEEE Transactions on Power Systems*, vol. 11, no. 2, May 1996, pp. 646-653.

[81] P.M. Mahadev and R.D. Christie, "Envisioning power system data: Concepts and a prototype system state representation," *IEEE Transactions on Power Systems*, vol. 8, no. 3, August 1993.

[82] T.J. Overbye, G. Gross, M.J. Laufenberg, and P.W. Sauer, "Visualizing power system operations in an open market," *IEEE Computer Applications in Power*, January 1997, pp. 53-58.

[83] P.M. Mahadev and R.D. Christie, "Case study: Visualization of an electric power transmission system," *Proceeding of Visualization 1994*, Washington D.C., October 17-21, 1994.

[84] H. Mitsui and R.D. Christie, "Visualizing voltage profiles for large scale power systems," *IEEE Computer Applications in Power*, July 1997, pp. 32-37.

[85] A. Thiyagarajah, B. Carlson, J. Bann, M. Mirheydar, and S. Mokhtari, "Seeing results in a full graphics environment," *IEEE Computer Applications in Power*, July 1993, pp. 33-38.

[86] J.A. Huang and F.D. Galiana, "An integrated personal computer graphics environment for power system education, analysis, and design," *IEEE Transactions on Power Systems*, vol. 6, no. 3, August 1991, pp. 1279-1285.

[87] J.D. Weber and T.J. Overbye, "Power system visualization through contour plots," *Proceedings of North American Power Symposium*, Laramie, WY, October 13-14, 1997, pp. 457-463.

[88] The Math Works Inc., *Reference Guide for MATLAB*. Natick, MA, 1992.

VITA

James Daniel Weber was born in Platteville, Wisconsin, on June 13, 1973. He received his Bachelor of Science degree in electrical engineering from the University of Wisconsin - Platteville in May 1995 and his Master of Science degree in electrical and computer engineering from the University of Illinois at Urbana-Champaign in January 1997. He worked as an intern at Wisconsin Power and Light Company in Madison, Wisconsin, during the summers of 1994 and 1995. He was a research assistant at the University of Illinois from August 1995 through August 1999. He was a teaching assistant for ECE 376, a power system analysis course, in 1997, and for ECE 333, an electrical machinery laboratory course, in 1998. His research interests include power systems, economics, and computer visualization. While pursuing his doctoral studies at the University of Illinois, he worked part-time as a power systems engineer and software developer at PowerWorld Corporation. He has been employed full-time at PowerWorld Corporation since February 1999. He is a member of Theta Tau, Eta Kappa Nu, Tau Beta Pi, and the Institute of Electrical and Electronic Engineers.